MULTI-STATION ARTIFICIAL INTELLIGENCE BASED ENSEMBLE MODELING OF REFERENCE EVAPOTRANSPIRATION USING PAN EVAPORATION MEASUREMENTS

A THESIS SUBMITTED TO THE GRADUATE SCHOOL OF APPLIED SCIENCES OF NEAR EAST UNIVERSITY

By
JAZULI ABDULLAHI

In Partial Fulfilment of the Requirements for the Degree of Doctor of Philosophy

in

Civil and Environmental Engineering

NICOSIA, 2020

JAZULI ABDULLAHI
MULTI-STATION ARTIFICIAL INTELLIGENCE BASED ENSEMBLE MODELING OF REFERENCE EVAPOTRANSPIRATION USING PAN EVAPORATION MEASUREMENTS
NEU 2020

MULTI-STATION ARTIFICIAL INTELLIGENCE BASED ENSEMBLE MODELING OF REFERENCE EVAPOTRANSPIRATION USING PAN EVAPORATION MEASUREMENTS

A THESIS SUBMITTED TO THE GRADUATE SCHOOL OF APPLIED SCIENCES OF NEAR EAST UNIVERSITY

By
JAZULI ABDULLAHI

In Partial Fulfilment of the Requirements for the Degree of Doctor of Philosophy in Civil and Environmental Engineering

NICOSIA, 2020

Jazuli ABDULLAHI: MULTI-STATION ARTIFICIAL INTELLIGENECE BASED ENSEMBLE MODELING OF REFERENCE EVAPOTRANSPIRATION USING PAN EVAPORATION MEASUREMENTS

Approval of Director of Graduate School of Applied Sciences

Prof. Dr. Nadire ÇAVUŞ

We certify this thesis is satisfactory for the award of the degree of Doctor of Philosophy in Civil and Environmental Engineering

Examining Committee in Charge:

Prof. Dr. Gözen Elkiran		Supervisor, Civil Eng. Dept., NEU
Prof. Dr. Vahid Nourani		Co-supervisor, Civil Eng. Dept., NEU
Prof. Dr. Hüseyin Gökçekuş		Committee Chairman, Civil Eng. Dept., NEU
Prof. Dr. Derin Orhon		Environmental Eng. Dept., NEU
Prof. Dr. Bülent Bilgehan		Electrical Eng. Dept., NEU
Doç. Dr. Mustafa Ergil		Civil Eng. Dept., EMU
Yrd. Doç. Dr. Bertuğ Akıntuğ		Civil Eng. Dept., METU/NC

I hereby declare that all information in this document has been obtained and presented in accordance with academic rules and ethical conduct. I also declare that, as required by these rules and conduct, I have fully cited and referenced all material and results that are not original to this work.

Name, Last name: Jazuli Abdullahi

Signature: 

Date: 03-05-2020

ACKNOWLEDGEMENT

My words of acknowledgement go to the two most important people in my life, my parents you are my pillars, you are the reason why I endured such a difficult and rough journey. Without you, there would be no me. I appreciate your charisma, composure and resilience in helping me reached a height that I initially never dreamed of. May Allah prolong our days together in this dunya and bless you with place in the highest Jannah, Amin.

I would like to thank my supervisors, Prof. Dr. Gozen Elkiran and Prof. Vahid Nourani, for their patience, motivation, enthusiasm, and immense contribution, towards achieving this success. Besides my Supervisors, I would like to thank each and every committee member of my jury more especially Committee Chairman and Dean of Civil and Environmental Engineering Faculty Prof. Dr. Hüseyin Gökçekuş. I appreciate all your encouragement and useful recommendations.

It is with great pleasure I would say thank you to my siblings. No matter the situation you never left me alone, your prayers and words of encouragement always keep me hitting and dismantling any obstacles that come to my way. Your patience keeps me calm my love, you have always been understandable, and you have made sacrifices in this journey. These make the success to be ours together. I would not forget your individual contributions my friends and well-wishers, you were always supportive and wishing me success. I remain appreciative. May we all fulfill our lives wishes and may our final home be Jannatil Firdaus, Amin. I say thank you once again.

To my parents…

ABSTRACT

Reference evapotranspiration (ET_0) plays a major role in the fields of irrigation scheduling, climatological studies, agricultural water management, hydrological studies, etc. Lysimeters is used to measure ET_0 directly, but high installation and maintenance cost makes it difficult to use. Pan evaporation method is found to be of practical value for ET_0 estimation. However, artificial intelligence (AI) techniques and empirical equations are also used for ET_0 modeling. This study investigates the capability of ensemble learning approaches to improve modeling and multi-step ahead modeling of ET_0. To achieve this aim, 12 meteorological variables from 14 different climatic data stations across Turkey, Cyprus, Iraq, Iran and Libya were used as inputs. To ensure the quality standard and acceptability of the obtained data, quality control test was applied for all variables. Initially, empirical models including Ritchie (RT), Makkink (MK), Hargreaves and Samani (HS) and Modified HS (MHS) were applied for the ET_0 estimation. Thereafter, AI based sensitivity analysis was employed to determine the most appropriate input variables for Artificial Neural Network (ANN), Adaptive Neuro-fuzzy Inference System (ANFIS), Support Vector Regression (SVR) and Multiple Linear Regression (MLR) models which were applied for single ET_0 modeling. *K*-fold cross validation was applied for models validation. Simple Average (SA), Weighted Average (WA) and Nonlinear Ensemble (NE) were the 3 ensemble approaches applied in 2 phases of the ET_0 modeling. Phase 1 involved ensemble ET_0 modeling using the outputs of AI and empirical models. Phase 2 involved single and multi-step ahead ET_0 modeling using outputs of AI based models. The results showed that valuable performance could be achieved by the applied single models, but AI based models produced more reliable performance than MLR and empirical models. The results also demonstrated that ensemble models could be employed successfully for performance improvement of the single models in phase 1 up to 55% for ET_0 modeling and in phase 2 up to 60% for multi-step ahead ET_0 modeling in the validation step.

***Keywords*:** Ensemble learning; reference evapotranspiration; station, Turkey; artificial neural network; adaptive neuro-fuzzy inference system

ÖZET

Referans Evapotransporasyon (ET_0); sulama planlaması, iklimsel çalışmalar, tarımsal su yönetimi, hidrolojik çalışmalar vb. alanlarda önemli bir rol oynamaktadır. ET0'ı doğrudan ölçmek için Lisimetreler kullanılır, ancak yüksek kurulum ve bakım maliyeti kullanımı zorlaştırmaktadır. Alet buharlaşma yönteminin ET_0 tahmini için pratik bir değer olduğu bilinmektedir. Ancak Yapay Zeka (AI) teknikleri ve Ampirik Denklemler de ET0 modellemesi için kullanılmaktadır. Bu çalışma ET_0 modellemesini ve çok adımlı ileri modellemeyi geliştirmek için topluluk öğrenme yaklaşımlarının kapasitesini araştırmaktadır. Bu amaca ulaşmak için Türkiye, Kuzey Kıbrıs, Irak, İran ve Libya'daki 14 farklı iklimsel veri istasyonundan 12 meteorolojik değişken girdi olarak kullanılmıştır. Elde edilen verilerin kalite standardını ve kabul edilebilirliğini sağlamak adına tüm değişkenler için kalite kontrol testi uygulanmıştır. İlk olarak, ET_0 tahmini için Ritchie (RT), Makkink (MK), Hargreaves ve Samani (HS) ve Modifiye edilmiş HS (MHS) gibi ampirik modeller kullanılmıştır. Daha sonra uygulanan Yapay Sinir Ağı (ANN), Uyarlanabilir Nöro-Bulanık Çıkarım Sistemi (ANFIS), Destek Vektör Regresyonu (SVR) ve Çoklu Doğrusal Regresyon (MLR) modellerinde en uygun girdi değişkenlerini belirlemek için AI tabanlı duyarlılık analizi tekil ET_0 modellemesi için kullanılmıştır. Model validasyonu için K-fold çapraz validasyonu kullanılmıştır. Basit Ortalama (SA), Ağırlıklı Ortalama (WA) ve Doğrusal Olmayan Topluluk (NE), ET_0 modellemesinin 2 fazında kullanılan 3 topluluk yaklaşımıdır. Faz 1, AI ve ampirik modellerin çıktılarını kullanarak birleştirilmiş ET_0 modellemesini, faz 2 ise AI tabanlı modellerin çıktılarını kullanarak tek ve çok adımlı ileri ET_0 modellemesini içermektedir. Sonuçlar, uygulanan tekil modeller ile iyi performans elde edilebilmiş, ancak AI tabanlı modeller, MLR ve ampirik modellerden daha güvenilir sonuçlar vermiştir. Sonuçlar ayrıca, topluluk modellerinin, faz 1'de ET_0 modellemesi için % 55'e kadar ve faz 2'de validasyon aşamasında çok adımlı ileri ET_0 modellemesi için % 60'a kadar tekil modellerin performans iyileştirmesinde başarılı bir şekilde kullanılabileceğini göstermiştir

***Anahtar kelimeler* :** Topluluk Öğrenimi; Referans Evapotransporasyon; İstasyon, Türkiye; Yapay Sinir Ağı; Uyarlanabilir Nöro-Bulanık Çıkarım Sistemi

TABLE OF CONTENTS

LIST OF TABLES

LIST OF FIGURES

LIST OF ABBREVIATIONS

AI	Artificial Intelligence
ANFIS	Adaptive Neuro Fuzzy Inference System
ANN	Artificial Neural Network
BGNN	Bagged Neural Network
BLS	Black Sea
BNN	Boosted Neural Network
BP	Back Propagation
CCAN	Continental Central Anatolia
CEAN	Continental Eastern Anatolia
CMED	Continental Mediterranean
DC	Determination Coefficient
DDM	Data Driven Models
ELM	Extreme Learning Machine
ET	Evapotranspiration
ET_0	Reference Evapotranspiration
FAO	Food and Agricultural Organization of United Nations
FFNN	Feed Forward Neural Network
FG	Fuzzy Genetic
FIS	Fuzzy Inference System
GANN	Generalized Artificial Neural Network
GEP	Genetic Expression Programming
GPR	Gaussian Process Regression
GWNN	Generalized Wavelet Neural Network
GWR	Generalized Wavelet Regression
HS	Hargreaves and Samani
KP	Kimberly Penman
LM	Levenberg-Marquardt
LSSVR	Least Square Support Vector Regression
LULC	Land Use Land Cover

M5tree	M5 Model Tree
MARS	Multivariate Adaptive Regression Splines
MED	Mediterranean
MEDT	Mediterranean to Central Anatolia Transition
MFG	Mamdani fuzzy genetic
MHS	Modified Hargreaves and Samani
MK	Makkink
MLR	Multiple Linear Regression
MNLR	Multiple Non-Linear Regression
MRT	Marmara (Mediterranean to Black Sea) Transition
MSE	Mean Square Error
NC	North Cyprus
NE	Nonlinear Ensemble (Neural Ensemble)
PM	Penman Monteith
PMT	Penman Monteith Temperature
PT	Priestley-Taylor
RBF	Radial Basis Function
RMSE	Root Mean Square Error
RBFNN	Radial Basis Function Neural Network
RT	Ritchie
SA	Simple Average Ensemble
SEBAL	Surface Energy Balance Algorithm for Land
SFG	Sugeno fuzzy genetic
SVM	Support Vector Machine
SVR	Support Vector Regression
Tansig	Tangent Sigmoid
TMO	Turkish Meteorological Organization
WA	Weighted Average Ensemble

LIST OF SYMBOLS

P_R	Precipitation
R_H	Relative Humidity
S_P	Surface Pressure
T_D	Dew point Temperature
T_{max}	Maximum Temperature
T_{min}	Minimum Temperature
T_{mean}	Mean Temperature
U_{min}	Minimum Wind Speed
U_{max}	Maximum Wind Speed
U_{mean}	Mean Wind Speed
R_S	Solar Radiation
E_P	Pan Evaporation
K_p	Pan Coefficient

CHAPTER 1

INTRODUCTION

1.1 Reference Evapotranspiration

Evapotranspiration (ET) refers to the transfer of water from the earth's surface to the atmosphere by evaporating from wet plant, water, and soil surfaces and by transpiration via plant stomata (Odhiambo et al., 2001). The reference surface of the reference crop evapotranspiration or evapotranspiration is a hypothetical grazing reference crop with an approximate field depth of 0.12m, a fixed surface resistant of 70 sm-1 and an albedo of 0.23 (Allen et al., 1998).

Water scarcity particularly in arid and semi-arid climatic regions is becoming a major problem. It has a detrimental impact on the irrigation system, resulting in very low to no crop yields for seasonal and multiannual crops (Papadavid and Diafantos, 2010). However, according to Oladipo, (1993), one of the key factors restricting agricultural development after soil fertility is deficiencies in water supply. Therefore, it is important to estimate Reference Evapotranspiration (ET0) with reasonable accuracy in order to have efficient soil water balance for crop productions and water resources management in these regions.

The history of ET with meteorological variables can be traced back to the beginning of the 19th century (see, Brutsaert, 1982; Chen et al., 2005). Since then, several methods have been developed (classified into 6 groups) (Chen et al., 2005): (1) radiation-based methods (e.g. Makkink, 1957; Jones and Ritchie, 1990); (2) temperature-based methods (Blaney, 1952; Hargreaves and Samani, 1985); (3) combination methods (e.g. Penman, 1948, Monteith, 1965); (4) Pan evaporation methods (e.g. Allen et al., 1998); (5) water-budget methods (e.g. Guitjens, 1982) and (6) mass transfer methods (e.g. Harbeck, 1962). The practical importance of pan evaporation (Ep) has been demonstrated, and therefore its use with empirical coefficients (which relate Ep to ET_0) have been generally applicable for period of 10 or longer days (Allen et al., 1998). Ep measurements account for cumulative impacts of humidity, wind speed, solar radiation and temperature on the ET_0. Such measurements for the ET_0 estimation could successfully achieve a good accuracy (Irmak et al., 2002). As

shown by various studies, higher correlations between, Ep and ET_0 are expected if Ep is properly maintained (Khoob, 2008).

While physical and conceptual models are accurate tools to investigate a phenomenon's actual physics, they contain practical constraints, and when detailed predictions are more of concern than physical understanding, it may be more useful to use black box models. Multilinear Regression (MLR) is a traditional modeling approach for linear relations between dependent and one or more independent variables (Tabari et al., 2012). Such categories of models that are literally linear lose their value in modeling processes in many fields that are integrated in both spatial and temporal scales of high complexity, dynamism and nonlinearity. The use of Artificial Intelligence (AI) for instance, Adaptive Neuro-Fuzzy Inference System (ANFIS), Artificial Neural Network (ANN) and Support Vector Regression (SVR) has been widely adopted in recent years, through which many research papers have been published.

Although these black box models (e.g., ANN, ANFIS, SVR, and MLR) could lead to a very accurate results, it is well-known fact that different models can provide different outcomes for a specific problem. Furthermore, it is apparent that performance of one intelligent technique may exceed another for a given set of data, and when different data sets are used, the results may be quite the opposite. In order to exploit the advantages of all the intelligent methods and also not to sacrifice generality, a recently introduced modeling technique called ensemble model produces better predictive efficiency by using the single output of each intelligent method with some kind of priority level, which is assigned to the output of each intelligent method and the combined output is then provided with the aid of an arbitrator (Kiran and Ravi, 2008). In the ensemble model, the individual components received as outputs from each implemented method are used as inputs to the model, which are processed to provide overall output based on the arbitrator's design (Kiran and Ravi, 2008). Consequently, Bates and Granger (1969) seminal work indicated that a collection of different approaches would result in minimal variance in error compared to individual techniques or approaches in solitary mode. Furthermore, Makridakis et al., (1982) reported that combining multiple single models to improve predictive accuracy has become a standard practice. Some techniques of ensemble nature for predicting problems with continuous variable dependence consist of Nonlinear ensemble for example neural network-based ensemble (Yu et al., 2005)

and linear ensemble, such as Weighted average (Perrone and Cooper, 1993), Simple average (Benediktsson et al., 1997), and Stack regression (Breiman, 1996). The idea behind ensemble learning is to create unique characteristics for the constituent models to generate various patterns presented in the dataset (Kiran and Ravi, 2008; Sharghi et al., 2018).

1.2 Problem statement

In the recent decades, increase in the world population, expansion of industrial activities, as well as the destruction of the environment resulted in the escalation and rise of greenhouse gases which are detrimental to global climate. Evapotranspiration is among the primary and most significant components of hydrologic cycle being the biggest source of water loss. The water loss due to evapotranspiration increases with increase in global warming which leads to major drawbacks in water resources occurrence and distribution especially in the arid and semiarid regions of the globe. Therefore, estimation of evapotranspiration with reliable efficiency is of paramount important for proper use of the available water resources, design of hydraulic structures, irrigation practices and water resources management.

1.3 Objectives of the Study

In the context of hydro-climatic processes in general and ET_0 modeling in particular, based on the present literature, so far, no research has been performed using empirical models and AI-based techniques to perform ensemble modeling. Therefore, this study was performed in two phases as; (1) ensemble modeling of ET_0 and (2) ensemble modeling for multi-step ahead ET_0. Hence, the main objectives of this study were to;

i. Perform sensitivity analysis of 12 meteorological parameters from 14 meteorological stations across Turkey, Cyprus, Iraq, Iran and Libya in order to determine the appropriate input combinations.
ii. Apply AI (particularly ANN, ANFIS and SVR) and MLR techniques to model ET_0 in the study stations.
iii. Perform multi-step ahead prediction of ET_0 using same AI and MLR techniques.
iv. Compare the performances of the AI and MLR models with classical (empirical) models including Hargreaves and Samani (HS), Modified Hargreaves and Samani (MHS), Makkink (MK) and Ritchie (RT) for the ET_0 modeling.

v. Improve the accuracy and reliability of the single models through the application of Simple Average (SA), Weighted Average (WA) and Neural Ensemble (NE) techniques.

1.4 Hypothesis

Following are the hypothesis in this study;

- Due to vulnerability to hot climate condition, temperature would be most dominant parameter especially in arid and semi-arid stations of this study.
- AI models would have superior performance in comparison to MLR and empirical models because of their ability to deal with nonlinear aspect of ET_0.
- By increasing the prediction horizon the performance of the models will decrease owing to inability of inputs at previous time step to predict for future ET_0 for multi-step ahead modeling of ET_0.
- Ensemble modeling will improve performance of single models.

1.5 Significance of the Study

Being the first study that utilized the application of ensemble techniques for ET_0 modeling using several AI models, after completion, this study will serve as the basis upon which numerous studies could be conducted in hydro-climatic fields in general and ET_0 in particular due to its rich content. The current study will add value to the existing tools for ET_0 modeling and will significantly enhance the prediction of the complex ET_0 process.

1.6 Limitation of the Study

This study employed the application of a novel approaches to enhance prediction and multi-step ahead prediction of ET_0. The study is limited to data obtained from 14 meteorological stations from Turkey, North Cyprus, Iraq, Iran and Libya. The data period ranges from the minimum of 16 years to a maximum of 31 years. The oldest data used was 2010 and the latest was 2018. Two radiations and two temperature based models were used for empirical modeling, multiple linear regression was used to cover for linear conventional models, while ANN, ANFIS, SVR were employed as artificial intelligences models. Finally, two linear and one nonlinear ensemble models were used for performance improvement.

CHAPTER 2

LITERATURE REVIEW

2.1 Reference Evapotranspiration Modeling over the Study Regions

Several studies that involved the application ANN, ANFIS, SVR, MLR, HS, MHS, MK and RT models for ET0 modeling in the regions of this study could be found in literature. These include;

2.1.1 Reference evapotranspiration studies in Turkey

Pour-Ali Baba et al. (2012) modeled daily ET_0 using sunshine hours, relative humidity, air temperature and wind speed from 1985 – 1992 (for 8 years) from two meteorological stations in South Korea. ANN and ANFIS were the two models employed for the daily ET_0 modeling. Different combinations of input variables tallying with FA0-56-PM, PT and HS equations were trained, validated and tested in the first part of the equations. For the second part of the study, instead of recording sunshine hours, solar radiated was estimated and used with same input combinations as the first part. The results showed that using the available climate data, the ET_0 process could be efficiently simulated with the applications of ANN and ANFIS. In addition, the models accuracy decreased with the estimation of solar radiation data as replacement to recorded sunshine hours data.

Kisi (2013a) employed Sugeno and Mamdani fuzzy genetic techniques (SFG and MFG) to model ET_0 in Antalya and Adana stations using solar radiation, wind speed, air temperature and relative humidity as inputs to the fuzzy models. FAO-56-PM was used as reference ET_0. HS, Priestley-Taylor (PT) and Valiantzas were the three empirical equations employed for the study. The results demonstrated that SFG had a better performance and was faster than MFG and the two AI models performed better all the three empirical models utilized. For Antalya and Adana stations, in modeling daily ET_0 process, SFG1 model was found to be superior to other models.

Kisi (2013b) investigated the applicability of a newly developed Valiantzas equation for the estimation of ET_0 in Mersin, Antalya, Isparta and Adana stations in the Mediterranean region

of Turkey. Copais, Turk, HS, Irmak, RT and Hargreaves were also employed for comparison and the models performance were determined by FAO-56-PM. The results showed that in Antalya, Isparta and Adana stations, with full weather data, Valiantzas's equation had superior performance than other empirical models. Copais equation had a better performance in Mersin station and the Turc method performed the worst among the empirical models.

Todorovic et al. (2013) assessed the possibility of applying PM temperature (PMT) and HS mothods to estimate ET_0 from 577 weather stations obtained from CLIMWAT data base across several Mediterranean climatic regions. The results revealed that PMT and HS performances were similar in hyper-arid and arid zones. PMT outperformed HS method in semi-arid to humid zones. In the estimation of dew point temperature, the PMT method performance could be improved when aridity/humidity corrections are adopted from minimum temperature data. High variability of ET_0 could be seen from spatial elaboration results by different methods. Hence, sufficient quality dataset is needed for a site specific analysis for calibration and validation of temperature methods for ET_0 modeling.

Kisi and Cengiz (2013) used air temperature, wind speed, relative humidity and solar radiation from Isparta and Antalya stations of Turkey Mediterranean region to ascertain the applicability of fuzzy genetic (FG) in modeling ET_0 using FAO-56-PM as reference. Comparison were made between FG models and ANN models. The results implied the superiority of FG model in ET_0 modeling in Turkey Mediterranean region in comparison to ANN model.

Kisi and Zounemat-Kermani (2014) compared the performance of subtractive clustering (SC) and grid partitioning (GP) methods of adaptive neuro-fuzzy inference system (ANFIS) for daily ET_0 modeling. Daily weather data from Adana station of Turkey Mediterranean region consisting of including wind speed, relative humidity solar radiation and air temperature were used as inputs to the two fuzzy models. Fuzzy models were used to investigate the effect of each meteorological parameter on FAO-56-Pm ET_0 in the first part of the study. The most effective variable was found to be wind speed. The missing data effect on fuzzy models on training, validation and testing were also examined in the second part of the study. ANFIS-GP model was found to be unaffected by the missing data while ANFIS-SC model's accuracy decreases with more percentage of missing data. The duration or data

length for training, validation and testing in the third part of the study were investigated. The results showed that the training data length has no significant effect on fuzzy models for the ET_0 modeling. The last part of the study compared the fuzzy models with calibrated Hargreaves, Turc, RT and Valiantzas' equations. The results showed that calibrated RT and Valiantzas' equations with two-parameters outperformed two-input ANFIS models while four and three-input ANFIS models performed better than the applied empirical equations.

Citakoglu et al. (2014) applied ANN, ANFIS, HS and RT models to estimate ET_0 using several combinations of long-term average monthly climate data of wind speed, air temperature, relative humidity, and solar radiation, recorded at stations in Turkey. FAO-56 PM was used as the basis of comparison of the models performances. The results showed that the ANFIS and ANN schemes can be employed successfully in modeling the monthly mean ET0, because both approaches yield better estimates than the classical methods, and yet ANFIS being slightly more successful than ANN.

Cobaner et al. (2016) proposed the modification of HS model for ET_0 modeling from 275 climate stations in Turkey. The study was organized first with application of HS model for ET_0 modeling, then FAO-56-PM was used to calibrate the coefficient of HS model, the finally, as an extra explanatory variable, wind speed was added to modify the HS model. The results revealed that for better accuracy in ET_0 modeling, the modified HS model can be used in regions with scare meteorological measurements.

Kisi (2016) applied three heuristic regression approaches including M5 model tree (M5tree), multivariate adaptive regression splines (MARS), and least square support vector regression (LSSVR) for ET_0 modeling in ISparta and Antalya stations in Turkey Mediterranean region. Cross-validation was also applied. In the first part of the study, the accuracy of the applied models were investigated using local input and output data. The results showed better performance of LSSVR than MARS and M5tree models. In the second part, the input data from nearby stations were used instead of local inputs. The result depicted higher accuracy of MARS in comparison to LSSR and M5tree models. The last part involved the use of both inputs and output data from nearby station. The results demonstrated the superiority of M5tree against LSSR and MARS models. The results also revealed that when all the local inputs and output data are available, LSSVR could model ET_0 sufficiently, in case of missing

local inputs, MARS model showed greater efficiency and when local inputs and output data are not available, M5tree would be a better choice between the three applied models.

2.1.2 Reference evapotranspiration studies in Cyprus

Papadavid et al. (2011) applied FAO-56-PM to estimate ET_0 using maximum and minimum temperature, wind speed and relative humidity as inputs. The FAO-56-PM ET_0 was compared with low-resolution satellite data (MODIS-TERRA). Moreover, geographic information system (GIS) was used to map the automatic meteorological stations in Cyprus. Thiessen polygons methodology was applied to categorize the agricultural area of the island, which is considered as area representative. The results depicted that with utilization of appropriate meteorological data, then the ET_0 correct deviation might be obtained leading to crop water stress and water losses.

Papadavid et al. (2013) ET_0 of groundnut was estimated by integrating remote sensing and modeling techniques in Paphos district of Cyprus. For the first time in Cyprus, the surface energy balance algorithm for land (SEBAL) was employed. The needed spectral data was capture using 7 ETM+ and Landsat-5 TM images. Empirical equations were used to enhance SEBAL model in order to increase its accuracy regarding crop canopy factors. For the interest area, SEBAL modified model (CYSEBAL) used to create ET_0 map. Measurements from pan evaporation were also compared with the results of SEBAL and CYSEBAL. The results revealed that the results of pan evaporation were comparable to the results yield by CYSEBAL. The results from T-test application also showed a quite crucial and significant statistical difference between CYSEBAL and SEBAL models especially in underground water resources and limited surface place.

Abdullahi and Elkiran (2017) applied feed forward back propagation data driven algorithm to perform an investigative study to examine the effect global climate might have on ET_0 using Larnaca and Girne meteorological variables of Cyprus. The first approach of the study the number of hidden neurons was altered while the input parameters remained the same. In the second approach, the hidden neurons double the number of inputs while the inputs ranged from 2 to 6 parameters. The results revealed that ANN in both approaches could successfully accomplish the prediction of ET_0 in Larnaca and Girne stations of Cyprus, but the models performance increases with more inputs.

Abdullahi et al. (2017) examined the accuracy of ANN model in predicting monthly ET_0 in Famagusta station of Cyprus. The results of the ANN models were compared with MLR model. Different input combinations were adopted in training the models. FAO-56-PM was employed for evaluating the performance of the developed models. The obtained results showed that wind speed was the most dominant parameter. Moreover, the results demonstrated that ANN model outperformed MLR in the estimation of ET_0 in Famagusta station.

2.1.3 Reference evapotranspiration studies in Iraq

Awchi (2008) investigated redial basis function neural network (RBFNN) potential in the prediction of daily ET_0. Data from Mosul meteorological station in the north of Iraq were collected for 5 years including wind speed, relative humidity, sunshine hours, rainfall and temperature. Varied input combinations were used to developed thirteen RBFNN models and their performances were compared with FAO-56-PM ET_0. FFNN model was also developed to compare with the RBFNN models. The results depicted that RBFNN could be used effectively for the prediction of ET_0 and could be compared to FFNN and RBFNN is faster and easier to train.

Abdullah et al. (2014) proposed the application of ANN-genetic algorithm (ANN-GA) hybrid model in comparison with FFNN and FAO-56-PM for daily ET_0 estimation in arid and semi-arid regions of Iraq using radiation hours, maximum and minimum air temperatures, wind speed and relative humidity as inputs to the models. Correlation coefficient (R^2) and mean square error (MSE) were the evaluation functions used. The results showed promising performance by all the applied models. However, the proposed hybrid model showed greater efficiency and therefore, was recommended for ET_0 estimation in arid and semiarid regions.

Aljumaili et al. (2014) analyzed five ET_0 estimation models FAO-24-PM model, FAO-56-PM model, Jensen-Haise (JH) model, Hargreaves model and Penman-Kimberly (PK) model for irrigation projects in Karbala, Iraq. Pearson correlation coefficient, root mean square error and bias were used for performance evaluation of the models. The results showed a close performance for models developed by more climatic inputs including PK, PF and PM. The wind function used in each model result in differences between the models. With slope

of 1.254, the minimum climate data used for linear regression model development, R^2 of 0.988 and an interception point of -1.801 very closely matched with PK model values.

Abdulllah et al. (2015a) examined the capabilities of ANN and hybrid ANN and genetic algorithm (ANN-GA) to model ET_0 in Baghdad meteorological station, Iraq. Sunshine hours, wind speed, relative humidity, and minimum and maximum air temperature were used as inputs. The performance of the models were evaluated using Determination coefficient (R^2), mean absolute error (MAE) and root mean square error (RMSE). The results obtained from each models were promising though, the hybrid model demonstrated better performance capability and was recommended for ET_0 modeling in arid and semiarid climate regions.

Abdullah et al. (2015b) study investigated the accuracy of extreme learning machine (ELM) algorithm in prediction of FA0-56-PM ET_0 in Basrah, Baghdad, and Mosul meteorological stations in the southern, middle and northern parts of Iraq. The input meteorological variables used from 2000 – 2013 include, relative humidity, sunshine hours, wind speed and maximum and minimum air temperatures. Four different combinations of inputs were used with complete and incomplete data sets. The ELM model performance was compared to FAO-56-PM and FFNN models. Determination coefficient (R^2), mean absolute error (MAE) and root mean square error (RMSE) were used as evaluation criteria. The results showed an encouraging performance of both models especially ELM model produced with incomplete data sets. The ELM model proved to be of high speed, simple application, efficient of good generalization performance and was therefore, recommended for climatic and geographical locations similar to arid and semiarid regions of Iraq.

Jassas et al. (2015) study employed the application of water balance and surface energy balance algorithm for land (SEBAL) to conduct spatial and temporal ET_0 estimation in Al-Khazir Gomal basin, northern Iraq. In the winter season, one of the most important activities is the rainfed farming of barley and wheat, while agricultural activities are limited to narrow strips of vegetable cultivation and small rice fields in the summer, along the Al-Khazir River. Land use land cover (LULC) map results were compared to the SEBAL results. The results showed the potential of SEBAL model in the estimation of ET_0 in the study area and could be employed in future water budget studies of the basin.

Jaber et al. (2016) applied SEBAL model to predict ET_0 in Al-babil city of Iraq. Two reference data sets from the Al-babil meteorological station were used to evaluate the performance of the SEBAL model. The first and second data sets on March and September overall accuracies were achieved as R^2 = 0.86 and R^2 = 0.85, respectively. The results revealed that SEBAL model could be employed for ET_0 prediction in the study area.

Najmaddin et al. (2017) assessed the accuracy of ET_0 estimated using remote sensing data ($ET_{0\text{-}RS}$) in comparison to ET_0 developed with the use of four ground-based stations ($ET_{0\text{-}G}$) over the period 2010 – 2014 in Iraq's Kurdistan region. Wind speed, cloud cover fraction, relative humidity and air temperature were used as inputs variables. Four empirical models were developed for the study purpose including Jensen-Haise (JH), (HS), FAO-56-PM and McGuiness-Bordne (MB) models. FAO-56-PM was used as the benchmark ($ET_{0\text{-}G}$). JH and MB overestimated ET_0 by 8% to 40%, while HS underestimated ET_0 by 2 to 3%. The annual average values of ET_0 reflected low bias in daily estimate indicating that ground-based data and RS data were similar to one another. The results revealed that $ET_{0\text{-}RS}$ could be successfully employed in the management of water resources as it can yield unbiased and accurate ET_0 estimate.

2.1.4 Reference evapotranspiration studies in Iran

Odhiambo et al. (2001) examine the suitability of estimating daily ET0 using fuzzy logic with fewer and simpler parameters in arid and humid climate regions. Two or three parameters from two fuzzy evapotranspiration models were developed for the ET0 estimation. The results obtained by fuzzy model was compared to FAO-56 PM, HS equations and measurements from grass cover weighing Lysimeters. The results demonstrated that accurate estimation of ET0 could be achieved by fuzzy logic with fewer and simpler parameters.

Sudheer et al. (2003) examined ANN potentials in estimating ET0 by limited climate data. Various input combinations were used and the models were developed, trained, and tested and compared to the measured lysimeter ET0. The results revealed that ANN could be applied successfully in predicting ET0 with air temperature as input.

Chen et al. (2005) performed an investigative study that compared the Penman-Monteith method as a reference, and its temporal and spatial variations with the pan measurement and Thornthwaite method. The revealed results in terms of spatial variation display a consistent regional pattern by pan measurements, while the Thornthwaite estimates show different regional patterns. In addition, pan measurements show much better representation of ET_0 in the temporal variability than the Thornthwaite estimates. Overall, to appropriately determine pan coefficients, pan measurements are more useful than the Thornthwaite estimates.

Dinpashoh (2006) used 30-year meteorological data from 81 weather stations based on spatial and temporal procedures to estimate the ET0. Results indicated that the long-term mean annual ET_0 varies across the country from 830 mm to over 3627 mm. The annual least and monthly ET_0 belonged to the coasts of the Caspian Sea while the highest ET_0 belonged to the southeastern and central parts of Iran. The mean annual ET_0 in the southeastern part of Iran was around 33 times that of its annual mean precipitation.

In order to estimate daily ET_0 from weather data, Kisi (2006) applied two separate feed-forward neural network algorithms, conjugate gradient (CG) and Levenberg – Marquardt (LM). The performance of the LM and CG algorithms in estimating ET_0 was evaluated and discussed, and the analysis explores different combinations of soil and air temperature, solar radiation, wind speed and relative humidity as data inputs to the ANN models to determine the degree of impact of each of these variables on ET_0. The findings of the ANN models were contrasted to those of the Penman and Hargreaves empirical models and multi-linear regression (MLR) model. Based on the comparisons, the neural computing technique from the available weather data was found to be effective in modeling the evapotranspiration process.

Kisi and Ozturk (2007) evaluated the ability of ANFIS for estimation of ET_0 using daily climate data of relative humidity, air temperature, wind speed, and solar radiation from Santa Monica and Ponoma stations in Lose Angeles as inputs the empirical and neurofuzzy models. the results obtained by neurofuzzy model were compared with that of ANN and empirical models including HS, RT, Penman and California Irrigation management system. The obtained results implied that in modeling the ET0 process, the neurofuzzy models could be of successful application.

Khoob (2008) estimated ET_0 using ANN from pan evaporation measurements. The ANN was assessed under semi-arid climate environments in Iran southwest's Safiabad Agricultural Research Center (SARC), comparing daily estimates by the standard FAO-56 Penman – Monteith equation (PM) with those from ANN and traditional empirical method. The comparison depicts that, the ET_0 obtained by the PM method was underestimated by conventional method. The ANN method provided better estimates than the traditional method, which needs data on humidity and wind speed.

Rahimikhoob (2010) based on air temperature data examined the potential of ANNs in the estimation of ET_0 in eight stations of humid subtropical regions located in the southern coast of Caspian Sea, Iran. Extraterrestrial radiation, minimum and maximum temperature were the input variables used. There was also a comparison of the estimates given by the ANNs and by the equation of HG. The Penman – Monteith FAO-56 model was utilized as the standard model to test the efficiency of both the methods. The obtained results by the study demonstrated that using air temperature data, the daily ET_0 was successfully estimated by ANNs and that using the ANNs, simulation of ET_0 was better with RMSE of 0.41 mm day^{-1} and R^2 of 0.95 compared to Hargreaves equation, which had RMSE of 0.51 mm day^{-1} and R^2 of 0.91.

Karimaldini et al. (2011) estimated daily ET0 under arid conditions using ANFIS from limited climate data in Iran. For the calibration of the model, to determine the number of sufficient data points and to find the best input combination, gamma test technique was used. K-fold cross-validation method was chosen to obtain the optimal classifier for training and testing data sets. Calibrated FAO-56 reduced-set PM ET_0 approach and some calibrated empirical ET_0 equations such as Makkink, Hargreaves, Blaney-Criddle and Priestley-Tailor equations were compared with the estimates of the ANFIS models. The FAO-56 full-set PM was adopted as the ET_0 equation of reference, and it was used to calibrate other ET_0 equations and ANFIS models. The results of the analysis suggested that the ANFIS models performed better than all the methods used when identical meteorological inputs are used. This fact strongly suggests that ANFIS is an accurate ET_0 estimation technique, even in the absence of complete meteorological data. Under arid conditions, the minimum data needed to construct a good ANFIS model are wind speed, maximum and minimum air temperatures.

Due to the constraint of FA0-56-PM to large amount of climate data, which are difficult to have especially in the developing countries, Tabari and Talaee (2011) study employed the use of PT and Hargreaves (HG) models that require limited amount of data from 12 meteorological stations in the cold and arid climates of Iran. The results implied that the PT coefficient for the climatic regions, which was originally 1.26 was very small, with the latest PT coefficients of 2.14 and 1.82 being the best match in cold and arid climates compared to the FAO-56-PM process. Overall, calibration of the equations of HG and PT led to improvement of the equations by reducing the errors of the estimates of ET_0.

Dinpashoh et al. (2011) used several regions that covered for over 16 weather stations in Iran to estimate ET_0. After eliminating the important lag-1 serial correlation effect from all of the ET_0 time series by pre-whitening, trend of ET_0 was evaluated using Mann-Kendall. The magnitude of the trend was found to be at it strongest positive (or negative) in April (July) with slope equal to 14 mm/year per decade for Theil–Sen. Considering the entire study domain, there was no homogeneity between months and stations for the ET_0 trends as indicated by the results of homogeneity test. The most influential variable to ET_0 in Iran was found to be wind speed in all months with exception of winter months.

Zanetti et al. (2007) used minimum climatological data which comprised of maximum and minimum air temperatures, daylight hours, and extraterrestrial radiation to test the potential of ANN model for the estimation of ET_0 in the Campos dos Goytacazes county, State of Rio de Janeiro. The results revealed that it is possible to have reliable estimation of ET_0 with the application of ANN model from maximum and minimum air temperatures only in Campos dos Goytacazes.

Tabari et al. (2012) performed investigation about the potential of SVM, ANFIS, MLR and multiple non-linear regression (MNLR) to estimate ET_0 in Iran's semi-arid highland environment using six climatic data input variables. Additionally, the PMF-56 model has been tested against eight radiation-based and four temperature-based ET_0 equations. The results obtained for the ET_0 estimated by the SVM and ANFIS models were better than those obtained using the climate and regression-based models and demonstrated the capability of these techniques to provide effective tools for ET_0 modeling in semi-arid environments. Based on the overall performance comparison, it was found that the models SVM6 and

ANFIS6, which used wind speed, relative humidity solar radiation and mean air temperature as input variables, had the highest efficiency.

Valipour (2012) performed an investigative study to determine the ability of Box-Jenkins models for the estimation of ET_0 for Mehrabad synoptic station in Tehran, Iran. The results were compared with FAO-56-PM, FAO radiation macking (FRM), Turc, corrected Jensen Haise (CJH), FAO blaney criddle (FBC), thornthwaite (TW) and HS models. Also ANN, genetic programming and remote sensing were also employed for the ET_0 modeling. To increase accuracy, the models were developed with increasing number of frequency up to 5. The results revealed the capability of Box-Jenkins models in modeling ET_0.

Rahimikhoob et al. (2013) applied conventional method and M5 model tree for the estimation of ET_0 from pan evaporation data in semi-arid climate of Khuzestan plain, southwest Iran. Results suggested that the M5 model tree was the best model to be applied for ET_0 estimation over test sites, which provided RMSE of 0.5 mm/day and R^2 of 0.98. Conversely, the two Kp equations worked poorly.

Shiri et al. (2013) applied GEP and ANFIS based on solar radiation and temperature modeling procedures and compared with radiation/temperatures-based estimation equations for ET_0 modeling in Shahrood, Semnan, Esfahan, Kerman and Bam stations via two management scenarios. In the first scenario, the GEP and ANFIS models were found to be superior in terms of performance compared to the equations by Makkink, Turc ET_0 and Hargreaves–Samani. Comparison of ANFIS and GEP models for each station with pooled data trained and tested depicted that the GEP models performed less than ANFIS models generally. However, the comparison of pooled data trained and tested GEP and ANFIS models indicated that the ANFIS models were outperformed by the GEP models in the second scenario.

Rahimikhoob (2014) Estimated ET_0 in four meteorological stations using M5 model tree and ANN in arid climate of Iran. Results from the analysis showed that better estimation of ET_0 were achieved by ANN than the M5 model tree but within the confinement of the study area, both models developed promising performance and produced results similar to the FAO56-PM process. The overall findings are of significant practical benefit since the moisture and

temperature-based model can be used when data on wind speed and radiation are not available.

Shiri et al. (2014a) compared different heuristic and empirical models for the prediction of ET_0 in a several climatic regions in Iran. The data driven models (DDM) include ANN, ANFIS, SVM and genetic expression programming (GEP) compared with HS, MK, Priestley-Taylor (PT) and Turk (T). The results demonstrated the superiority of GEP based models. Among the applied empirical models, calibrated HS model produced the best performance in both pooled and local scenarios. The DDM provided superior performance over the rest of the empirical models. The poorest result was obtained from arid region while the best result was obtained from humid regions. High advective and higher ET_0 values could be attributed to such results.

Shiri et al. (2014b) applied genetic expression programming (GEP) model for estimating ET_0 according to spatial and temporal criteria in coastal environment in Iran.

Snyder et al. (2005) evaluated equations for ET0 estimation from pan evaporation measurements and provided a simpler to make conversion from pan evaporation to ET0 in arid climate conditions such as California. The results show that the proposed method is conceptually easier and simple to use such as in coding for computer applications, the method gave better results within California than methods based on wind speed and relative humidity.

Valipour (2015a) used data from 31 provinces in 181 synoptic stations of Iran and compared the performance of 11 temperature-based and FAO-56-PM models to determine the best approach for estimating ET_0 under the influence of several climatic conditions. The results showed that in most Iranian provinces the updated Hargreaves–Samani 1 predicted the evapotranspiration process with more accuracy than other models. Nevertheless, the R^2 values for 20 Iranian provinces were < 0.9930. The most accurate approach for Alborz province (AL) was the updated Hargreaves – Samani 4. Finally, a list of each model's best results was provided for implementation in different regions based on minimum, maximum and mean temperature elevation, precipitation, wind speed, mean and minimum relative humidity and sunshine. The study results are also particularly useful in identifying the

appropriate model when researchers have to apply temperature-dependent models based on available data.

Valipour (2015b) compared Turk, PT and 5 different Valiantzas models for ET_0 modeling from 181 synoptic stations under different weather conditions in Iran. Findings showed that the optimal climatic conditions to be used in the methods of Valiantzas are 1.50–2.50 m s−1, 16–18 ° C, > 24.2 MJ m−2 day−1 and 40–50 percent for wind speed, temperature, solar radiation and relative humidity. Results are also valuable in choosing the best model if researchers are expected to apply such models based on the available data.

Wen et al (2015) used limited climatological data to test the use of a support vector machine (SVM) to model the daily ET_0. For the SVM, in the extremely arid area of Ejina basin, China, four combinations of minimum air temperature (T_{min}), maximum air temperature (T_{max}), daily solar radiation (R_S) and wind speed (U_2) were used as inputs with T_{min} and T_{max} as the baseline data. The results of the SVM models were assessed by comparing the performance with the ET_0 determined using the equation of Penman – Monteith FAO 56 (PMF-56). The results showed that the approximate ET_0 using SVM with limited climatological data was in strong agreement to those achieved using the traditional equation by PMF-56 using the maximum meteorological data complement. Notably, three climatic parameters- Rs, Tmin and Tmax were sufficient to satisfactorily predict the daily ET_0. In addition, SVM system performance was also compared with that of ANN and three empirical models including Ritchie, Hargreaves and Priestley-Taylor. The results suggested that the SVM system performance was the better among these models. This provides important potential for a more precise estimate of the ET0 in severe arid regions with insufficient data.

Feng et al. (2016) compared the performances of backpropagation neural networks optimized by genetic algorithm (GANN), extreme learning machine (ELM), wavelet neural network, HS, MHS, MK, Priestley-Taylor and RT models for reference evapotranspiration estimation in humid region southwestern China. Results suggested that ELM and GANN models were much superior than WNN models among the proposed models, and that the ELM and GANN temperature-based models performed better than modified Hargreaves and Hargreaves models, radiation-based, the performance demonstrated by ELM and GANN were more accurate than Ritchie, Priestley-Taylor and Makkink models. Both radiation-

based ELM could be employed to estimate ET_0 at reasonable level of accuracy, and without adequate climatic data, they are highly recommended for ET_0 estimation.

Djaman et al. (2016) study focused on determination of ET_0 using FAO-56-PM and two Valiantzas ET_0 models in eight meteorological stations across Burkina Faso. The climate parameters used include solar radiation, maximum and minimum relative humidity, wind speed and maximum and minimum air temperature. The results demonstrated that with missing solar radiation, ET_0 can be accurately estimated using maximum and minimum air temperatures for solar radiation estimation. The Valiantzas 1 model that utilizes only relative humidity and air temperature is not recommended and not suitable in the climate condition of Burkina Faso. Efficient estimations of ET_0 with regards to FAO-56-PM with full climate data was achieved using Valiantzaz 2 model. It was finally concluded that due to limitation of Valiantzas equation with limited data, FAO-56-PM was recommended.

Kisi and Kilic (2016) assessed the generalization capability of ANN and M5 model tree for ET_0 modeling in two different regions of the USA. Climatic data of daily measurements including wind speed, average temperature, relative humidity and solar radiation from six different stations located in San Joaquin region and Southern region. Empirical equations were also developed for comparing to the ANN and M5 model tree. The AI models performed better than the empirical models. However, better performance were achieved by ANN models in comparison to RT, HS, Turc and CIMIS Penman models, while generally M5 model tree performed better than empirical models in both regions. Also in the third part of the research, M5 tree and ANN models with four inputs were superior to CIMIS Penman models in one station only but with only 2 inputs, ANN model performance surpasses Turc, RT, and HS models in two stations.

Adamala et al. (2019) applied generalized wavelet neural network (GWNN), HS, and Turc models for daily ET_0 modeling in humid, subhumid and semiarid regions of India. The developed models were also compared with generalized artificial neural network (GANN), generalized wavelet regression (GWR), generalized linear regression (GLR) and other conventional methods. FAO-56-PM was used as the reference ET_0 to determine the performance of the applied models. The results indicated that GWNN followed by GANN

models provided better prediction than GWR and GLR and are therefore recommended foe ET_0 modeling in the three regions of study.

Manikumari et al. (2017) employed boosted neural network (BNN) and bagged neural network (BGNN) ensemble learning to improve the forecasting accuracy of daily ET_0 for the period 2004 – 2014 consisting of 4018 number of observations in India. The results revealed that the efficiency of BNN and BGNN in prediction of ET_0 was higher than individual neural network models. Among the applied ensemble models, BNN was found to have better performance than BGNN.

Gao et al. (2017) applied FAO-56-PM, FAO-24 radiation, Blaney Criddle (BC), HS, PT, Turc and MK models for daily, monthly average and total annual ET_0 estimation in AKsu, an arid region of China, Tongchuan, a semiarid region of China and Mississipi, a humid region of United States. Comparison of models performances were based on modeling efficiency root mean square error and index of agreement. The results revealed that for arid and semiarid regions, HS and PT have the best performance while in humid region, performed better.

Mehdizadeh et al. (2017) investigated the performances of SVM-radial basis function (SVM-RBF), SVM-polynomial (SVM-Poly), MARS, GEP and 16 empirical equations including mass transfer based, temperature based, meteorological parameters based and radiation based for the estimation of monthly ET_0 in Iran. The MARS and SVM-RBF methods were found to typically achieve better results than the SVM-Poly and GEP methods. The accuracy of empirical equations and AI methods were compared at the end part of the analysis. In general, MARS and SVM-RBF worked better than empirical equations used.

Shiri (2017) assessed the performance of several estimation techniques including GEP, HG, PT, Turk (Tr), Kimberly Penman (KP) for ET_0 modeling ET_0 in the hyper arid regions of Iran. The findings obtained revealed that the GEP models in all three studied categories (radiation, humidity /temperature, and combination-based methods) outperformed the corresponding semi-empirical and empirical models. The research further revealed that the calibrated models of Tr (with estimated relative humidity) and PT (original) provided the most reliable performance among the similar groups.

Karbasi (2018) performed multi-step ahead daily ET_0 forecasting from 1 to 30 days ahead using the Gaussian Process Regression (GPR) and Wavelet-GPR models at the Zanjan synoptic station, Iran. The study considered 10 years statistical period between 2000 and 2009. For this reason, 2000–2006 datasets (7 years) were utilized for training and 2007–2009 the (final 3 years) datasets were used for validation of several models. The revealed results indicated that the accuracy of the models is increasing by decreasing the forecasting time span from 30 days to 1 day with RMSE = 0.816 mm/day for 30 days ahead and RMSE = 0.068 mm/day for one day ahead. Summer season application of the proposed model showed that the model's performance during the summer season is more reliable than its performance year-round.

Duo and Yang (2018) applied extreme learning machine (ELM), ANFIS, ANN, and SVM to predict daily ET with observations of flux towers in four major ecosystem categories. The findings suggested that all of the models applied had good performance for daily ET modeling. Among the ELM models implemented, in most cases the three hybrid ELM methods outperformed the original ELM method at the four locations, and the computational time needed to learn these ELM models was substantially reduced. Generally, the fuzzy c-means clustering and subtractive clustering algorithms for ANFIS were stronger than the grid-partitioning algorithm. It was concluded that owing to their robustness and versatility, the advanced ANFIS and ELM models can be recommended as essential complements to conventional methods. In addition, there was a substantial difference between the four major types of ecosystems regarding the modeling results. The models usually performed best in the forest environment, while offering the worst in the cropland environment.

Farzanpour et al. (2018) compared the performances of twenty prediction models for ET_0 estimation using daily meteorological parameters from 10 stations for the period of 12 years in semiarid climate of Iran. Cross-station and local calibration scenarios were compared against FAO-56-PM. The results showed that cross-validation could serve as a good substitutes to local calibration of ET_0 models when similar stations are used for the training matrix.

Mohammadrezapour et al. (2018) compared the performances of GEP, ANFIS and SVM for ET_0 modeling in baluchestan and and sistan province, an arid region of Iran. The study

involves the combination of five different inputs. Determination coefficient, mean absolute error and root mean square error were the employed criteria for performance evaluation. The obtained results showed that SVM with wind speed, sunshine hours current and one month lag, air temperature and relative humidity as inputs performed better than other models for Zabol, Chabahar, Zahedan and Iranshahr stations. Comparison of the heuristic models revealed that for estimation of ET_0, the first, second and third performances models were SVM, GP and ANFIS across all stations.

Mehdizadeh (2018) applied gene expression programming (GEP) and multivariate adaptive regression splines (MARS) based on external and local performance to estimate daily ET_0 by providing a new strategy to lagged data-based modeling of ET_0. Daily historic data was used during 2000–2014 from six stations with various climates in Iran, including Yazd and Zahedan (hyperarid), Isfahan and Shiraz (arid), Urmia and Tabriz (semi-arid). The applied models local performance exhibited the capability of the GEP and MARS methods to estimate daily ET_0 using the lagged data and the climate variables as inputs to the ET_0. Nevertheless, the MARS performed best in the weather-based data scenarios. In addition to that, the accuracy of the models for the lagged ET0 data-based scenarios was not observed with significant differences. In the innovation of this research, through the conjunction of GEP and MARS models with time series model of autoregressive conditional heteroscedasticity (ARCH), novel hybrid models were proposed in the lagged data-based scenarios of ET_0. It was concluded that the GEP-ARCH and MARS-ARCH novel models proposed, enhanced ET_0 modeling efficiency compared to single GEP and MARS models. Furthermore, the external performance review of models at locations with identical weather conditions suggested the applicability of nearby station data to estimate the daily ET0 at the target station.

In Brazil, Ferreira et al. (2019a) proposed a new method for estimating the ET_0 using SVM and ANN with minimal climatological data. The results revealed that even though they were calibrated, the ANN and SVM models displayed higher efficiency than the equations which were studied. The methods analyzed (clustering and preceding days) received substantial efficiency gains. The ANN developed the best performance for the temperature-based models with the clustering strategy and the use of data from two previous days as input; although, owing to the identical reliability and greater generalization efficiency, the ANN

produced from four previous days with the use of data and without clustering is recommended. The ANN established with data from four days before was the best choice for the relative humidity and temperature-based models.

Huang et al. (2019) implemented a new learning algorithm using gradient boosting for ET_0 estimation on decision trees with support for categorical features (i.e., CatBoost), SVM and Random Forests (RF). The results depicted that all three algorithms in subtropical China could achieve adequate accuracy for the estimation of ET_0 by using inputs of T_{min}, T_{max} and R_S or Hr, T_{min} T_{max} and U in the absence of complete climatological variables. The rise in RMSE and MAPE testing over RMSE and MAPE training showed positive relationships with the number of input variables for the AI models. For the local models, SVM provided the best prediction accuracy and consistency among the three algorithms, with insufficient combinations of climatological variables as inputs, whereas CatBoost performed best with the full combination of variables. Generalized model trends were almost the same as local models, however the former models showed a decrease of less than 10% in RMSE or MAPE relative to the latter. Additionally, CatBoost's running time and memory use for data processing was much less than SVM and RF. Overall, as a tree-based algorithm, as opposed to RF, CatBoost has made major improvements in precision, reliability and computational costs. The CatBoost algorithm therefore has a very high potential for estimating ET_0 in humid regions of China, and probably even in other parts of the world with similar humid climates.

Granata (2019) performed a comparative study based on machine learning algorithms to model ET. SVM, M5P regression tree, random forest and bagging were the machine learning algorithms applied using data from experimental site of humid subtropical climate of central Florida. Three different input combinations based on different parameters were developed. The results revealed that, model 1 provided the best outcome with soil moisture, mean temperature, sensible heat flux, mean relative humidity, wind speed and net solar radiation. A satisfactory result was also obtained from model 3 which comprised of mean relative humidity, mean temperature and net solar radiation. Model 2 which has addition of wind speed to same inputs of M3, led the results comparable to those of M3 itself.

Zhu et al. (2019) used 838 stations daily meteorological data of 12 consecutive years to calibrate HS model through comparison between produced ET_0 values by PM model and those calculated by original HS model. Values of statistical indices and distribution were used to evaluate HS model. The ET_0 estimation provided by the calibrated HS model was found to be greatest in the southwestern and subtropical monsoon climate zone. Despite the improvement achieved by HS model due to applied calibration in the monsoon, mountain and plateau climate zones, high enough accuracy was achieved by the original HS model. For regions of tropical climate, reliable results were failed to be achieved by HS model even in calibrated form. The overall results demonstrated that higher accuracy was achieved by the calibrated HS model for most climate zones.

Dinpashoh et al. (2019) study was aimed at determining the trend analysis of annual and monthly ET_0 time series in the NW and west of Iran. 36 stations were selected for the ET_0 estimation using FA-56-PM method, the ET_0 trend was determined by nonparametric Mann-Kendall method while Sen's estimator approach was applied for the slopes of trend lines. The results showed an upward trend of about 86% of the ET_0 time series. In contrast, a significant downward trend of less 0.7% was observed for the whole monthly ET_0 time series. August was detected to be the month with strongest positive upward trend at Kermanshah station. Khodabandeh station has the strongest negative upward trend. Monthly ET_0 slopes with steepest upward and downward trend were observed at Khodabandeh and Maragheh stations. Upward trend slopes of above 94% were observed on an annual time scale. It was concluded that for most of the stations in NW and west of Iran, ET_0 has an increasing trend.

Raoof and Mobaser (2019) applied generalized reduced gradient in determining Angstrom radiation models coefficient a_s and b_s for the estimation of ET_0 for Ardabil plain cold arid region. The results revealed that compared to the original models, the errors were reduced and the performance of the calibrated models were improved. Moreover, it is necessary to calibrate bot FAO-56-PM and Angstrom radiation model for ET_0 prediction.

Ferreira et al. (2019b) applied multivariate adaptive regression splines (MARS) and calibrated alternative equations to model ET_0 with limited climate data. The data from 2002 – 2016 were used for the study purpose from eight weather stations in Brazil. Different

scenarios of input combinations were used to developed the models including wind speed and temperature, solar radiation and temperature, relative humidity and temperature, and temperature only. The results revealed that MARS models have superior performances across all scenarios. The models created using wind speed showed less accuracy, followed by relative humidity, and finally models with solar radiation provided the best performance.

Keshtegar et al. (2019) investigated the feasibility of response surface method (RSM) and polynomial chaos expansion (PCE) models for ET_0 modeling in Antalya and Isparta stations of Mediterranean Turkish region. Multilayer perceptron neural network (MLPNN) and M5 model tree were also employed for comparison. Daily meteorological data including air temperature, relative humidity, wind speed and solar radiation were used in different input combinations. PCE with four inputs were found to be the most accurate models in the estimation of ET_0 in Antalya and Isparta, respectively.

Sanikhani et al. (2019) utilized six AI techniques including radial basis neural networks (RBNN), generalized regression neural networks (GRNN), multilayer perceptron (MLP), GEP, ANFIS with subtractive clustering (ANFIS-SC) and ANFIS with grid partitioning (ANFIS-GP) for ET_0 modeling in Isparta and Antalya stations of Turkey. The HS as well as calibrated HS (CHS) models were also applied for comparison. The results revealed a reliable and highly practical ET_0 modeling for the stations under study. The GEP and GRNN models performance was better at Antalya station, while at Isparta station, RBNN and ANFIS-SC performed better than other models. When cross-station scenario was applied, all the models under investigation with the exception of MLP performed better than HS and CHS models. Comparing the performance of original HS and CHS models, it was found that CHS performed better across both stations.

Shiri et al. (2019) used climatic data from 29 meteorological stations to evaluate calibrated version and PT and original PT models for ET_0 estimation with k-fold validation for external and local data scrutinizing procedures. Additionally, using net radiation (Rn) and vapor pressure deficit (VPD) records, external calibrated models were reevaluated. GEP models were developed using solar radiation and air temperature data. The results depicted that for estimating ET_0, the accuracy of original PT model was generally improved by both external and internal calibration of PT model especially in arid and humid regions. Non-calibrated

and locally calibrated PT models were comparable to VPD and Rn data external calibration. Non-calibrated and locally calibrated PT models were found to be inferior to GEP models. In comparison to non-calibrated PT models, GEP models were found to be of higher accuracy.

2.1.5 Reference evapotranspiration studies in Libya

Ali (1997) compared the performance of FAO-56-PM and Budyko-Zubenok methods for the estimation of ET_0 in an arid climate. The findings show that the evapotranspiration would rise from north to south owing to temperature increase resulting from an increase in CO2 content, as well as other greenhouse gasses in the atmosphere of the Earth.

Ekhmaj (2012) applied ANN with back propagation algorithm and empirical methods using sunshine hours, relative humidity and air temperature as inputs to the models for the prediction ET_0 in coastal area, western Libya. The results showed that ANN forecasts were superior to the ones obtained by Blaney and Criddle and Radiation methods. Due to its little input data, ANN is considered to be more efficient as compared with the modified Penman method. However, this application of ANN as a fitting tool should be useful in evapotranspiration modeling.

Todorovic et al. (2013) used HS and PM-temperature (PMT) methods from CLIMWAT data base which contains 577 weather stations data for ET_0 modeling across 16 Mediterranean countries (including Libya) categorized in to dry sub-humid, moist sub-humid humid, semi-arid, arid, and hyper-arid regions. Results of spatial elaboration showed high variability of estimates of ET_0 using various methods. Thus, a location-specific study is required to validate and calibrate temperature methods for estimating ET_0 using regular data sets of adequate quality. Maps showing suggestive effects on under/over estimate of ET_0 by both methods of temperature may be useful for their more precise application across different Mediterranean climates.

Benzaghta and Lawgali (2014) estimated ET_0 in Sirte Libya using three climate models including FAO-56-PM, HS and Penman. The meteorological data used include wind speed, air temperature and relative humidity. The results based on the performance statistics indicated that Penman ET_0 model, showed better performance than HS method.

El-Wahed and El-Mageed (2014) modified Blaney-Criddle equation for the estimation of ET_0 in Ghadames, Ghat and Obary stations located in arid region of Libya. The results showed that the ETo values calculated based on the modified Blaney-Criddle which applied calibrated coefficient values were better than the results of ETo values calculated based on Blaney-Criddle when compared with the ETo estimation from the PM.

2.2 Global Reference Evapotranspiration Studies

Kumar et al. (2002) investigated the performance of ANN model for the prediction of daily ET0 for two different data sets at Davis California. The meteorological data used as inputs were maximum and minimum temperatures, wind speed, maximum and minimum relative humidity, and solar radiation. Three different learning methods were considered in the study including backpropagation with momentum, backpropagation with 0.2 learning rate and backpropagation with 0.8 learning rates. Based on the obtained results, it was concluded that ANN could perform better than conventional method for ET0 estimation in Davis.

Kisi (2011) put forward a basic Wavelet Regression (WR) method for ET_0 modeling. The WR model has been improved by integrating two methods: a model of linear regression (LR) and a discrete wavelet transform (DWT). The WR models' accuracy has been compared with that of the LR models. Based on the results review, the WR models in daily ET_0 modeling were found to perform better than the empirical models.

Shiri et al. (2012) applied gene expression programming (GEP), ANFIS, HS, and Priestley-Taylor (PT) models using 5 years meteorological data including relative humidity, solar radiation, air temperature and wind speed to estimate daily ET_0 from four weather stations in northern Spain. Comparison of the results obtained from each model showed that, GEP performed better than ANFIS, HS and PT models.

Shiri et al. (2012) proposed a five-year (1999–2003) Gene Expression Programming (GEP) method to estimate daily ET_0 at four meteorological stations in Basque Country located in Northern Spain. The findings of the GEP were compared to the models Adaptive Neuro-Fuzzy Inference System (ANFIS), Hargreaves – Samani and Priestley – Taylor. The GEP was found to work better on the basis of the comparisons than the ANFIS, Hargreaves – Samani and Priestley – Taylor versions. The ANFIS model is rated second best model.

Manikumari et al. (2017) applied the neural network Boosted and Bagged (Boosted-NN, Bagged-NN) for ET_0 estimation in India. It has been demonstrated that the Boosted-NN and Bagged-NN ensemble models are better in terms of accuracy than individual NN models. Boosted-NN reduces the prediction errors among the ensemble models compared to the individual NNs and Bagged-NN.

Djaman et al. (2016) examined the application of two new Valiantzas ET_0 equations and FAO-56 Penman-Monteith equation for estimating ET_0 with minimal weather data in Burkina Faso. Climatic variables from eight weather stations used, including minimum and maximum relative humidity, wind speed, minimum and maximum air temperatures and solar radiation. The results showed that solar radiation estimates from minimum and maximum daily air temperatures provided accurate estimates of ET_0 when solar radiation data were missing. The equation of Valiantzas 1, which uses only data from relative humidity and air temperature, was found to be inappropriate and thereby not advised for use in climatic conditions of Burkina Faso. With full climate data, the Valiantzas 2 equation relative to the FAO-PM ET_0 model resulted in good ET_0 estimates under the climatic conditions of Burkina Faso; however, limited data conditions the FAO-PM ET_0 equation is recommended due to limitations of the Valiantzas 2 equation.

Kisi and Kilic (2016) assessed the potential and ability of ANNs and model tree M5 (M5Tree) in six different climate data stations in the USA to model ET_0 using California Irrigation Management Information System (CIMIS). They considered the ANN and M5Tree models better than the empirical models. The results showed the superiority in terms of performance by ANN models over the Ritchie, CIMIS Penman, Turc and Hargreaves models in two stations, whereas the general accuracy was demonstrated by M5Tree models than the corresponding empirical models in all stations.

Dou and Yang (2018) carried out investigation in to the feasibility and effectiveness of both extreme learning machine (ELM) and ANFIS for daily ET estimation with flux tower observations in the ecosystem's four main categories. The potential of the models were determine through a comparative study that was undertaken between the conventional ANN and SVM models. Conclusion drawn based on the obtained results recommended the advanced ELM and ANFIS models owing to their role as traditional methods' important

complements and due to their flexibility and robustness. In addition, there was a substantial difference between the four main types of ecosystems regarding the modeling results. The models usually performed best in the forest ecosystem, while delivering the least performance in the cropland ecosystem.

Yang et al. (2019) proposed a model using public weather forecasts and the reduced-set Penman-Monteith for short-term forecasting of daily ET_0. For the purpose of the study, different types of wind speed data were used including the default wind speed, annual average wind speed, daily average long-term wind speed, and forecasted wind speed to forecast daily ET0 up to 7 steps ahead in eight weather stations of China. The results while compared to HS model performance showed that reduced-set Penman-Monteith proposed approaches were better than the results obtained by HS model for sub-arid and arid regions whereas in sub-tropical areas the results were found to be opposite, which implies that wind speed parameter inclusion has a profound effect on ET_0 modeling for semi-arid and arid climate regions.

Zhang et al. (2019) performed a study to assess the variability of ET_0 based on daily weather data from 598 stations to statistically determine spatial clusters significance of low and high ET_0 in China using hot spot geospatial analysis over the period of 1970 – 2014. The obtained results implied that hot and cold spots statistically significant clusters exhibited between months a migration trend. The results of ordinary least square regression revealed that the meteorological variables controlling the estimation of ET_0 over China were wind speed, relative humidity and maximum temperature. The results of local geographic weighted regression showed that over China, the most influential parameters affecting ET_0 were minimum and maximum temperatures. For modeling ET_0 in China, the ordinary least square regression method was found to be less powerful than geographic weighted regression method.

Wang et al. (2019) investigated the generalization capability of random forest (RF) and gene-expression programming (GEP) algorithms to model ET_0 in 24 meteorological stations in the southwest karst region of China using different input combinations. The GEP-based and RF-based models performances were assessed by ET_0 derived from FAO-56 PM model. The obtained results depicted that the RF-based model was successful in modeling ET_0 at the

study station with incomplete and complete meteorological variables. Promising results were also obtained by GEP-based model. Despite the slight performance increment of RF-based model ET_0 models over GEP-based ET_0 models, explicit expression could be achieved by GEP approach between independent and dependent variables, which for irrigators with less computer skills would be more convenient.

Čadro et al. (2019) considered the impact of elevation, spatial distribution of ET_0 was studied by applying reliable methods. Using kriging with external drift method, spatial interpolation of ET_0 was analyzed for the period 1961 – 2016 from 108 weather stations. A 20 m spatial resolution map was developed for national spatial resolutions, regional, municipality annual temporal resolution, vegetation period and monthly mean ET_0 values. Each grid node elevation of ET_0 estimation required was extracted from Bosnia and Herzegovina digital elevation model. FAO-56-PM and HS models were also developed. Based on the obtained results, a gradual increase of mean ET_0 values is observed from central to northern and from central to southern part of the country. Moreover, the southern region has greater ET_0 than the central-east, west and north for the annual, vegetation, and monthly seasons.

Ferreira et al. (2019a) made evaluation of the accuracy of alternative equations, ANN and SVM, for estimating daily ET_0 in Brazil using temperature data only or relative humidity and measured temperature. The results showed that, even when tuned, ANN and SVM models had best accuracy than the equations that were tested. The methods analyzed (clustering and preceding days) received major efficiency gains. The ANN developed the best performance for the temperature-based models using data from two previous days as input with the clustering strategy; however, due to the similar output and greater generalization efficiency, the ANN developed with the use of data from four previous days and without clustering is recommended. The ANN established with data from four days before was the best choice for the relative humidity and temperature- based models.

Huang et al. (2019) using limited data in the humid meteorological regions of China, assessed the ability of a new machine learning algorithm using gradient boosting on decision trees with support for categorical features (i.e., CatBoost) to accurately estimate daily ET_0. Support Vector Machine (SVM) and Random Forests (RF) were the two other widely used machine learning algorithms tested for comparison. Generalized trends of the models were

almost similar to that of local models, but the former models with respect to RMSE or MAPE in relation to the latter showed less than 10% decrease. Additionally, CatBoost's running time and memory use for data processing were much less than RF and SVM's. Overall, as a tree-based algorithm, as opposed to RF, CatBoost has made major improvements in precision, reliability and computational costs. In humid regions of China, the CatBoost algorithm therefore has a significant potential for estimating ET_0, and probably also in other areas of the world having similar climatic conditions.

Saggi and Jain (2019) provided the H_2O model system for Punjab's districts of Patiala and Hoshiarpur for assessing daily ET_0. The results of four supervised learning algorithms, including Generalized Linear Model (GLM), Deep Learning-Multilayer Perceptrons (DL), Gradient Boosting Machine (GBM), and Random Forest (RF) and also to determine the overall ability to predict potential ET_0. Study of the four models was performed in H_2O context. This approach provides a new criteria for preparing, validating, evaluating and enhancing the efficiency of classification using machine-learning algorithms. The DL model's efficiency is contrasted with other state of the art models like RF, GLM, and GBM. In this regard, their research showed that the models provided greater efficiency for daily modeling of ET_0.

Carter and Liang (2019) used ground-measured ET data, high-level Moderate-Resolution Imaging Spectroradiometer (MODIS) data and Global LAnd Surface Satellite (GLASS) radiation data to provide an overview of ten machine learning methods from 184 flux tower sites for estimating daily ET. The strongest results for evergreen, grassland sites and shrub and the worst results for wetland sites were shown by comparison of findings from sites with various types of habitats. In general, efficiency has not been enhanced by training with data only of the same type of ecosystem.

Granata (2019) applied four machine learning algorithms including Random Forest, M5P Regression Tree, Support Vector Regression and Bagging and compared the variants of each model for ET_0 modeling in central Florida’s subtropical humid climate. Model 1, whose input variables were soil moisture content, net solar radiation, wind speed, sensible heat flux, mean temperature and mean relative humidity produced the best results. For the results of the models developed by using data only of mean relative humidity, mean temperature, and

net solar radiation, Model 3 has still achieved satisfactory results. Model 2, which includes addition of wind speed to the Model 3 input variables, has provided results that are totally comparable with those of Model 3 itself.

Zhang et al. (2019) performed geospatial hot spot analysis to assess statistical significance of high and low ET_0 spatial clusters in China from 1970–2014, based on the daily data obtained from 598 weather stations. General ordinary least square regression (OLS) model was used cross continental China to investigate the global controlling factors that affect ET_0. Cold and hot spots statistically relevant clusters showed a trend in migration between months. OLS analytical findings indicated that the relative humidity, maximum temperature and wind speed were the governing meteorological variables affecting ET_0 over China. Based on GWR tests, the most controlling climatic variables affecting ET_0 over China were minimum and maximum temperature. GWR has been found to be a more effective tool for modeling ET_0 in China than OLS. The findings of this study can be used to help policy makers, planners, end users and predict their decision-making, which in effect would boost China's regional water management.

Wang et al. (2019) used 24 weather stations data from southwest's karst area of China to investigate the random forest (RF) algorithm generalization ability in modeling ET_0 with different input combinations (see specific instances in missing data). The results of the RF algorithm were compared with the gene expression programming (GEP) approach. The results showed that the derived RF-based generalized ET_0 models were successfully implemented to model ET_0 with incomplete and complete climate variables. In addition, due to the climate change effect on the ET_0 the performance of the models decreased with periods. Finally, both methods have the potential to determine the value of predictors, in Guangxi the order of the effect of meteorological variables on ET_0 : air temperature, wind speed, sunshine period and relative humidity.

Čadro et al. (2019) research explored accurate methods to measure and spatially distribute ET_0, while effect of the elevation in Bosnia and Herzegovina was also considered. The results showed that for all seasons including monthly and annual vegetation periods, the north, central and west east regions have less ET_0 compared to the southern region. The

Bosnia and Herzegovina's long-term annual average ET_0 is 716 mm, of which around 78 per cent (559 mm) occur during the vegetation season.

Zhu et al. (2019) used 12-year daily weather data from 838 stations across China and calibrated the HS model by comparing the ET_0 values determined from PM model with those from the ordinary HS. The calibrated results by HS model indicated the largest estimate of ET_0 in both the temperate monsoon and subtropical monsoon climate zones situated in the south-western region of China. The HS model struggled to produce consistent results, even in optimized form, for tropical climate regions. In general, the study showed that the calibrated HS model is more reliable for most climatic zones.

Aschonitis et al. (2019) introduced a new framework for the success of ranking models with respect to ET0. The method is based on the hierarchical Ranking Performance Index (sRPI), which incorporates outcomes from various simulation scenarios of any number and type of parameters. The sRPI varies from 0 to 1 (from worst to best performance of model) depending on the relative distance of the accuracy of the models. The sRPI methodology could greatly decrease the complexity of evaluating the outcomes of models based on numerous scenarios and could identify the most concise criteria which minimize their overuse in modeling studies.

Adamala et al. (2019) for daily ET_0 estimation used generalized neural wavelet network (GWNN) models and compared to Hargreaves (HG), Turc and FAO-56-PM empirical methods. The inputs to GWNN models were from 15 different locations daily pooled climate data from 4 different agro-ecological regions in India. For evaluating the superiority of one model over another, the developed GWNN models were compared with the classical generalized wavelet regression (GWR), generalized linear regression (GLR), generalized neural artificial network (GANN), and corresponding conventional methods. The results showed that for four AERs, the GWNN models had the best performance over GANN, GWR and GLR models but GANN was found to be the second best. The test results showed that for almost all, locations the GWNN and GANN models produced outstanding performance than the GWR and GLR.

Yang et al. (2019) used wind speed and temperature data derived from public weather forecasts to predict near-future and short-term daily ET_0 using empirical temperature-based

and Reduced-set Penman-Monteith (RPM) models forecasting. By comparing the performance of RPM approaches with one of the temperature-based models that is most widely used, the Hargreaves-Samani (HS), it was deduced that for sub-arid and arid regions, RPM was found to be better than the HS model, while for subtropical regions, the results happened to be opposite. This implies that wind speed parameter inclusion would positively affect ET_0 prediction for semi-arid and arid regions.

Djaman et al. (2019) under limited climatic data examined 34 simple ET_0 equations and Penman-Monteith ETo equation for modeling ET_0 in New Mexico. Data from five meteorological stations were used between 2009 – 2017 under dry and semiarid climates. The results implied that engineers, university researchers, producers and irrigation managers could use the alternative equations to improve management of water resources across the New Mexico particularly in arid dry and semiarid zone, as well as other semiarid areas where water scarcity is the most alarming factor to fiber and food production.

Raoof and Mobaser (2019) examined the capacity of the Angstrom's Radiation Model Locally Adjusted Coefficient in an Arid-Cold Area for estimating ET_0. Locally calibrated models yielded better reliability in the estimation of Rs and ET_0 values beyond the original ones and it is necessary to calibrate both the PM FAO equation and Angstrom radiation model for every region.

In their original and optimized versions, Ferreira et al. (2019b) made comparative analysis of alternative equations and the multivariate adaptive regression splines (MARS) to estimate daily ET_0 with limited amount of meteorological data. Eight Brazilian weather stations daily data were used for the period 2002 to 2016. The best results were achieved by models developed with solar radiation as input, followed by those using relative humidity and, eventually, wind velocity. The models based on air temperature as the sole input variable performed the worst.

Keshtegar et al. (2019) performed a study to assess the feasibility of response surface method (RSM) and polynomial chaos expansion (PCE) models for the simulation of ET_0. The simulation results of the proposed models were verified against the methods of multilayer perceptron neural network (MLPNN) and M5 model tree. The accuracy of the modeling was improved by increasing the number of inputs. Wind speed inclusion in to the modelling

inputs greatly improved their ET_0 modeling accuracy. The PCE was found to be the most reliable model for estimating the ET_0 per day.

Sanikhani et al. (2019) study investigated the applicability of radial-based neural networks (RBNN), generalized neural regression networks (GRNN), multilayer perceptron (MLP), gene expression programming (GEP) and subtractive clustering and grid partitioning integrated adaptive neuro-fuzzy inference systems (ANFIS-SC and ANFIS-GP), for ET_0 estimation in Antalya and Isparta stations, Turkey. The calibrated and ordinary Hargreaves – Samani version (CHS and HS) of equation, verified the established AI models. Except for the MLP model, when implemented in a cross-station situation, all the other investigated models offered a better output accuracy compared to the empirical HS and CHS models. A cross-station scenario test implies the estimation of any station's ET_0 using nearby station input data. In all cases, the performance of the CHS models in the ET_0 modeling was higher than that of the original HS.

Wu et al. (2019) study applied five-fold cross-validation approach to examine the performance of extreme learning machine (ELM) models optimized by four bio-inspired algorithm including flower pollination algorithm (ELM-FPA), ant colony optimization (ELM-ACO), cuckoo search algorithm (ELM-CSA) and genetic algorithm (ELM-GA) for daily ET_0 prediction across China. The results recommended the application of bio-inspired optimization algorithms, more specifically the CSA and FPA algorithms, for boosting the accuracy and reliability of the conventional ELM model in the contrasting climates of China for daily estimation of ET_0.

CHAPTER 3

MATERIALS AND METHODS

3.1 Study Location and Data

Fourteen stations were considered in this study, which involves prediction and multi-step ahead ET_0 modeling in several climatological regions across 5 countries including Turkey, NC, Iraq, Iran and Libya. The details of the locations of the study are thus provided based on the countries where the stations are located.

3.1.1 Turkey stations

Turkey is a transcontinental country located predominantly in Asia (see Figure 3.1), certain area of its land enters some portion on the Balkan Peninsula which is located in the southeast Europe. Sea of Marmara separated Anatolia with Europe's East Thrace. Turkey is bordered by Georgia to its northeast, Bulgaria and Greece to its northwest, Iran, Azerbaijan exclave of Nakhchivan and Armenia to the east, Syria and Iraq to the south. Turkish geographical area is covered between latitudes 360 and 420 N and longitudes 260 and 450 E. Due to large inland plateau surrounded by rough topographical terrain of Anatolia Peninsula, variation of temperature in the region is high. The maximum temperature recorded at Sanliurfa station is +46.8 ^{0}C in the southeast, while minimum temperature at Agri station recorded as -42.8 ^{0}C in the northeast. Pan evaporation varies annually between 435 and 2,800 mm/year. Turkish annual average precipitation is 643 mm/year (Citakoglu et al., 2014). Using seasonality index and total seasonal rainfall percentage ratio to the annual amount, seven climatic regions in Turkey were formed including Continental Eastern Anatolia (CEAN), Continental Central Anatolia (CCAN), Mediterranean to Central Anatolia Transition (MEDT), Continental Mediterranean (CMED), Mediterranean (MED), Marmara (Mediterranean to Black Sea) Transition (MRT) and Black sea (BLS) (Turkes, 1996). MED region is the geographical location of Adana station; it tends to have cool and heavy rainy winter and a hot dry summer due to its semi-humid and humid subtropical nature. Ankara station is a semi-arid steppe climate located in Continental Central Anatolia (CCAN); it possesses cool rainy spring, cold rainy winter and warm and light rainy summer. Izmir and Adana stations

share semi-humid and humid subtropical owing to their location in MED region. Samsun station is a temperate climate from the Black Sea region (BLS); it attains its peak of uniformly rainy climate in autumn. The Turkey stations' coordinate locations and data statistics are given in Appendix 1a.

As demonstrated in Appendix 1a, the maximum daily average values for monthly P_R are around twice in Izmir and Adana than Samsun and Ankara. This is due to the presence of MED region, which has partly semi-humid and humid climates for Adana and Izmir stations, Ankara is located in semi-arid climate in the CCAN region, while Samsun climate is temperate located in the BLS region. However, a bit higher precipitation can be seen in Samsun than in Ankara, because increase in aridity index decreases precipitation of a region. Meanwhile, Table 3.1 also depicts that owing to the moderate nature of BLS climate, the values of T_{min} and T_{max} for Samsun station are found to be within the ranges of other stations under investigation. Table 3.2 gives independent and dependent correlation matrix between the study variables.

3.1.2 North Cyprus (NC) stations

Cyprus is the third largest island in the East Mediterranean and its climate is generally Mediterranean, with hot dry summers and mild wet winters, the occurrence of rainfall mostly happens from November to March. As a whole, the Island annual average precipitation is 500 mm. The highest point of the Trodos Mountain has an average of 1200mm rainfall, while at the central plain it is around 300-400mm (Elkiran and Ergil, 2006). Average temperature in NC rises higher in July and falls between 5 to 15^{0}C in January. However, according to class A pan reading, annual evaporation reaches up to 2200mm/year. As reported by Elkiran and Ongul (2009), latest studies revealed that water returns to the atmosphere of about 80% of rainfall through evapotranspiration. This study utilized data from four stations including Kyrenia, Nicosia, Famagusta and Morphou. The Famagusta climate is classified as temperate and warm. The average temperature in Famagusta is 19.3 ^{0}C, with an average annual rainfall of 407 mm. Kyrenia has an average July temperature of 29 ^{0}C (hottest month), and January temperature of 10 ^{0}C (coldest month). In hilly areas, average rainfall varies from 500 mm to 750 mm, rarely falling in the summer and specifically in winter. Kyrenia Mountains is experiencing the highest rainfall rate due to the altitude, as it ranges from 750

mm to 1110 mm. Morphou's climate is known as being a local steppe climate. Morphou receives little rainfall year-round with annual precipitation drops of around 363 mm and an average annual temperature of 18.5 ^{0}C. Nicosia is an inland city as such the Mediterranean Sea's influence compared to the other coastal cities is less in Nicosia. Colder winters and hotter summers are therefore felt in Nicosia than in the other coastal regions, and the difference between minimum night and maximum daytime temperatures is therefore greater. The difference in daytime temperature between Nicosia and other cities along the coastline is around 4 ^{0}C to 7 ^{0}C for July and August (the hottest months). In January and February (the coldest months), the difference in daytime temperature in Nicosia is 2 ^{0}C to 3 ^{0}C lower than on the coast. Figure 3.1 shows northern Cyprus research stations, whereas Appendix 1b shows coordinates, locations and data statistics of the study stations in North Cyprus.

Low, medium and high temperatures can be seen as shown by Appendix 1b, with relatively dry hot summer and mild or cool winter being a Mediterranean climate. The pan evaporation minimum values are 1.1 mm/day, 0.9 mm/day, 1.11 mm/day and 1.10 mm/day for Famagusta, Kyrenia, Morphou and Nicosia stations, respectively, while for Nicosia its maximum value is as high as 12.6 mm/day. Relative values for humidity differ broadly across all stations. Temperature at dew points fluctuates from peak 22.48 ^{0}C to lowest 2.86 ^{0}C to.

3.1.3 Iraq stations

Iraq is historically called Mesopotamia, located in western Asia (Figure 3.1). Iraq population is about 37.2 million in 2016 and it has an area of land that covers 437,072 km^{2}. Iraq is bordered by 6 countries including Jordan, Saudi Arabia, Turkey, Kuwait, Syria and Iran. The longitudes and latitudes of Iraq are between 38°45' and 48°45' E and 29°5' and 37°22' N (Tahsin, 2018). Erbil is the capital city of Kurdistan province, in northern Iraq. Erbil falls within a continental and semi-arid climate. It is experiencing cold, rainy winters and dry, warm summers (Rasul et al., 2015). Salahaddin is situated in the Kurdistan region, in the far north of Iraq. Salahaddin's climate is semi-arid, according to a report by Sarlak and Agha, (2018). Appendix 1c reveals details of the study stations in Iraq, their location and their coordinates.

With their susceptibility to semi-arid climate conditions, the stations Erbil and Salahaddin have nearly identical statistics as shown in Appendix 1c. Salahaddin is more humid than Erbil, which results in higher relative humidity. The T_{max} at station in Salahaddin is also lower which has a value up to around 0 ^{0}C as can be seen and as high as 39.9 0C.

3.1.4 Iran stations

Tabriz City is located between latitudes 38^{0}08`N and 46$^0$15`E in northwestern Iran. It is situated at an altitude of 1350 m, at the junction of Aji and Quri Rivers. Tabriz has an annual rainfall of about 380 mm, and enjoys good and moderate spring, semi-hot and dry summer climate. The average annual temperature is around 13 ^{0}C, with possible rate of evapotranspiration estimated at around 1733 mm/year. Urmia is a city situated at latitude 37^{0}34`N and longitude 44$^0$58`E in northwestern Iran. Maximum freezing days in Urmia are about 120 days, with very low summer precipitation and a heavy rise in downfall for late autumn and winter. The station has annual rainfall of about 300 mm/year (Nourani and Fard, 2016). Figure 3.1 shows the locations of Tabriz and Urmia stations in Iran and Appendix 1d shows the descriptive statistics of the data from Tabriz and Urmia stations.

Higher altitude means quicker transmission of solar irradiance to the earth's surface, causing the temperature to rise and therefore the evapotranspiration increases. For Urmia station, therefore, both the maximum pan evaporation and the maximum temperature are lower (10,96 mm/day and 33.90 ^{0}C) than Tabriz (15.33 mm/day and 35.15 ^{0}C). However, Urmia Lake's presence increases the station's evaporation bodies and thus has provided more precipitation in the maximum and average amount (3.74 mm / day and 0.67 mm / day) than Tabriz (2.91 mm / day and 0.59 mm / day).

3.1.5 Libya stations

Sabha is an inland station situated at 14^{0}43`E longitude and 27$^0$04`N latitude in the southern part of Libya. It contains dry arid climate with 52 percent of an annual average relative humidity, an annual average temperature of 26.5 ^{0}C and precipitation of an annual average not exceeding 100 mm/year. Tripoli is the capital of Libya, a coastal city located in the Mediterranean region. It is a semi-arid climate with hot dry summers and rainy winters. The annual rainfall ranges from 140 to 550 mm/year, an average air temperature of around 14.2

to 21.6 0C and an average relative humidity of about 70% (Ageena, 2013). The two study stations for Libya are given in Figure 3.1 while the descriptive statistics of the used data from the stations are shown in Appendix 1e.

Specific characteristics of the meteorological variables are observed as seen by the data descriptive statistics displayed by Appendix 1e, being a distinct climate stations. Sabha station has higher evaporation, less precipitation and higher temperature (24.70 mm/day, 1.42 mm/day and 41.95 ^{0}C) in comparison to Tripoli station, which has evaporation 14.10 mm/day, precipitation 4.79 mm/day, and temperature 36.21 ^{0}C because of the severe weather conditions. Figure 3.1 shows the regions and stations used in this study.

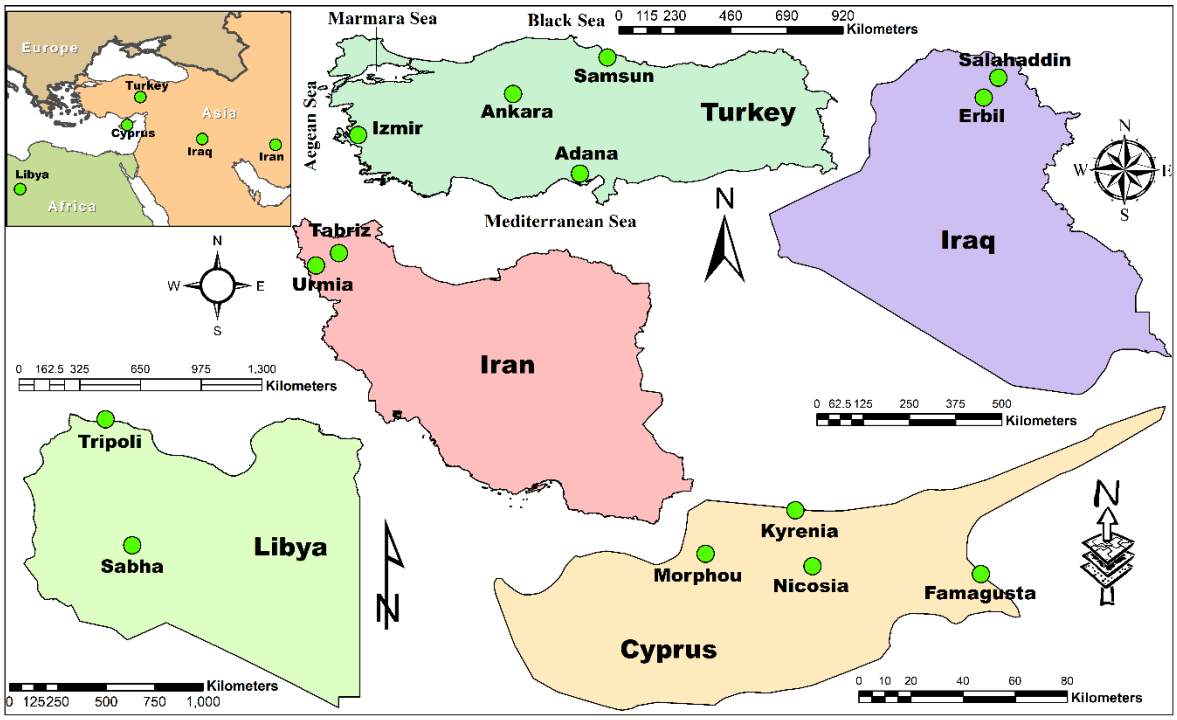

Figure 3.1: Location of study regions and stations

The study data were collected from meteorological organizations of the respective study countries including Kurdistan Meteorological Organization, North Cyprus Meteorological Organization, Turkish Meteorological Organization (TMO), Libya National Meteorological Centre and Iran Meteorological Organization for Iraq, Cyprus, Turkey, Libya and Iran stations, respectively. A stratified *k*-fold cross-validation approach was employed for model validation. In the *k*-fold cross-validation method, *k* number of subsamples of equal size are formed by randomly dividing the original sample of the dataset. *k*-1 subsamples are used as

training data of the *k*-subsamples that are formed initially, while the single subsample left behind is used as validation data to test the model. The process of the cross-validation is then repeated in *k* number of times, with each of the model been validated once by the *k*-subsample not used in training. The result of single estimation is then provided by combining or otherwise taken an averaging of the *k*-fold results. The *k*-fold cross-validation approach has the advantage that all observations are used both for training and validation and each observation is used only once for validation (Sharma et al., 2018).

In this study, as shown in Figure 3.2, the 14 stations data samples were partitioned into k = 4 random subsamples. By randomly dividing total sample size by k (4) folds as seen in Table 11, each subsample was obtained. The $k - 1$ (4 – 1) random subsamples were used to train the model while the remaining single subsample was drafted for testing the model. The process was repeated 4 times to equal the number of *k*-fold subsamples for different $k - 1$ training subsamples and for different single test subsamples. The *4*-fold cross-validation approach adopted in this study is schematically illustrated in Figure 3.2 while datasets duration and number of observations are shown in Table 3.11.

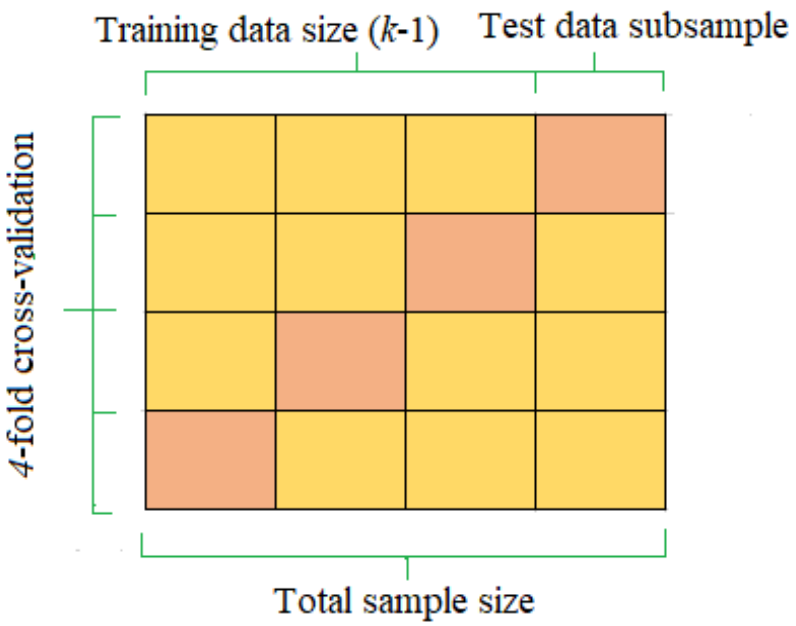

Figure 3.2: Schematic illustration of the k-fold cross-validation applied

Table 3. 1: Data duration and validation method applied across the study stations

Country	Station	Data Duration	No. of Years	No. of Observations	*k*-folds Partitioning	No. of Observations for each Subsample
Turkey	Adana	1988 - 2018	31	371	4	93
	Ankara	1988 - 2016	29	348	4	87
	Izmir	1987 - 2017	31	372	4	93
	Samsun	1988 - 2017	31	372	4	93
Cyprus	Famagusta	1995 - 2017	23	276	4	69
	Kyrenia	1995 - 2017	23	276	4	69
	Morphou	1995 - 2017	23	276	4	69
	Nicosia	1995 - 2017	23	276	4	69
Iraq	Erbil	1992 - 2011	20	240	4	60
	Salahaddin	1993 - 2011	20	240	4	60
Iran	Tabriz	1992 - 2018	27	317	4	79
	Urmia	1992 - 2015	24	282	4	70
Libya	Sabha	1995 - 2010	16	192	4	48
	Tripoli	1995 - 2010	16	192	4	48

Usually, data are normalized in AI-based modeling to eliminate dimensions of variables and to ensure that equal attention is received by all variables during model training (Nourani et al., 2012). Two primary benefits of data normalization are gained in the application of the AI-based predictions. The first is to prevent overshadowing of smaller numerical ranges by the attributes of larger numeric ranges. The second benefit is that computational problems are minimized while calculation. The data were scaled within 0 and 1 in this study.

$$ET_{0n} = \frac{ET_{0i} - ET_{0min}}{ET_{0max} - ET_{0min}} \tag{3.1}$$

Where ET_{0n} is the observed normalized ET_0 value, ET_{0i} is the ith observed ET_0 value, ET_{0min} and ET_{0max} are the maximum and minimum observed ET_0 values, respectively.

For efficiency and performance analysis of the models, several globally accepted statistical indicators can be used including Mean Absolute Error (MAE) (Yaseen et al., 2018), Correlation Coefficient (R) (Fotovatikhah et al., 2018), Root Mean Square Error (RMSE) (Moazenzadeh et al., 2018), Nash-Sutcliffe efficiency criterion or Determination Coefficient (DC) (Ghorbani et al., 2018). Nevertheless, according to Legates and McCabe (1999),

RMSE and DC are sufficient for any hydro-climatic modeling and are therefore employed in this study as the models performance evaluation criteria. The Equations are given as:

$$DC = 1 - \frac{\sum_{i=1}^{N}(R_i - \hat{R}_i)^2}{\sum_{i=1}^{N}(R_i - \bar{R})^2} \quad (3.2)$$

$$RMSE = \sqrt{\frac{\sum_{i=1}^{N}(R_i - \hat{R}_i)^2}{N}} \quad (3.3)$$

Where, $\hat{R}_i$ $\bar{R}$, R_i and N are respectively the predicted values, observed values average, observed data and number of observations.

RMSE tests the precision of the forecasted values, which gives positive value by squaring the error. As difference between observations and forecasts becomes increasingly high, the RMSE increases from zero to large positive values for perfect forecasts. Understandably, DC ($-\infty<DC\leq1$) with high value up to 1 and RMSE ($0\geq RMSE<\infty$) value close to 0 imply high model efficiency.

3.2 Proposed Methodology for Phase 1 Study

Sensitivity analysis was applied during the first phase of the study to determine the most suitable input parameters for the models. Black box models including FFNN, ANFIS, SVR, and MLR were then separately developed, trained, and validated for modeling the ET_0. To estimate the ET_0, two radiation-based models including MK and RT and two temperature-based models including HS and MHS were also used. The proposed ensemble approaches were implemented for AI based and empirical models using the outputs of the single models through strategies 1 and 2.

(i) Strategy 1

In the first ensemble strategy, the outputs of the black box models including $ET_{FFNN}, ET_{ANFIS}, ET_{SVR}$ and ET_{MLR} are used as independent variables, which ET_0 depends on, given as:

$$ET_0 = f(ET_{FFNN}, ET_{ANFIS}, ET_{SVR}, ET_{MLR}) \quad (3.4)$$

(ii) Strategy 2

In the second ensemble strategy, the ET_0 is used as a function of the outputs of the four empirical models which are $ET_{HS}, ET_{MHS}, ET_{MK}$ and ET_{RT}:

$$ET_0 = f(ET_{HS}, ET_{MHS}, ET_{MK}, ET_{RT}) \quad (3.5)$$

The fundamental notion behind ensemble simulation is attributed to the following circumstances (Sharghi et al., 2018): (i) In practice, it is often difficult to decide whether one particular model or method is better than others or whether the underlying process under analysis for a time series is created by a linear or non-linear phenomenon. Hence, choosing the right approach or methodology for a particular problem is a challenging task before predictors. Applying the ensemble strategy will thus deal with the question of selecting correct model. (ii) Time series can include both non-linear and linear characteristics in a real world process. In such a case, for the prediction of the time series, neither AI nor MLR could be adequate as errors of a linear trend might be exacerbated by AI models and non-linear relationship could not be handled by MLR model. Thus, the dynamic underlying nature of the data could be described more accurately by integrating the AI and MLR models. (iii) There is no unique or specific approach that can thoroughly examine processes as previous studies have shown (such as Zhang, 2003 and Sharghi et al., 2018). Complex nature of the real world problem could be largely the cause, whereby a distinct process could not be detected by a specific model. The proposed methodology of the first phase of the study is shown in Figure 3.3. It is valuable to mention that for sufficient comparing of ET_0 computed over several regions (from five countries including Iraq, Libya Turkey, Iran and NC), the proposed methodology is applied to all the 14 data stations. In Figure 3.3, U_{min}, T_{max}, R_H, T_{mean}, T_D, U_{mean}, S_P, P_R, T_{min}, U_{max}, R_S and E_P are defined in Tables 3.1, 3.3, 3.5, 3.7 and 3.9; ET_{ANFIS}, ET_{FFNN}, ET_{SVR}, ET_{MLR}, $ET_{MK,}$ ET_{HS}, ET_{RT} and ET_{MHS} given in Equations 3.3 and 3.4 represent computed ET_0 by ANFIS, FFNN, SVR, MLR, MK, HS, RT, and MHS models, respectively; whereas the ensemble ET_0 including $ET_{NE,}$ ET_{SA} and ET_{WA} are obtained from NE, SA and WA techniques.

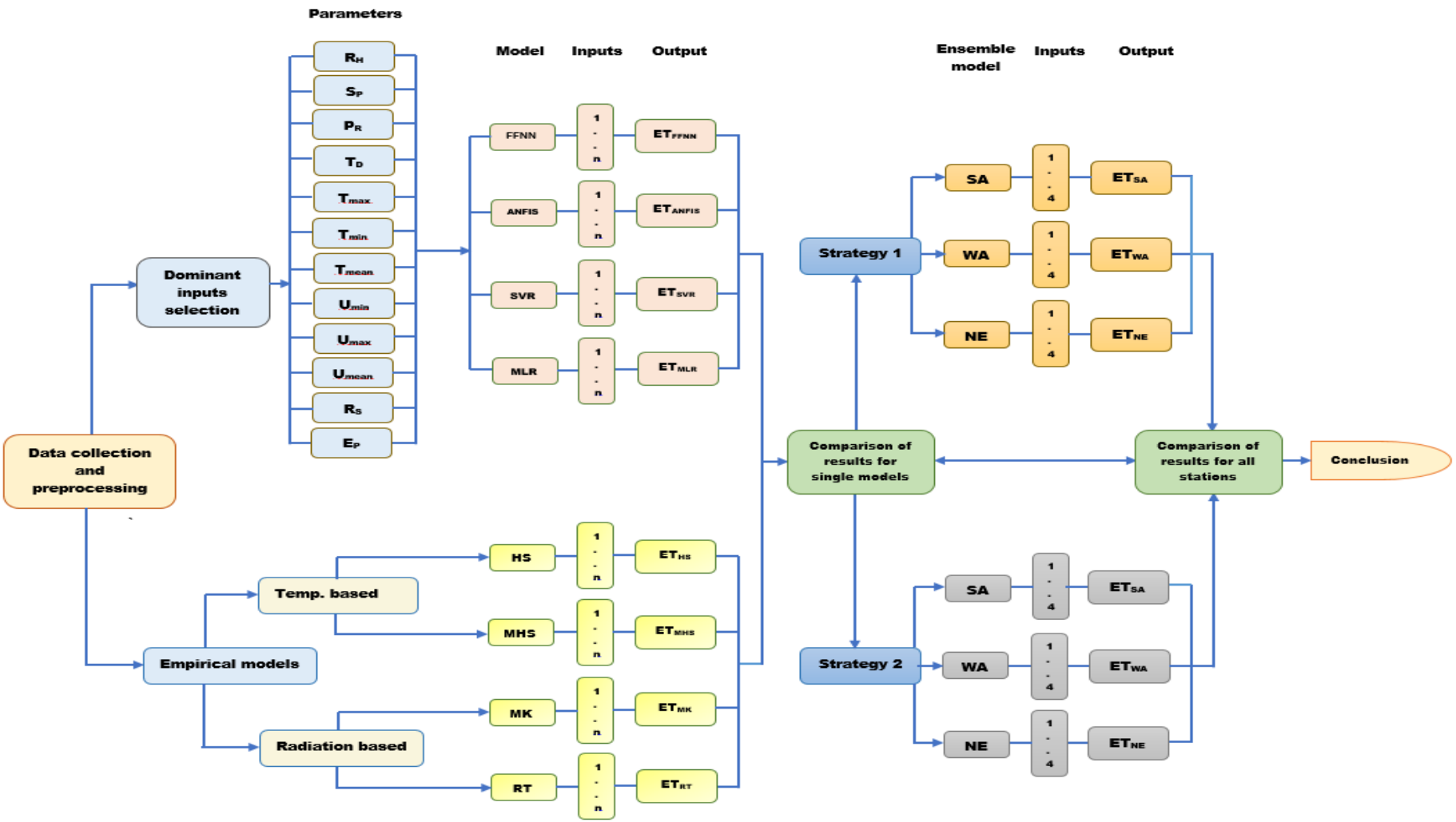

Figure 3.3: Schematic diagram of the phase 1 proposed methodology applied for all stations

3.3 Proposed Methodology for Phase 2 Study

The second phase of this study assessed the feasibility of applying the concept of ensemble learning for AI based and MLR models' performance improvement for single and multi-step ahead predictions of ET_0. Initially, one, two and three-step ahead models were developed by three AI based and MLR techniques. Finally, the proposed ensemble modeling was carried out using the outputs produced by the single models.

The fundamental notion behind model ensemble is owing to the following: (i) Most of the times, in practice, it is difficult to determine for a time series under study if the underlying process is induced by a nonlinear or linear circumstance or whether the application of one model or a particular method yields better results than others. Consequently, selection of the best technique or choosing the best befitting method is a difficult task before the predictors for a unique issue. Therefore, the problem arises while selecting the appropriate model could be handled by the application of ensemble learning (Sharghi et al., 2018). (ii) Both linear and non-linear characteristics may be involved in time series predictions for a real world process. Neither MLR nor AI could be satisfactory in such situation for the time series prediction as non-linear relationship cannot be handled by MLR model, whereas AI models could magnify errors of a linear pattern. Thus, the data complex stochastic nature could be grabbed more appropriately by combination of MLR and AI models. (iii) As revealed by previous studies (such as Sharghi et al., 2018; Nourani et al., 2019a), there is no specific method or a unique model that can completely examine a process. The complex and uncertain nature of real world problem could be largely the cause whereby distinct patterns of the process might not be detected accurately by a unique model. The proposed study methodology is shown in Figure 3.4. To have a proper comparison of the computed ET_0 over the study regions, same methodology (given in Figure 3.4) was used for all stations (10 stations from Turkey, north Cyprus and Iraq). The next sub-sections present details of the used tools and components of the models.

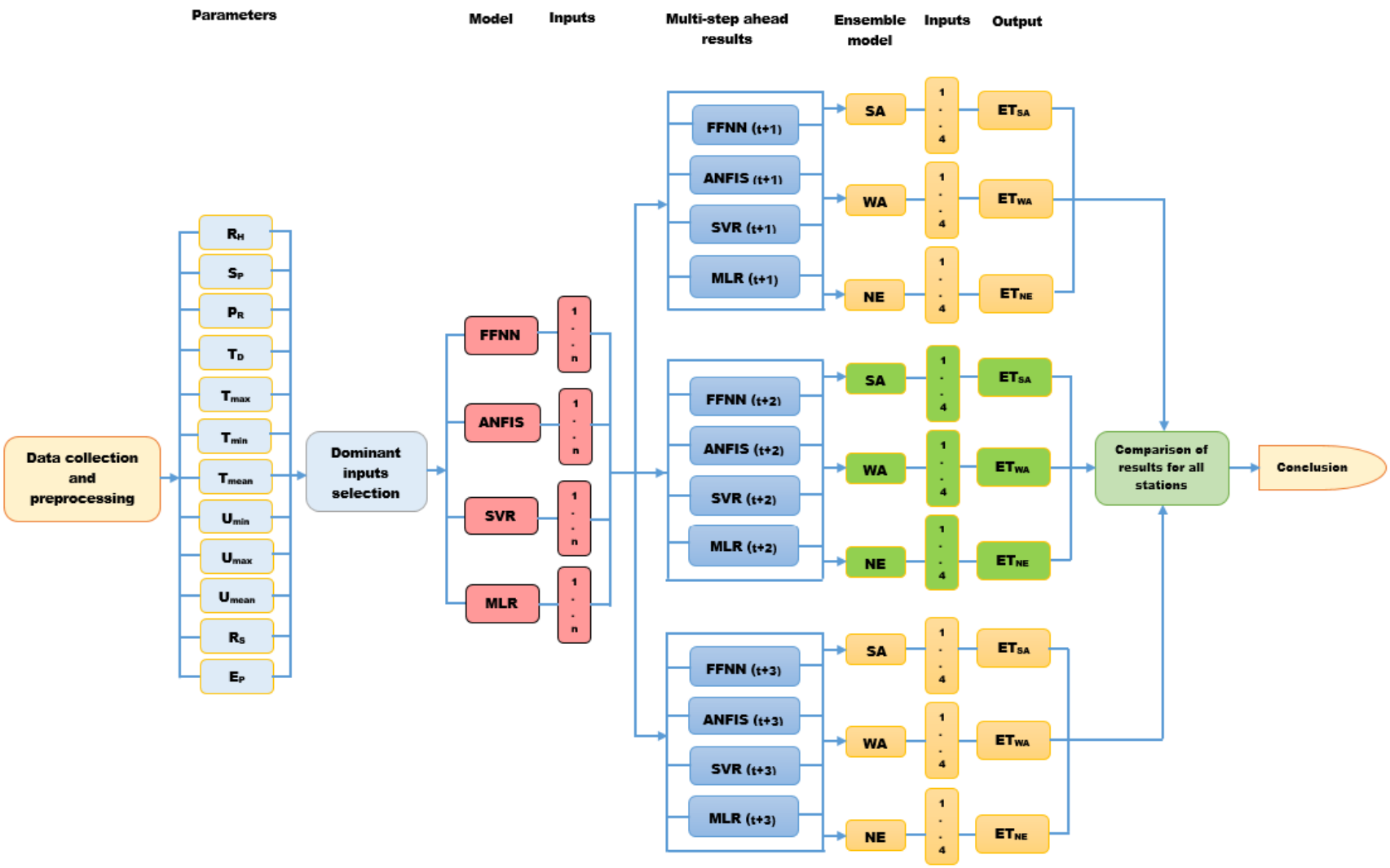

Figure 3.4: Proposed phase 2 study methodology applied for all stations

3.4 Artificial Neural Network (ANN)

ANN provides a compelling approach for handling enormous amounts of noisy, nonlinear, and dynamic data, specifically when the underlying physical relationships are not fully understood. This makes ANN an ideal approach for data-driven modeling of a time series (Nourani et al., 2015).

ANN constitutes a number of simple interconnected processing elements known as nodes or neurons with fascinating peculiarity of information processing characteristics, such as noise tolerance, nonlinearity, generalization capability, parallelism, and learning. A FFNN with Back Propagation (BP) training algorithm are the most common methods used by neural networks to solve several engineering issues (Hornik et al., 1989). The FFNN technique is composed of parallel processing element layers known as neuron, and every layer is being connected fully by weights to the proceeding layer. Generally, those ANNs learning are accomplished by BP algorithm (Hornik et al., 1989).

The Levenberg-Marquardt (LM) training algorithm among the various training methods, was selected in this research, taking into account its ability to converge quickly as described by Sahoo et al. (2005). In addition, the transfer function of Tangent Sigmoid (Tansig) was implemented for both the hidden and the output layers. Similarly, the hidden layer nodes and epoch number for model calibration were calculated by trial and error method. Figure 3.5 shows the three layered FFNN structure.

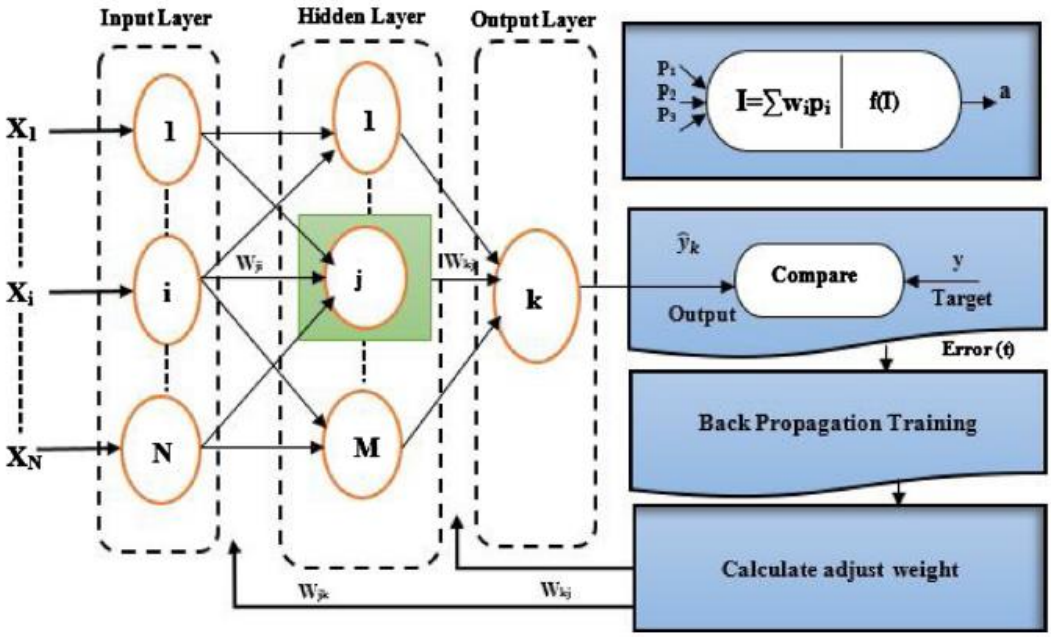

Figure 3.5: A three layered FFNN (Nourani and Fard, 2012)

3.5 Adaptive Neuro-fuzzy Inference System (ANFIS)

Neuro-fuzzy simulation refers to methods of applying various learning algorithms in the neural network literature or the fuzzy inference (FIS) method to fuzzy modeling (Akrami et al., 2014). A distinctive approach to neurofuzzy development is ANFIS, first proposed by Jang (1993) and using NN's learning algorithm.

Every fuzzy system consists of three main components; fuzzy database, fuzzifier, and defuzzifier (Nourani et al., 2015; Nourani and Komasi, 2013). The two principal parts of the fuzzy database are the fuzzy rule base and the inference engine. Fuzzy rule base contains rules related to fuzzy prepositions, as demonstrated by Jang et al., (1997). Subsequently, operation analysis was implemented by Fuzzy inference. Many fuzzy inference engines can be used to achieve this purpose, of which Mamdani and Sugeno are the two most popular.

As a universal approximator, ANFIS will compact the set of precision for any particular continuous function to any degree. ANFIS is functionally identical to FIS according to Jang et al., (1997). Precisely, the ANFIS system's value here is fundamentally identical to the Sugeno fuzzy model of the first order (Jang et al. 1997). The general structure of the ANFIS is given in Figure 3.6.As shown in Figure 3.6, ANFIS is known to have inputs of x and y

and f outputs . According to Aqil et al. (2007), the first-order Sugeno fuzzy model has an ideal set of rules that are two fuzzy if-then rules:

Rule (1): If μ(x) is A_1 and μ(y) is B_1; the $f_1 = p_1x + q_1y + r_1$ (3.6)

Rule (2): If μ(x) is A_2 and μ(y) is B_2; the $f_2 = p_2x + q_2y + r_2$ (3.7)

In which, A_1 and A_2 are x inputs MFs, B_1 and B_2 are y inputs MFs, respectively. While the function parameters the of the output are p_1, q_1, r_1, and p_2, q_2, r_2. The functions of each ANFIS layer are as follows:

Layer 1: Each node in this layer produced membership grades of an input variable. The output of the ith node in k layer is represented as Q_i^k. Assuming as the membership function (MF) of a generalized bell function (gbellmf), the output (Q_i^1) can be obtain from Jang and Sun (1995) as:

$$Q_i^1 = \mu_{A_i}(x) = \frac{1}{1+((x-c_i)/a_i))^{2b_i}} \quad (3.8)$$

Where a_i, b_i, c_i are adaptable variables called premise parameters.

Layer 2: In this layer, the incoming signals are multiplied by each node:

$$Q_i^2 = w_i = \mu_{A_i}(x).\mu_{B_i}(y) \; i = 1, 2, \ldots \quad (3.9)$$

Layer 3: In this layer, the ith node calculated the normalized firing strength:

$$Q_i^3 = \overline{w}_i = \frac{w_i}{w_1 + w_2} \qquad i = 1, 2 \quad (3.10)$$

Layer 4: In this layer, node i calculated the contribution given by the ith rule to the model output:

$$Q_i^4 = \overline{w}_i(p_ix + p_iy + r_i) = \overline{w}_i f_i \quad (3.11)$$

Where, p_1, q_1, r_1 is the perimeter set, $\overline{w}_i$ is the output of layer 3.

Layer 5: In this layer, single node calculated the overall output of the ANFIS (Jang and Sun, 1995).

$$Q_i^5 = \sum_i \overline{w}_i f_i = \frac{\sum_i w_i f_i}{\sum_i w_i} \quad (3.12)$$

The learning algorithm for ANFIS is a hybrid algorithm that combines the least squares with the methods of gradient descent (Aqil et al., 2007). The parameters of optimization are a_i, b_i, c_i which are the parameters of the proposition, while, p_i, q_i, r_i are the corresponding parameters. Through the hybrid learning approach to forward pass, the node output goes forward until layer (4), and the resulting parameter has been defined by the least-square technique. The error signals propagate backwards, and the premise parameters are updated by the gradient descent in the backward pass (Nourani and Komasi, 2013).

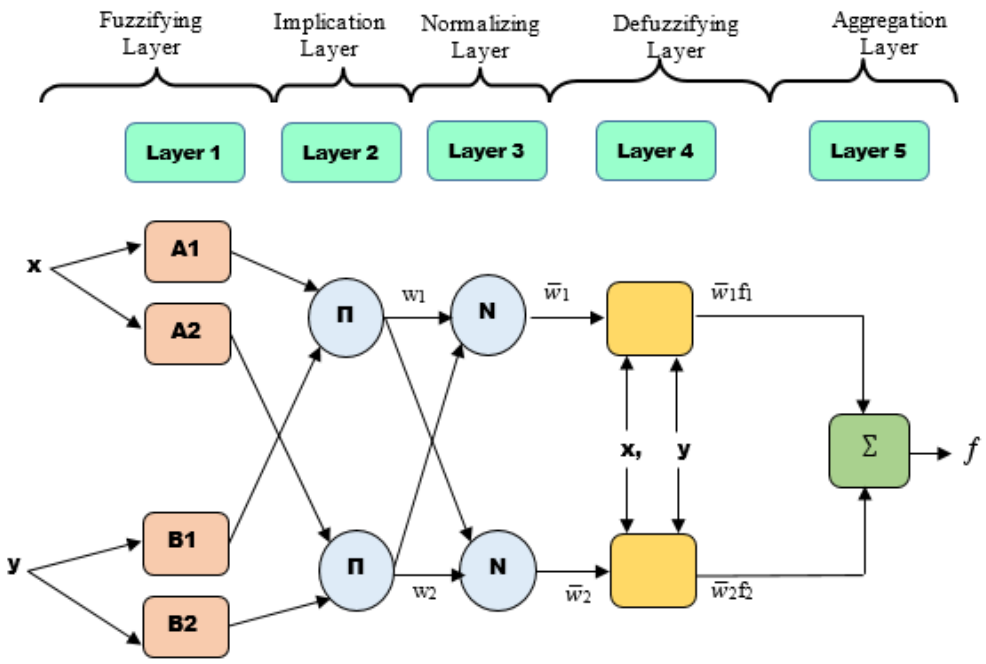

Figure 3.6: General structure of ANFIS (Nourani et al., 2017)

3.6 Support Vector Regression (SVR)

SVR is built based on the principle of SVM and is used in non-linear regression problems. Unlike many other black box prediction techniques, SVM-based techniques such as SVR find operational risk to be minimized as the objective function instead of reducing the error between the observed and the calculated values. In SVR, the data is equipped first with a linear regression, and then the outputs go through a non-linear kernel to capture the data's non-linear pattern. For a given training dataset $\{(x_i, d_i)\}_i^N$ (d_i is the actual value, N is the

data patterns' total number and x_i is the input vector), the SVR function is generally given as (Wang et al., 2013):

$$y = f(x) = w\varphi(x_i) + b \tag{3.13}$$

where $\varphi(x_i)$ denotes function spaces, mapped non-linearly from x input vector (Vapnik, 1998). By assigning positive values for the minimization of the objective function and for the slack parameters of ξ and ξ^*, regression parameters of b and w could possibly be determined (Wang et al., 2013).

Minimize: $\frac{1}{2} \| w \|^2 + C[\sum_i^N (\xi_i + \xi_i^*)]$

Subject to: $\begin{cases} w_i\varphi(x_i) + b_i - d_i \leq \varepsilon + \xi_i^* \\ d_i - w_i\varphi(x_i) + b_i \leq \varepsilon + \xi_i^* \\ \xi_i, \xi_i^* \end{cases}$ i=1,2,…,N

where $\frac{1}{2} \| w \|^2$ is the norm weights vector and C is denotes to constant of regularization which determines the tradeoff between the regularized term and the empirical error . ε is called the tube size and is equal to the precision of approximation imposed inside the training data points. With the concept of Lagrange multipliers α_i and α_i^*, the stated optimization problem can be modified to the dual quadratic optimization problem. After finding solution to the quadratic optimization problem, the vector w can be computed as (Wang et al., 2013):

$$w^* = \sum_{i=1}^{N} (\alpha_i - \alpha_i^*)\varphi(x_i) \tag{3.14}$$

So, the SVR in its final form can be described as (Wang et al., 2013):

$$f(x, \alpha_i, \alpha_i^*) = \sum_{i=1}^{N} (\alpha_i - \alpha_i^*) K(x, x_i) + b \tag{3.15}$$

$k(x_i, x_j)$ performed the feature space non-linear mapping and is called the kernel function whereas b is bias term. One commonly used kernel function is the Gaussian Radial Basis Function (RBF) kernel as (Haghiabi et al., 2016):

$$k(x_1, x_2) = \exp(-\gamma \|x_1 - x_2\|^2) \tag{3.16}$$

where, γ denotes the kernel parameter. The SVM general structure is represented in Figure 3.7.

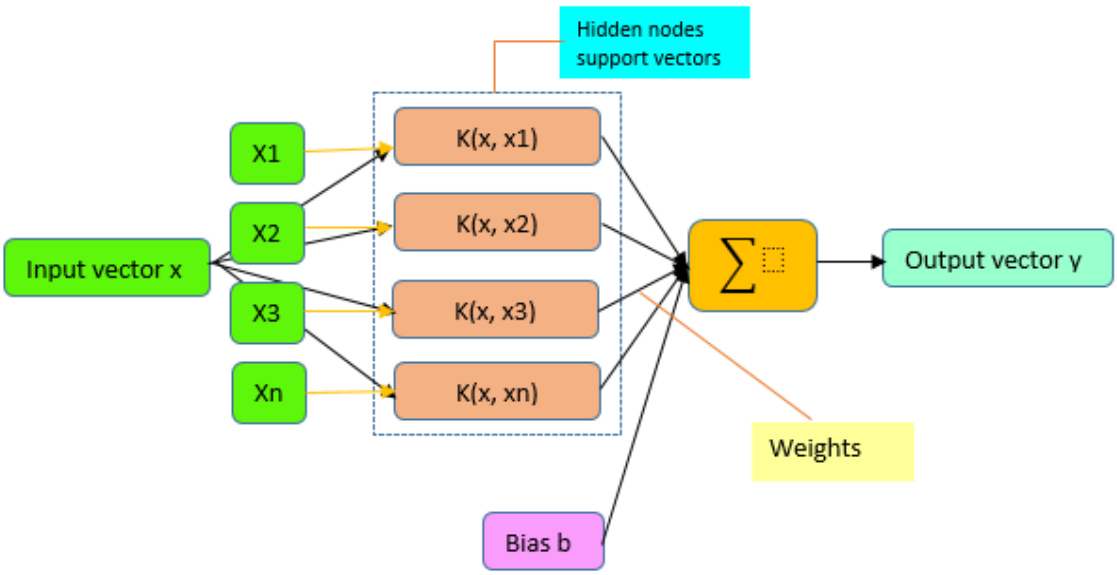

Figure 3.7: The structure of SVM model (Ghorbani et al., 2018)

3.7 Pearson Correlation

A Pearson correlation is a number between -1 and +1 that indicates to which extent 2 variables are linearly related. Assume that the data are an *n* x *m* matrix where *n* is the number of instances and *m* is the number of attributes of an instance. Let *X* and *Y* be instances that contains m attributes. Mathematically, the Pearson correlation coefficient, $r_{X,Y}$ between two instances *X* and *Y* is defined as:

$$r_{X,Y} = \frac{\sum_{i=1}^{m}(X_i - \bar{X})(Y_i - \bar{Y})}{\sqrt{\sum_{i=1}^{m}(X_i - \bar{X})^2}\sqrt{\sum_{i=1}^{m}(Y_i - \bar{Y})^2}} \tag{3.17}$$

where $\bar{X}$ and $\bar{Y}$ are defined as:

$$\bar{X} = \frac{1}{m}\sum_{i=1}^{m} X_i \tag{3.18}$$

$$\bar{Y} = \frac{1}{m}\sum_{i=1}^{m} Y_i \quad (3.19)$$

The Pearson correlation coefficient is a measure of how two instances are linearly related. The value of $r_{X,Y}$ ranges from -1 to 1. It is closed to zero if two instances are uncorrelated. When it is positive, *X* and *Y* are correlated. The higher the value, the stronger the correlation. If the value of rx,y is negative, then *X* and *Y* are negatively correlated.

3.8 Multi-Linear Regression

Multi-linear regression (MLR) is a popular mathematical modeling technique that relates dependent variable to one or many independent variables linearly. Generally, the n regressor variables and dependent variable y can usually be correlated by (Elkiran et al., 2018):

$$y = b_0 + b_1x_1 + b_2x_2 + b_3x_3 + \cdots + b_ix_i + \xi \quad (3.20)$$

Where x_i is the ith predictor value, b_0 is the constant of regression, and b_i is the ith predictor coefficient and ξ is refers to error term.

3.9 Empirical Equations

3.9.1 Pan evaporation

The evaporation rate from pans filled with water is easily obtained. In the absence of rain, the amount of water evaporated during a period (mm/day) corresponds with the decrease in water depth in that period. Pans provide a measurement of the integrated effect of radiation, wind, temperature and humidity on the evaporation from an open water surface. Although the pan responds in a similar fashion to the same climatic factors affecting crop transpiration, several factors produce significant differences in loss of water from a water surface and from a cropped surface. Reflection of solar radiation from water in the shallow pan might be different from the assumed 23% for the grass reference surface. Storage of heat within the pan can be appreciable and may cause significant evaporation during the night while most crops transpire only during the daytime. There are also differences in turbulence, temperature and humidity of the air immediately above the respective surfaces. Heat transfer through the sides of the pan occurs

and affects the energy balance.

Notwithstanding the difference between pan-evaporation and the evapotranspiration of cropped surfaces, the use of pans to predict ET_0 for periods of 10 days or longer may be warranted. The pan evaporation is related to the reference evapotranspiration by an empirically derived pan coefficient:

$$ET_0 = K_p * E_p \quad (3.21)$$

Where K_p is a pan coefficient which ranges between 0.3 and 1.1 and it is inversely proportional to wind speed and directly proportional to relative humidity (Aschonitis et al., 2012; Heydari and Heydari, 2014). Cuenca approach (Cuenca, 1989) was applied in this study owing to its performance and application in many studies (including Sabziparvar et al., 2010; Snyder et al., 2005; Heydari and Heydari, 2014). The equation is given by (Snyder et al., 2005):

$$K_p = 0.475 - 2.4\,X\,10^{-4}U_2 + 5.16\,X\,10^{-3}R_H + 1.18\,X\,10^{-3}F - 1.6\,X\,10^{-5}{R_H}^2 - 1.01\,X\,10^{-6}F^2 - 8\,X\,10^{-9}R_H U_2 - 1.0\,X\,10^{-8}{R_H}^2 F \quad (3.22)$$

Where U_2 and R_H were previously defined and F is fetch distance (green crop windward side distance).

3.9.2 Hargreaves model (Hargreaves and Samani, 1985) (HS)

Hargreaves and modified Hargreaves (Hargreaves and Samani, 1985 and Hu et al., 2011) are the two temperature based models selected. The models require minimum, maximum and mean air temperature as input (Feng et al., 2016)

$$ET_0 = 0.000939R_a(T_{mean} + 17.8)(T_{max} - T_{min})^{0.5} \quad (3.23)$$

Where T_{min}, T_{mean}, and T_{max} were define previously in equation.. , R_a is extraterrestrial radiation (MJ/m^2/day)

3.9.3 Modified Hargreaves model (Hu et al., 2011) (MHS)

Hu et al. (2011) applied modification to previous Hargreaves model, given by;

$$ET_0 = 0.000571R_a(T_{mean} + 13.1)(T_{max} - T_{min})^{0.7} \quad (3.24)$$

Where T_{min}, T_{mean}, and T_{max} and R_a were defined previously in equation…

3.9.4 Makkink model (MK)

Makkink and Ritchie models are the radiation based models applied in this study. Solar radiation and temperature might explain about 80% of ET_0 (Samani, 2000; Feng et al., 2016), and accurate estimation of ET_0 could be achieved by many radiation based ET_0 models.

$$ET_0 = 0.61\left(\frac{\Delta}{\Delta+\gamma}\right)\frac{R_s}{2.45} - 0.12 \tag{3.25}$$

Where Δ is the vapor pressure curve slope $(\text{kPa oC} - 1), \gamma$ is the psychometric constant (kPa $^{o}C^{-1}$) and R_s is solar radiation (MJ/m^2/day), respectively.

3.9.5 Ritchie model (Jones and Ritchie, 1990) (RT)

The Ritchie model is given by the following equation;

$$ET_0 = \alpha_1 * [0.00387R_s(0.6T_{max} + 0.4T_{min} + 29)] \tag{3.26}$$

Where α_1 has the following conditions:

$$5 < T_{max} \leq 35°\text{C}, \alpha_1 = 1.1; \tag{3.27}$$

$$T_{max} > 35°\text{C}, \alpha_1 = 1.1 + 0.05(T_{max} - 35) \tag{3.28}$$

$$T_{max} < 5°\text{C}, \alpha_1 = 0.01 \exp[0.18(T_{max} + 20)] \tag{3.29}$$

3.10 Multi-Step Ahead Predictions

Multi-step ahead predictions are the predictions of parameters for some future time steps i.e. φ_{N+h}, with $h = 1,2,3, \ldots H$, while H is the integer having value greater than one, in view of the current and previous observations i.e. $\varphi_t, t = 1,2,3 \ldots N$. Multi-step ahead modeling is good for decision making and could be used to provide warning and counter measures for the persistent climate change impact on hydro-climatic processes such as ET_0. Iterated and direct algorithms are the two most commonly applied methods for the multi-step ahead modeling (Bao et al., 2014). For iterated algorithm, a prediction model is constructed by minimizing the squares of one step ahead residual, thereafter, the predicted values are used as inputs to predict the next values. In direct algorithm, prediction models are constructed for each horizon by applying only its past observations (Bao et al., 2014). In this study, direct

algorithm was employed since the next step is independent of the previous step and there is susceptibility of error accumulation problem for iterated algorithm as it uses past predicted values to generate next step ahead prediction.

3.11 Ensemble Modeling

It is evident for a given collection of data that the output of one intelligent technique may exceed another, and when distinct data sets are used, the findings might be quite the opposite. To gain from the advantages of all techniques and not to lose generality, an ensemble model is developed using the single output of each technique with a certain priority level assigned to each technique with the aid of an arbitrator to produce the output (Kiran and Ravi, 2008). For prediction issues, some ensemble techniques include linear ensemble, such as Simple average (Benediktsson et al., 1997), Stack regression (Breiman, 1996), Weighted average (Perrone and Cooper, 1993); and Nonlinear ensemble, such as ensemble modeling using neural network (Yu et al., 2005). As reported by Kiran and Ravi (2008), there exist two ensemble methods: (i) linear ensemble method; which includes simple average linear ensemble, weighted average linear ensemble and weighted median linear ensemble. (ii) Nonlinear ensemble method; such as training an ANN model to produce ensemble output.

Non-linear FFNN, simple and weighted average ensemble methods are the types of ensemble modeling techniques employed in this study.

Simple average (SA) ensemble modeling is performed using:

$$\overline{ET} = \frac{1}{N}\sum_{i=1}^{N} ET_i \tag{3.30}$$

Where $\overline{ET}$ is the simple ensemble output produce by SA model, ET_i is the *i*th single model output (FFNN, SVR, ANFIS and MLR with respect to this study) and N is the number of single models (here, N is 4).

The weighted averaging (WA) ensemble is given by:

$$\overline{ET} = \sum_{i=1}^{N} w_i ET_i \tag{3.31}$$

Where w_i is the weight applied on *i*th model and can be obtained in accordance with the

performance of single models:

$$w_i = \frac{DC_i}{\sum_{i=1}^{N} DC_i} \tag{3.32}$$

DC_i is called determination coefficient. It indicates efficiency of the *i*th single model. Figure 3.8 gives the general methodology developed for ensemble modeling.

In the non-linear ensemble (NE), the ANFIS, FFNN, MLR and SVR individual outputs are used as inputs to generate a new FFNN non-linear model (for strategy 1 in the first phase of modeling) and finally by training and validating the model, the overall ensemble output is obtained. Data were partitioned into *4*-folds subsamples, to validate the ensemble model in similar process to the case of single modeling. The training subsamples used were $k - 1$ (4-1) while the validation was carried out using the remaining subsample. The process of training and validating the model was repeated until each subsample was once used as dataset for training and validation. Figure 3.8 depicts the ensemble modeling general procedure.

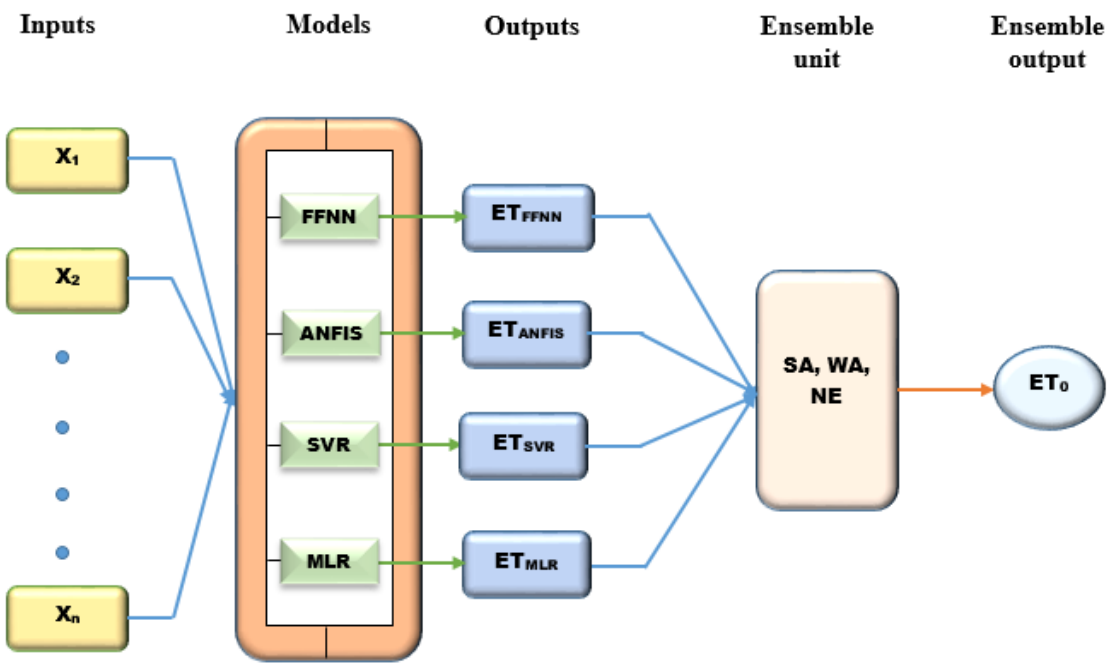

Figure 3.8: General procedure of the developed method for ensemble modeling

3.12 Validating the Meteorological Parameters

Quality assurance measures were applied to assess the incorrect and suspicious data from observations. Firstly, it is important to check that the right and full record structure is obtained and that all possible data are collected. Gaps found in the data files should be flagged as erroneous, and should not be included in the ET_0 estimation as input variable. The methods used for meteorological parameters quality control include: fixed or dynamic range test, step test, internal consistency test, and persistence test (Estévez et al., 2011, 2016). Range (fixed) testing technique was applied in this study because of its ability to detect erroneous data (i.e. data outside appropriate fixed target). Table 3.13 displays the test procedures implemented for testing the data quality of the variables used.

Table 3. 2: Data validation procedures for meteorological variables before their use as input data for ET_0 estimations.

Variable	Unit	Applied Data Validation Procedure
Relative humidity (R_H)	%	$0.8 < R_H < 103$ (Estévez et al., 2011)
Surface Pressure (S_P)	Kpa	$80 < S_P < 105$ (Shafer et al., 2000)
Precipitation (P_R)	mm	$0 \leq P_R < 508$ (Estévez et al., 2011)
Maximum air temperature (T_{max})	(°C)	$-20 < T_{max}, T_{min}, T_{mean} < 50$ (Estévez et al., 2016)
Minimum air temperature (T_{min})		
Mean air temperature (T_{mean})		
Mean wind speed (U_{mean})		
Maximum wind speed (U_{max})	m/s	$0 < U_{max} < 100$
Minimum wind speed (U_{min})		$0 < U_{mean}$ (Estévez et al., 2011)
Solar Radiation (R_S)	MJ/m^2/day	$0 < R_S < 121$
		$0.03R_a \leq R_S \leq R_a$ (Estévez et al., 2016)
Pan Evaporation (E_P)	mm	$0 \leq E_P < 500$ (Feng et al., 2004)

CHAPTER 4

RESULTS AND DISCUSSION

4.1 Results for Phase 1

In this phase of the study, four steps are contained in the proposed methodology, (i) application of conventional methods, (ii) selection of dominant input variables on ET_0 using neural network-based analysis (iii) application of linear MLR and non-linear AI based techniques for single modeling, and finally, (iv) Two strategies were used for results presentation via a non-linear and two linear approaches to ascertain the performance improvement by ensemble modeling over the single models. Accordingly, the results are provided with respect to the aforementioned steps in different sub-sections.

To validate and assure the quality standard of the input variables for the simulation of ET_0, quality control measures were utilized to determine faulty values from the input variables. The conducted fixed range test results implied there are no erroneous or flagged data pinpointed. Signifying that within the range of acceptable variables in Table 3.13, the tested variables showed compliance. The data descriptive statistics given in Tables 3.1, 3.3, 3.5, 3.7 and 3.9 can also be affirmed to this.

4.1.1 Results of the applied Pearson correlation

The Pearson correlation results for all stations across all regions from Turkey, North Cyprus, Iraq, Iran and Libya are given in Appendices 2a, 2b, 2c, 2d and 2e, respectively. For Turkey stations, it can be seen that P_R has higher correlation with ET_0 in Adana and Izmir than in Ankara and Samsun stations. This could be because the former stations are situated in the MED region which possesses cool and heavy rainy winter and hot and dry summer due to its semi humid and humid subtropical nature whereas, the latter stations are representing semiarid climate of CCAN region and temperate climate of BLS region. This is implying that the higher the aridity index of a climate, the lower the linear correlation and thus, the higher the nonlinear correlation between P_R and ET_0. For R_H, the correlation effect is also higher in Adana and Izmir station. This is because the ratio of the partial pressure of water

vapor to the equilibrium vapor pressure of water is higher in humid climate than semiarid or temperate climate, as the temperature increases, the vapor pressure present in air decreases and thus results in decrease in effect of R_H. Overall, E_P and R_S show better correlation with ET_0 in comparison to the other 10 variables used in this study. This followed by T_{mean} and T_{min} due the climate of the stations. For North Cyprus stations, the Pearson correlation results is shown in Appendix 2b. R_S demonstrated the highest correlation with ET_0 and U_{max}, U_{min} and U_{mean} are the least correlated variables. For Iraq stations, contrary to Turkey and Iraq stations, U_{max}, U_{min} and U_{mean} are more correlated with ET_0 than S_P, T_D and T_{max}. This shows how dynamic and unpredictable variables could be despite having similar climate (semiarid). For Iran stations, P_R is very significant variable next to E_P and R_S. For Libya stations, EP has the highest correlation followed by R_S, P_R, R_H, T_{mean}, T_{min}, and the least correlated variable is S_P for both Sabha and Tripoli stations.

4.1.1 Results of the empirical models

To evaluate the performance of the climate based models and for the basis of comparison, ET_0 computed by the empirical models were referenced by ET_0 values computed by Ep method. The radiation and temperature based empirical models results for the entire stations are presented in Table 4.1. It is worthy to acknowledge that comparison was made between the results of the empirical models with that of AI based models, therefore, for efficient comparison, the former results were calibrated on the basis of *4*-folds cross-validation, as the latter.

Table 4.1: Results of the empirical models

			Training		Validation	
Country	**Station**	**Model**	**DC**	**RMSE[a]**	**DC**	**RMSE[a]**
Turkey	Adana	HS	0.8425	0.1032	0.7910	0.1052
		MHS	0.8697	0.0828	0.8698	0.0924
		MK	0.6581	0.1496	0.4462	0.1701
		RT	0.6753	0.1468	0.5263	0.1611
	Ankara	HS	0.7721	0.1188	0.6863	0.1284
		MHS	0.7997	0.1152	0.7145	0.1239
		MK	0.6475	0.1512	0.5692	0.1487
		RT	0.8299	0.1048	0.6324	0.1395
	Izmir	HS	0.8029	0.1301	0.7817	0.1388

		MHS	0.8464	0.1136	0.8411	0.1161
		MK	0.8225	0.1208	0.8127	0.1253
		RT	0.8166	0.1292	0.8113	0.1241
	Samsun	HS	0.6324	0.1511	0.4097	0.1641
		MHS	0.6824	0.1403	0.4552	0.1579
		MK	0.6581	0.1493	0.5616	0.1429
		RT	0.6778	0.1431	0.5683	0.1398
Cyprus	Famagusta	HS	0.8012	0.1316	0.7727	0.2083
		MHS	0.8245	0.1274	0.7941	0.1232
		MK	0.7042	0.1494	0.6512	0.2473
		RT	0.7374	0.1410	0.6882	0.2341
	Kyrenia	HS	0.8684	0.1511	0.7567	0.1275
		MHS	0.8824	0.1449	0.7469	0.1359
		MK	0.7752	0.1993	0.7841	0.1216
		RT	0.8035	0.1879	0.8092	0.1172
	Morphou	HS	0.8897	0.1801	0.7184	0.1614
		MHS	0.8723	0.1878	0.6945	0.1671
		MK	0.8819	0.1847	0.7381	0.1572
		RT	0.8933	0.1742	0.7391	0.1546
	Nicosia	HS	0.9268	0.1417	0.7769	0.1183
		MHS	0.9311	0.1406	0.8035	0.1152
		MK	0.8946	0.1624	0.7701	0.1201
		RT	0.9047	0.1566	0.7881	0.1161
Iraq	Erbil	HS	0.8641	0.1021	0.8331	0.1134
		MHS	0.8689	0.1002	0.8004	0.1298
		MK	0.7745	0.1312	0.7964	0.1322
		RT	0.8176	0.1245	0.7477	0.1453
	Salahaddin	HS	0.4932	0.1721	0.3624	0.1843
		MHS	0.6043	0.1519	0.4587	0.1738
		MK	0.5861	0.1505	0.3747	0.1806
		RT	0.6689	0.1378	0.4598	0.1714
Iran	Tabriz	HS	0.8267	0.1189	0.7646	0.1425
		MHS	0.8735	0.1016	0.8149	0.1264
		MK	0.6665	0.1696	0.5989	0.1810
		RT	0.8547	0.1089	0.7757	0.1391
	Urmia	HS	0.8596	0.1074	0.7627	0.1395
		MHS	0.8705	0.1032	0.7797	0.1344
		MK	0.8012	0.1277	0.7646	0.1391
		RT	0.7949	0.1297	0.7524	0.1427
Libya	Sabha	HS	0.8362	0.1187	0.6663	0.1494
		MHS	0.8273	0.1219	0.6740	0.1477
		MK	0.8474	0.1146	0.5900	0.1656

	RT	0.8475	0.1146	0.6306	0.1572
Tripoli	HS	0.6241	0.1338	0.4252	0.1587
	MHS	0.6514	0.1288	0.4278	0.1583
	MK	0.6228	0.1340	0.4087	0.1610
	RT	0.4553	0.1611	0.3276	0.1716

RMSE[a] : Since the data were normalized, RMSE has no unit

As shown in Table 4.1, the performance of all models is appreciable in most stations; meaning that empirical models in most of the study locations could achieve accurate estimates of ET_0. Since the results of the models are comparable for similar weather conditions, it is nevertheless clear that one model output may be better than another due mainly to the environment (climate) from which the models were originally produced. This results in the least and highest performing models.

For Turkey stations, the empirical models performance at Adana and Izmir stations is a little better than at stations in Ankara and Samsun in relation to lower RMSE and higher DC. This may be because the MED climate receives higher precipitation, and condensation and precipitation occurs due to regular evapotranspiration according to the definition of water cycle. This suggests that evapotranspiration is easier to be estimated using empirical models with higher precipitation levels. The results obtained by empirical models in Ankara station have exceeded those obtained from Samsun station since Ankara station is located in CCAN, a semi-arid climate region, while Samsun is in BLS temperate climate and most empirical models are built on the basis of extreme climate predictions (including arid and semi-arid climate conditions) in order to properly handle and manage processes. Therefore, for stations that are not subjected to these climatic conditions, reliable predictions may not be provided by the empirical models. Comparing the performance of the models, it can be seen that models based on temperature usually have greater predictability than models based on radiation and MHS models performed better than models based on HS. Prediction of radiation-based models were increased by the temperature-based models in the validation phase up to 3% at the Izmir station, 14% at the Ankara station and 42% at the Adana station, while temperature-based models were increased by 16% in the Samsun region by radiation based models.

For Cyprus stations, the performance in Famagusta station by MHS model was found to be better, with training phase RMSE = 0.1274, DC = 0.8245 and validation phase RMSE =

0.1232, DC = 0.7941. During the validation process, HS model followed closely with RMSE = 0.2083 and DC = 0.7727. Radiation related models have been found to have better efficiency in Kyrenia station. RT model was found in the validation process to overestimate ET_0 with RMSE = 0.1172 and DC = 0.8092. Better output of the models based on radiation may be due to the rocks surrounding the site, which can lead to easier evaporation and transpiration. In this area (Kyrenia), atmospheric conditions such as slope of the saturation vapor pressure and extraterrestrial radiation may also be more effective as they can easily penetrate the earth's surface unlike in a flat setting like Nicosia. However, in Morphou, the correlation between ET_0 values calculated by Ep method and those calculated by methods based on radiation is significantly higher than when compared with ET_0 values calculated by methods based on temperature. In the validation, RT provided the highest simulated values with RMSE = 0.1546 and DC = 0.7391. MHS has the highest results in validation process for Nicosia station with RMSE = 0.1152 and DC = 0.8035. Based on the findings in Table 4.1, temperature-based models are superior in efficiency for all stations during the training phase, possibly due to the appropriateness of this study's used indicators. In the validation processes, however, the temperature-based models achieved better correlation for Famagusta and Nicosia while the radiation-based models provided better results for Kyrenia and Morphou areas. Therefore, both radiation-based and temperature-based models can predict ET_0 with some level of precision. Nonetheless, as shown in Table 4.1, the models' output across the four stations is identical, which may be because the stations share similar hot dry summer and mild cold winter of semi-arid Mediterranean climate. The principal discrepancy between their climates is the station they are located. That is, the temperature would be marginally moderate for a coastal region than for the inland. Hilly and valley areas may also affect the environment, and ultimately the ET_0 prediction. This may be the reason why the performance of radiation-based models in Kyrenia is higher than any other station.

For stations in Iraq, the models used at Erbil station provided better estimates of the ET_0 values but the empirical models at Salahaddin station achieved lower estimates. While Salahaddin has been identified as a semi-arid climate station, a Sarlak and Agha (2018) study reveals that the aridity of the station varies with the time and aridity index (defined by Ranjbar et al., 2018 as the mean annual potential evaporation to precipitation ratio) used for its analysis. For example, the station was found to be semi-arid between 1998-2011, sub-

humid between 1980-1997 and sub-humid between 1980-2011 using the UNEP (1992) aridity index. The station's climate incoherence makes it hard for empirical models to predict the ET_0. Since the long record of data includes elements from various climatic areas, the empirical models struggle to provide reliable estimates. This is why the models used produced the least performance for the station in Salahaddin compared to the other stations.

Table 4.1 also demonstrates the efficiency of the empirical models for Iran's stations of Tabriz and Urmia. The findings suggest that empirical models based on temperature and radiation could be used successfully in the stations for estimating ET_0. This is because the used input parameters to the models including temperatures (T_{max}, T_{mean} and T_{min}) and R_S have little variance from the mean, which implies less diversification of data and thus formed a close bond with the output target. In both stations, over all other empirical models, promising performance is shown by MHS model, which in the validation phase has performance increase that amount to about 3%, 2% and 2% for Urmia station and 3%, 2% and 5% for Tabriz station over RT MK and HS models. This justifies its upgrade from the HS original model.

For stations in Libya, distinct outcomes from two stations of Sabha and Tripoli can be seen in Table 4.1. In spite the arid nature of Sabha weather, both temperature and radiation dependent models performed better for station in Sabha than station in Tripoli. It may be because Tripoli is a heavily populated city, comprising of around one million of the six million population in Libya. High population can contribute to an increase in human activities and industrialization, which can cause deterioration of the environment and release of harmful gasses into the air. This can have a profound impact on ET and hence make it difficult to estimate ET_0 using physical methods. The scatter plots in the validation phase for the best RT model (Izmir station), MK model (Izmir station), MHS model (Adana station) and HS model (Erbil station) are shown in Figure 4.1.

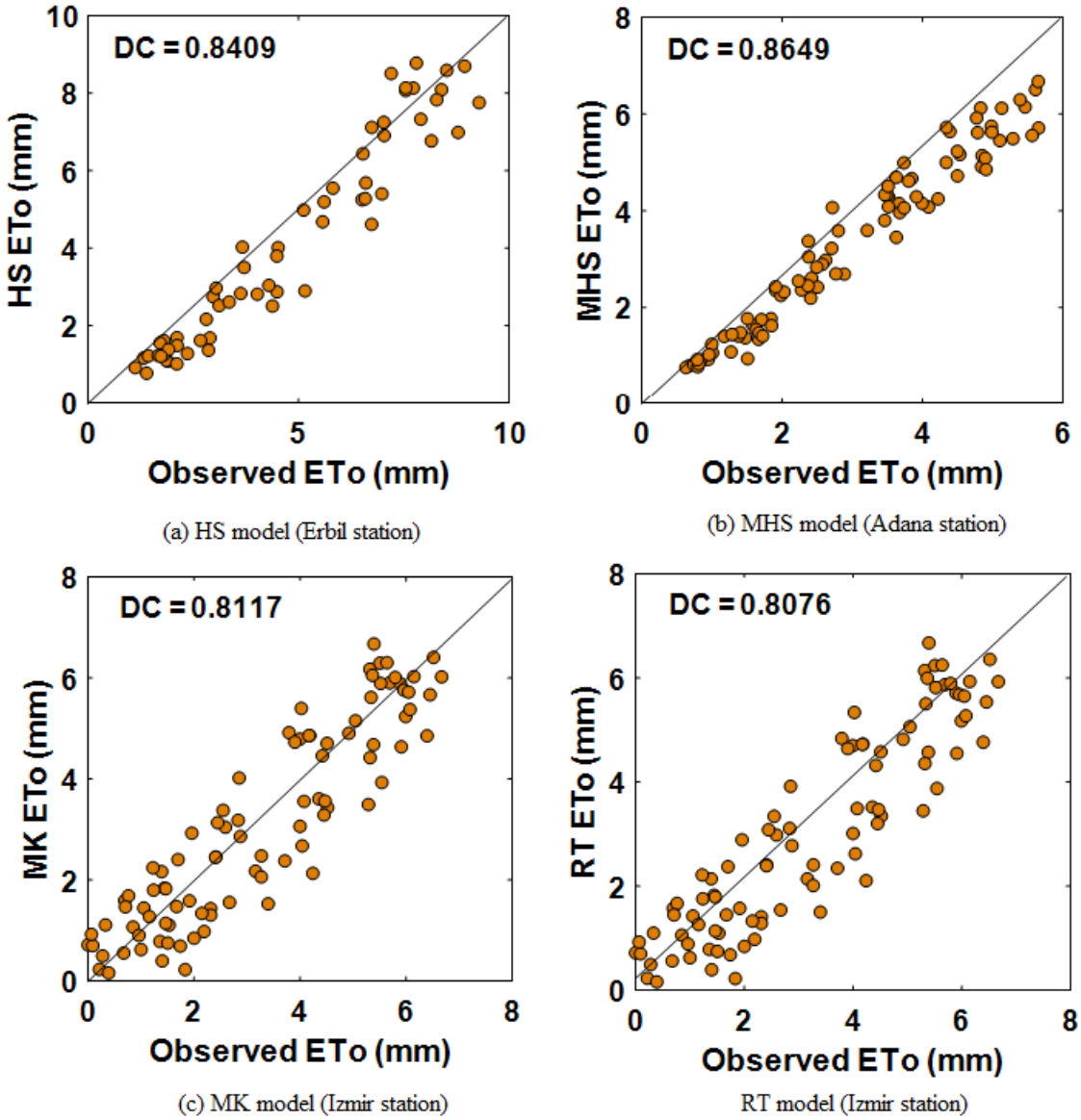

Figure 4.1: Best performance in the validation phase across all stations

In general, the empirical models based on temperature provided better predictions than models based on radiation. Any of the models may be used to achieve useful outcomes in regions similar to that of this research, and where only temperature data are available, temperature-based models could be successfully applied.

4.1.2 Sensitivity analysis results

A non-dimensional sensitivity analysis has already been used to assess the impact of meteorological variables on ET_0 increases or decreases including study by Beven (1979) and Estévez et al. (2009). Some earlier studies also show that single-input single-output sensitivity analysis by AI-based techniques can also be used to determine the impact of each meteorological variables on ET_0, for modeling ET_0 successful using AI techniques. For instance, Jain et al. (2008) used ANN to perform sensitivity analysis for the ET_0 estimation. Doğan (2009) determined each meteorological variable's impact on the benchmark ET_0 using ANFIS technique. Wang et al. (2011) conducted sensitivity analysis of meteorological variables to determine the dominant inputs for ET_0 modeling in arid regions of Africa using ANN. Eslamian et al. (2012) employed the services of ANN to find out the most appropriate parameters to be used as inputs for the ET_0 modeling. The most important weather parameters on ET_0 were calculated by Petković et al. (2015) using ANFIS. Consequently, a neural network-based single-input sensitivity analysis was used to define the key input parameters in this study for the modeling of the ET_0 over the selected stations. The models were then trained and tested with ET_0 value as a function to each parameter.

Results for all of the 12 parameters in this analysis are provided in Table 4.2. Table 4.2 highlights the significance of possible input parameters on the output ET_0 in the validation phase. RMSE was used to assess the efficacy of the parameters, while the lowest error signifies the most influential parameter.

Table 4.2: Sensitivity analysis results

			R_H	S_P	P_R	T_D	T_{max}	T_{min}	T_{mean}	U_{min}	U_{max}	U_{mean}	R_S	E_P
Country	**Station**	**Error term**	**%**	**Kpa**	**mm/day**	**^{0}C**	**^{0}C**	**^{0}C**	**^{0}C**	**m/s**	**m/s**	**m/s**	**MJ/m^2/day**	**mm/day**
Turkey	Adana	RMSE[a]	0.2081	0.0891	0.1722	0.1118	0.0989	0.1099	0.1010	0.1586	0.2067	0.3084	0.0828	0.0121
	Ankara	RMSE[a]	0.1633	0.1917	0.2275	0.1190	0.1141	0.1150	0.1101	0.2312	0.2278	0.2283	0.1029	0.0198
	Izmir	RMSE[a]	0.1534	0.1496	0.2183	0.1358	0.1179	0.1239	0.1129	0.2768	0.2938	0.2875	0.3193	0.0182
	Samsun	RMSE[a]	0.2195	0.1817	0.2150	0.2084	0.1186	0.1204	0.1140	0.2390	0.2306	0.2317	0.1335	0.0074
Cyprus	Famagusta	RMSE[a]	0.1194	0.0281	0.0792	0.0886	0.0493	0.0818	0.0411	0.1492	0.1771	0.1786	0.0227	0.0355
	Kyrenia	RMSE[a]	0.0763	0.0285	0.0695	0.0892	0.0786	0.0586	0.0381	0.2440	0.2109	0.2717	0.0203	0.0723
	Morphou	RMSE[a]	0.0734	0.0324	0.0690	0.0911	0.0496	0.2374	0.0382	0.2440	0.2396	0.2477	0.0225	0.0172
	Nicosia	RMSE[a]	0.0637	0.0297	0.0702	0.0913	0.0548	0.0545	0.0537	0.2225	0.2195	0.2722	0.0209	0.0108
Iraq	Erbil	RMSE[a]	0.1524	0.1212	0.2298	0.2215	0.1038	0.1130	0.1034	0.1927	0.2949	0.2228	0.1022	0.0269
	Salahaddin	RMSE[a]	0.1278	0.1284	0.1889	0.1935	0.1252	0.1193	0.1271	0.1576	0.2378	0.2343	0.1161	0.0124
Iran	Tabriz	RMSE[a]	0.1089	0.2771	0.2446	0.1199	0.0515	0.0641	0.1096	0.2987	0.2731	0.1144	0.0758	0.0107
	Urmia	RMSE[a]	0.1766	0.2387	0.2785	0.1507	0.1435	0.1489	0.1265	0.2778	0.2631	0.2678	0.1104	0.0182
Libya	Sabha	RMSE[a]	0.1190	0.1647	0.2552	0.1922	0.1178	0.1151	0.1172	0.2435	0.2230	0.2043	0.1389	0.0263
	Tripoli	RMSE[a]	0.1313	0.1538	0.1775	0.1852	0.1479	0.1722	0.1702	0.2028	0.2386	0.1989	0.1620	0.0110

RMSE[a] : Since the data were normalized, RMSE has no unit

For Turkey stations E_P, T_{mean} and $T_{max,}$ E_P, R_S and T_{mean}, E_P, T_{mean} and R_S, E_P, R_S and T_{max} are the three most important parameters for ET_0 modeling at Samsun, Izmir, Ankara and Adana stations, respectively, according to the findings in Table 4.2. For NC stations, on the other hand, $S_{P,}$ E_P and R_S are in descending order the 3rd, 2nd and 1st, most important parameters for both the training and validation phases at Famagusta station. The 6th, 5th, and 4th most significant parameters at Famagusta Station are T_{min}, T_{max} and T_{mean}, for the ET_0 process. Due to the station's hot climate and less precipitation, the water vapor presence in the air is low, which may be the reason why T_D and P_R in Famagusta station are 7th and 8th. Due to higher air moisture levels in the air, R_H will be more efficient in humid regions, hence rising aridity index, restricted air moisture levels thereby leading to reduced effects of R_H; this may be an explanation to why R_H is in 9th spot. The least efficient parameters are U_{min}, U_{mean} and U_{max} at Famagusta Station for estimating the ET_0. With Kyrenia as a coastal region, the parameters effects are identical to those of the Famagusta station, but the mountains presence surrounding the area for the region of Kyrenia results in easier evaporation and transpiration and hence higher precipitation. The effect of parameters on the estimate of the ET_0 at Morphou station is in the ascending order of U_{mean}, U_{min}, U_{max}, T_{min}, T_D, R_H, P_R, T_{max}, T_{mean}, S_P, E_P and R_S. The impact of the parameters on ET_0 are identical for Nicosia station, with location close to Morphou station. For the stations in the northern Iraq province of Kurdistan, the best 3 parameters that are most appropriate for Erbil's ET_0 modeling are E_P, T_{mean} and R_S, while the dominant parameters for Salahaddin station are E_P, T_{min} and R_S. For Iran's Tabriz and Urmia stations, E_p, T_{max} and T_{min} are the 3 most influential parameters for Tabriz station with RMSE of 0.0107, 0.0515 and 0.0641 and for Urmia station E_p, R_S and T_{mean} with RMSE of 0.0181, 0.1104 and 1.265. Therefore, for Sabha station, the 4 most important parameters are T_{mean}, T_{max}, T_{min} and Ep due to its arid climate as ET_0 rises with rise in temperature. As a coastal station receiving more precipitation at a lower elevation above mean sea level, for Tripoli station, the ET_0 4 most important parameters include R_H and S_P.

4.1.3 Results of the black box models (ANN, ANFIS, SVR and MLR)

This section presents the results of 14 different stations obtained from three AI-based techniques FFNN, ANFIS and SVR and conventional MLR technique for ET_0 estimation in

Iran, NC, Libya, Turkey and Iraq using different input combinations based on input selection results.

The FFNN simulation of ET_0 was done using Levenberg Marquardt algorithm to train the network with varying hidden neurons number and a single hidden layer. The optimum number of hidden layer nodes for each region was established using method of trial and error. Accordingly, for Samsun, Izmir, Ankara, Adana, Nicosia, Morphou, Kyrenia, Famagusta, Salahaddin, Erbil, Urmia, Tabriz, Tripoli and Sabha, the hidden layer nodes that received the best results were 11, 6, 9, 7, 11, 12, 9, 10, 10, 8, 7, 9, 12 and 14.

In this study, an ANFIS model using Sugeno type fuzzy inference algorithm was implemented, where calibration of the membership function parameters was performed using a collection of given input-output data through hybrid optimization algorithm. In order to develop ANFIS with the best construction, trial and error method was applied for the structure formulation of the ANFIS models. Across all stations, 3 categories of membership functions (MFs) were found to be suitable including Gaussian-shaped, Trapezoidal and Triangular MFs for the simulation of ET_0 while training epoch modification was examined to ascertain the number of MFs that will provide the most optimal output.

RBF kernel was used for the SVR models' development for all stations. The RBF kernel's tuning parameters are less than polynomial, and two sigmoid kernels. The RBF kernel also demonstrates improved performance in SVR modeling in the light of smoothness in assumptions (Sharghi et al., 2018). The parameters of the RBF kernel in SVR were tuned to achieve the best accuracy, reliability, and consistency for ET_0 estimates at each station. Finally, this study also employed MLR model to linearly simulate the dependent and independent parameters relationship for ET_0 process.

Each model was subjected to the combination of 3, 4 and 5 different inputs to ensure efficient performance from the best 5 most productive parameters determined through the applied sensitivity analysis of input parameters for the ET_0 estimation. Varied input combinations produced varied outcomes, 3 input models led to higher reliability for the simulation in some stations than 4 input models while in some the 4 input models were superior, but usually, models with 5 and 3 inputs provided the highest number of best performing models.

Therefore, in accordance with the number of input parameters, which provided the best output, the models were developed. The input combinations for the ET_0 simulation with respect to the study stations are thereby given as:

$$ET_0^{Ad} = f(E_p^{Ad}, R_s^{Ad}, T_{max}^{Ad}) \quad (4.1)$$

$$ET_0^{An} = f(E_p^{An}, T_{mean}^{An}, R_s^{An}, T_{max}^{An}) \quad (4.2)$$

$$ET_0^{Iz} = f(E_p^{Iz}, R_s^{Iz}, T_{mean}^{Iz}) \quad (4.3)$$

$$ET_0^{Sa} = f(E_p^{Sa}, T_{mean}^{Sa}, T_{max}^{Sa}, T_{min}^{Sa}, R_s^{Sa}) \quad (4.4)$$

$$ET_0^{Fa} = f(R_s^{Fa}, E_p^{Fa}, T_{mean}^{Fa}, T_{max}^{Fa}, S_p^{Fa}) \quad (4.5)$$

$$ET_0^{Ky} = f(R_s^{Ky}, E_p^{Ky}, T_{mean}^{Ky}, P_R^{Ky}, S_p^{Ky}) \quad (4.6)$$

$$ET_0^{Mo} = f(R_s^{Mo}, E_p^{Mo}, T_{mean}^{Mo}, T_{max}^{Mo}, S_p^{Mo}) \quad (4.7)$$

$$ET_0^{Ni} = f(R_s^{Ni}, E_p^{Ni}, T_{mean}^{Ni}, T_{min}^{Ni}, S_p^{Ni}) \quad (4.8)$$

$$ET_0^{Er} = f(E_p^{Er}, T_{mean}^{Er}, R_s^{Er}) \quad (4.9)$$

$$ET_0^{Sl} = f(E_p^{Sl}, T_{min}^{Sl}, R_s^{Sl}, T_{max}^{Sl}, T_{mean}^{Sl}) \quad (4.10)$$

$$ET_0^{Ta} = f(E_p^{Ta}, T_{max}^{Ta}, T_{min}^{Ta}) \quad (4.11)$$

$$ET_0^{Ur} = f(E_p^{Ur}, T_{mean}^{Ur}, R_s^{Ur}) \quad (4.12)$$

$$ET_0^{Sh} = f(E_p^{Sh}, T_{min}^{Sh}, T_{mean}^{Sh}) \quad (4.13)$$

$$ET_0^{Tr} = f(E_p^{Tr}, R_H^{Tr}, S_p^{Tr}, T_{max}^{Tr}) \quad (4.14)$$

where ET_0^{Ad}, ET_0^{An}, ET_0^{Iz}, ET_0^{Sa}, ET_0^{Fa}, ET_0^{Ky}, ET_0^{Mo}, ET_0^{Ni}, ET_0^{Er}, ET_0^{Sl} ET_0^{Ta}, ET_0^{Ur}, ET_0^{Sh} and ET_0^{Tr} are ET_0 at Adana, Ankara, Izmir, Samsun, Famagusta, Kyrenia, Morphou, Nicosia, Erbil, Salahaddin, Tabriz, Urmia, Sabha and Tripoli stations respectively and $R_s, E_p, T_{mean}, T_{max}, S_p, P_R$, R_H and T_{min} defined as in Table 3.1.

Table 4.3 shows for all the stations, the results of the SVR, ANFIS, FFNN, and MLR models. It is worthy to state that the results presented are only for the best output models. The x-y-z numbering of the FFNN structure mean input number of parameters, hidden layer neurons number and output number. For structure of ANFIS, MF-x describes MF type and number of MFs. For SVR, RBF denotes Radial Basis function utilized in the construction of SVR. The MLR form x-y corresponds respectively to number of inputs and outputs.

Table 4.3: Results of the black box models

				Training		Validation	
Country	**Station**	**Model**	**Structure**	**DC**	**RMSE**	**DC**	**RMSE[a]**
Turkey	Adana	FFNN	3-7-1	0.9010	0.0733	0.8895	0.0864
		ANFIS	Gaussian-3	0.8980	0.0742	0.8835	0.0887
		SVR	RBF	0.9330	0.0608	0.9184	0.0732
		MLR	3-1	0.7588	0.1294	0.7602	0.1238
	Ankara	FFNN	4-9-1	0.9045	0.0783	0.8416	0.0909
		ANFIS	Triangular-4	0.9043	0.0787	0.8412	0.0910
		SVR	RBF	0.8875	0.0863	0.7964	0.1038
		MLR	4-1	0.6197	0.1401	0.5743	0.1637
	Izmir	FFNN	3-6-1	0.8874	0.0942	0.8691	0.1067
		ANFIS	Triangular-3	0.8882	0.0937	0.8696	0.1053
		SVR	RBF	0.8687	0.1031	0.8379	0.1174
		MLR	3-1	0.7365	0.1508	0.6577	0.1684
	Samsun	FFNN	5-11-1	0.8873	0.0864	0.8388	0.0861
		ANFIS	Trapezoidal-5	0.8839	0.0843	0.8393	0.0856
		SVR	RBF	0.7956	0.0978	0.7844	0.1123
		MLR	5-1	0.5549	0.1628	0.5168	0.1507
Cyprus	Famagusta	FFNN	5-10-1	0.9178	0.1241	0.8172	0.1201
		ANFIS	Triangular-5	0.9273	0.1164	0.8285	0.1146
		SVR	RBF	0.9084	0.1267	0.7903	0.1237
		MLR	5-1	0.8177	0.1789	0.6638	0.1618
	Kyrenia	FFNN	5-9-1	0.9584	0.0959	0.8879	0.0891
		ANFIS	Triangular-5	0.9687	0.0769	0.8694	0.0926
		SVR	RBF	0.9795	0.0743	0.8281	0.1118
		MLR	5-1	0.8610	0.1579	0.7085	0.1419
	Morphou	FFNN	5-12-1	0.9365	0.1431	0.7842	0.1415
		ANFIS	Triangular-5	0.9346	0.1391	0.8692	0.1126
		SVR	RBF	0.9354	0.1408	0.7388	0.1548
		MLR	5-1	0.8734	0.1943	0.6593	0.1772
	Nicosia	FFNN	5-11-1	0.9387	0.1256	0.8890	0.0863

		ANFIS	Triangular-5	0.9576	0.1091	0.8967	0.0818
		SVR	RBF	0.9448	0.1217	0.8771	0.0900
		MLR	5-1	0.8469	0.1982	0.6667	0.1462
Iraq	Erbil	FFNN	3-8-1	0.9193	0.0781	0.8832	0.0958
		ANFIS	Trapezoidal-3	0.9187	0.0783	0.8784	0.1032
		SVR	RBF	0.9165	0.0813	0.8647	0.1082
		MLR	3-1	0.7975	0.1308	0.7535	0.1348
	Salahaddin	FFNN	5-10-1	0.8632	0.0895	0.7867	0.1102
		ANFIS	Gaussian-5	0.8741	0.0853	0.8064	0.1040
		SVR	RBF	0.8649	0.0886	0.7693	0.1132
		MLR	5-1	0.6050	0.1517	0.5669	0.1543
Iran	Tabriz	FFNN	3-9-1	0.9201	0.0808	0.8798	0.0932
		ANFIS	Trapezoidal-3	0.9261	0.0777	0.8925	0.0875
		SVR	RBF	0.8997	0.0905	0.8318	0.1205
		MLR	3-1	0.8906	0.0945	0.7581	0.1300
	Urmia	FFNN	3-7-1	0.8628	0.1062	0.8271	0.1191
		ANFIS	Gausian-3	0.8824	0.0983	0.8552	0.1090
		SVR	RBF	0.9049	0.0884	0.8342	0.1166
		MLR	3-1	0.8161	0.1230	0.7492	0.1327
Libya	Sabha	FFNN	3-14-1	0.8948	0.0952	0.7131	0.1385
		ANFIS	Triangular-3	0.9113	0.0874	0.8108	0.1125
		SVR	RBF	0.9049	0.0905	0.7095	0.1394
		MLR	3-1	0.8586	0.1103	0.6087	0.1618
	Tripoli	FFNN	4-12-1	0.7532	0.1084	0.7342	0.1079
		ANFIS	Triangular-4	0.8317	0.0895	0.7822	0.0977
		SVR	RBF	0.7575	0.1075	0.6855	0.1174
		MLR	4-1	0.7220	0.1151	0.5940	0.1334

RMSE[a] : Since the data were normalized, RMSE has no unit

Table 4.3 shows different performances of the models. AI-based models were found to be higher in efficiency and accuracy than linear models of all the models implemented. Both AI and MLR models received a good estimate of ET_0 for stations located in Turkey, except for Samsun station where the MLR model with RMSE = 0.1507 and DC = 0.5168 obtained fair output. This implies that the Samsun station's temperate BLS climate negatively affects the efficiency of both MLR and empirical models, but AI-based models can resolve the region's climate threat as they have provided reliable results because of their robustness and ability to cope with unpredictable climate behavior. Given their ability to deliver good results in the BLS climate zone, however, the performance of the AI-based models at Samsun

station is lower than their performance at other stations, indicating that the AI-based models can produce reliable results but not at the peak in that zone of climate. It is evident from the result displayed in Table 4.3 that all the applied models performance at stations of Adana and Izmir (situated in the MED region, with semi-humid and humid climates) was better than those at station of Ankara (located in CCAN region of semi-arid climate). By comparing Tables 4.1 and 4.3, it is certain that AI-based models in all modeling training and validation phases are superior in performance than the other models. The black box models' improved performance may be attributed to (i) the pan evaporation inclusion as their input data, which was also used with other coefficients to produce the benchmark ET_0 and (ii) their potential to manage nonlinear phenomenon of a process. The performance of empirical and MLR models differs across stations with certain empirical models getting an upper hand over MLR models. This is because the input requirements for empirical models are R_S, T_{min}, T_{max} and T_{mean} and in those stations, these variables were found to be influential and forefront parameters for the estimation of ET_0, which allowed empirical models to provide reliable and efficient estimation of ET_0 than MLR model in most stations. For Turkey stations, the overall results imply that modeling of ET_0 in the regions is affected by the climate of the regions, with the least performance in BLS region, followed by CCAN region and the best performance in MED region.

For NC stations, the MLR models for estimating ET_0 during the training phases led to appropriate values based on the applied statistical indicators. But in the validation process, MLR models did not offer much reliable performance with the exception of Kyrenia which got RMSE = 0.1419 and DC = 0.7085. The effectiveness of the used input combination may be the reason for better performance for Kyrenia, which has an inclusion of precipitation due to its dominance in the region for the ET_0 estimation. MLR models' inability to generate effective simulation beyond training steps may be due to their struggle to deal with nonlinear, dynamic processes. All models based on AI techniques provided promising performance in the study stations due to their ability to handle complex phenomenon like the ET_0 process. In the Famagusta station for validation process, ANFIS obtained higher predictions with RMSE = 0.1146 and DC = 0.8285. SVR performed better in Kyrenia's training phase but was 6 percent lower in the testing phase than FFNN. Morphou and Nicosia have also observed greater efficacy of ANFIS predictions over FFNN and SVR. The ANFIS's efficient

performance could be due to ANN's shortcomings in dealing with unclear or less reliable data notwithstanding its robustness in dealing with various real-world issues; as such ANFIS could be a better choice due to the fuzzy logic capability to manage process ambiguity (Moghaddamnia et al., 2009).

In the case of stations in Iraq, the model results shown in Table 4.3 reveal that in Erbil, the efficiency of the ET_0 simulation is higher than in Salahaddin, which is due to the distinct aspect of the climate environment between the two stations. Salahaddin station's aridity varies over time and the aridity index applied while Erbil station's remains constant regardless of the time and the applied indices (Sarlak and Agha, 2018). The station's irregular climate activity decreases the precision of the model predictions.

For Iran stations, with similarity to the empirical models' results (but in an enhanced form), a comparable performance of the AI models could be seen for the study stations due to their climate similarity. As with most stations, for both stations of Tabriz and Urmia, ANFIS has an outstanding performance in the validation phase among other AI models. FFNN has lower performance over SVR in Urmia station and higher performance over SVR at Tabriz station. Notwithstanding being produced on the basis of dominant inputs which have higher correlation to the benchmark output, the MLR model did not yield superior estimates over the empirical models (Table 4.3). This is could be because despite been fixed inputs for empirical simulations; there is strong agreement between the inputs and ET_0 output. The effective convergence of the meteorological parameters towards the mean led to better performance of the applied models in Tabriz station as demonstrated by standard deviation of the input parameters in the descriptive statistics of the study data shown in Table 3.7.

For Sabha and Tripoli stations of Libya, all the models performances are convincing, and with uncertainties and problems solving nature of AI models, the deficiencies of the underperformance empirical models at Tripoli station have been significantly dealt with. Performance improvements up to 26%, 26%, 28% and 33% were achieved in the validation phase by SVR (the least AI performing model) over HS, MHS, MK and RT models, respectively.

The scatter plots for the best FFNN model (Adana station), ANFIS model (Nicosia station), SVR model (Adana station), and MLR model (Adana station) across all the study stations in the validation phase are shown in Figure 4.2.

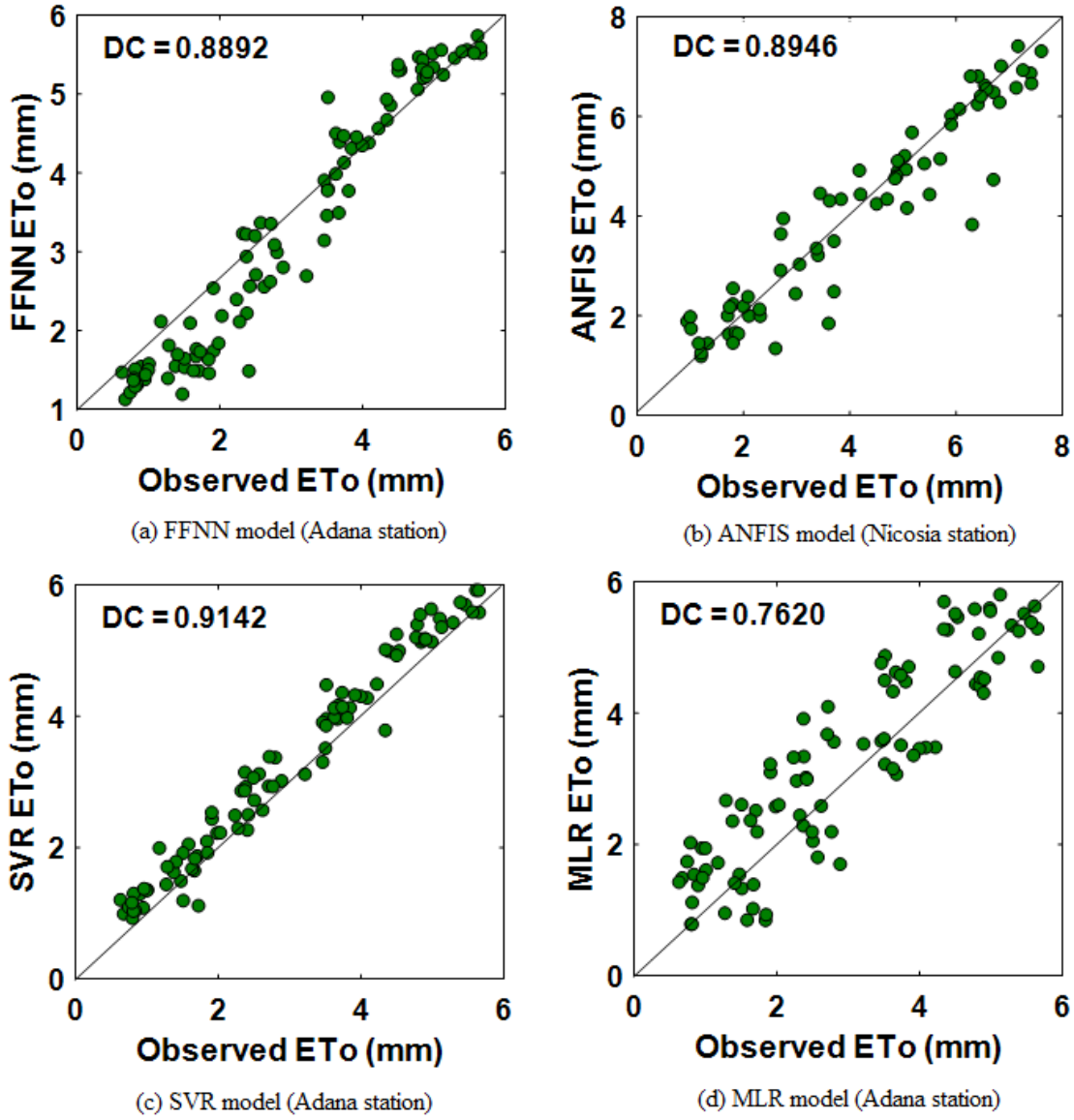

Figure 4.2: Best performance in the validation phase across all stations

Comparisons were made between the empirical, AI based and MLR models to ascertain the performance of one model over another for all stations. The results are presented in Figure 4.3 based on the DCs and RMSEs of the validation phase.

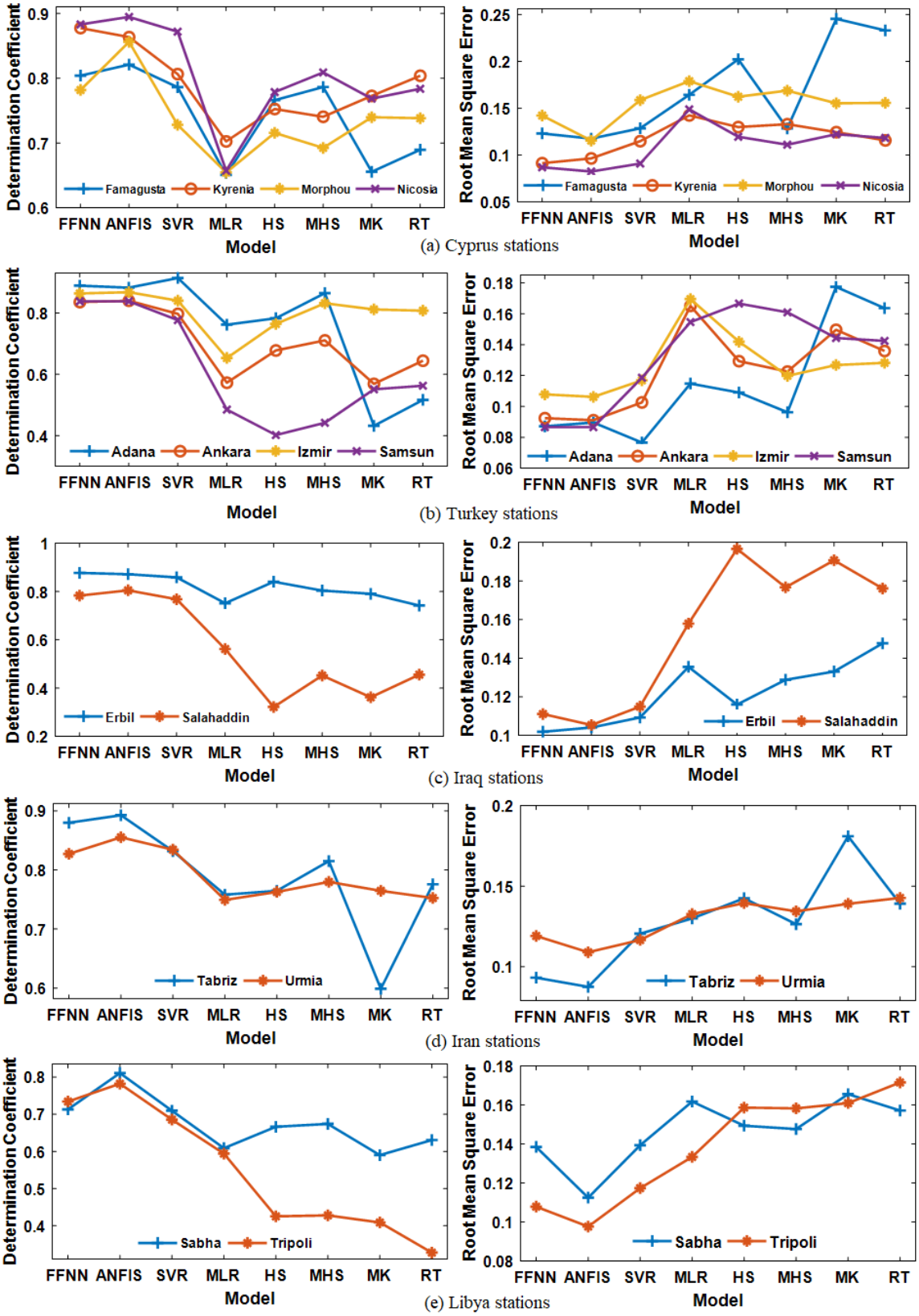

Figure 4.3: Models performances with respect to DCs and RMSEs

As depicted by Figure 4.3, across all stations, AI based models in terms of higher DC and lower RMSE outperformed all other applied models in this study. The reasons for the promising performance of AI models could be owing to one or all of the following reasons; (a) AI models are capable of dealing with complex and nonlinear process, (b) the input combinations of the AI models were used based on merit, implying that the input selection of the AI based models were due to their effectiveness in ET_0 estimation as derived from input selection step while the inputs for all other models (with exception of MLR models) were fixed regardless of their performances toward ET_0 modeling.

Figure 4.4a shows a time series in the validation phase of Adana station for the black box models (FFNN, ANFIS, SVR and MLR). In order to have proper visualization of the estimated ET_0 values by each model, Figure 4.4b is also plotted that contains only the 12 months period of the year 2014 (January, 2013 – December, 2013).

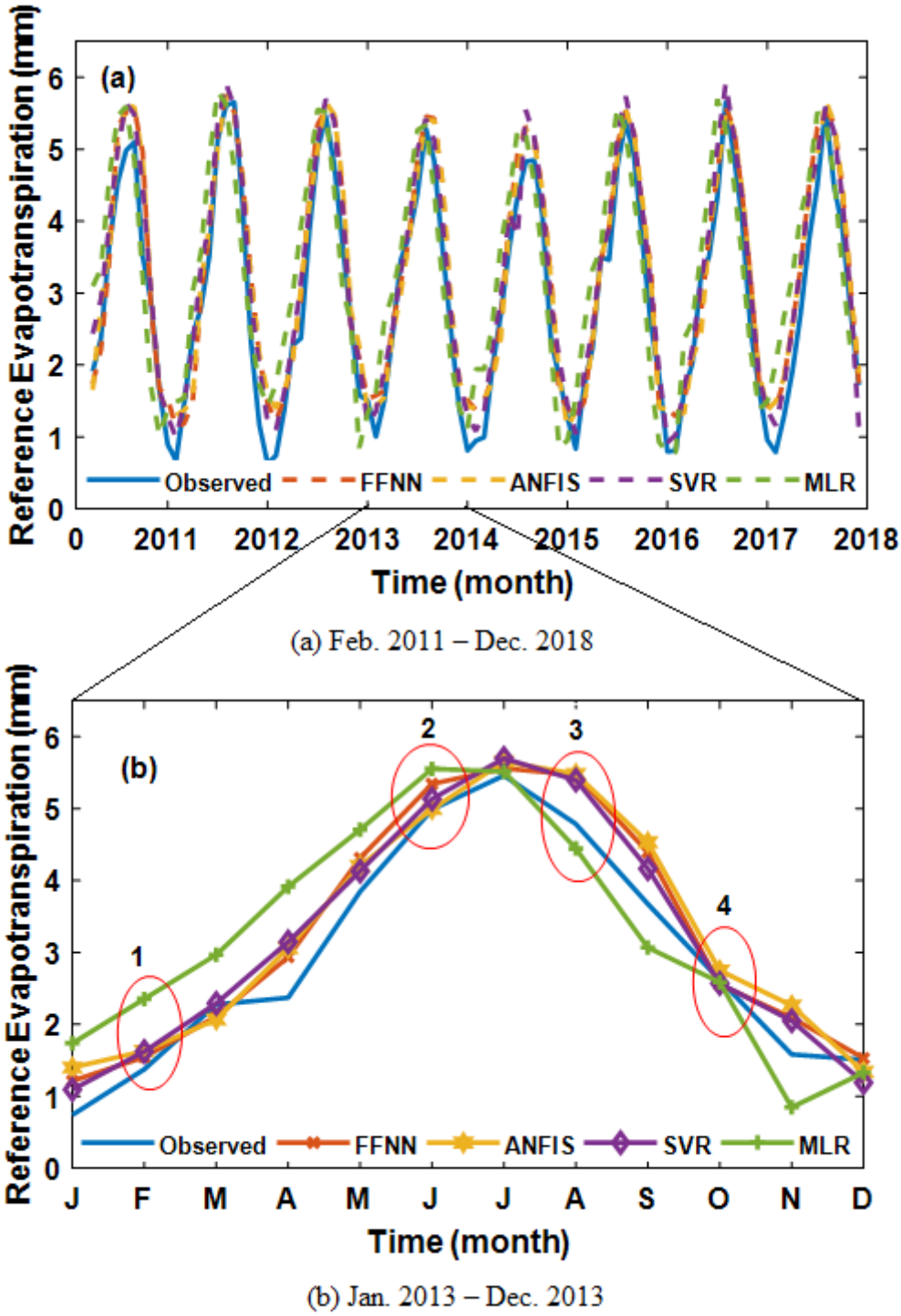

Figure 4.4: Observed versus predicted ET_0 values in the verification phase of Adana station in the year

As revealed in Figure 4.4b, four different points are randomly selected and numbered 1, 2, 3 and 4 which correspond to the months of February, June, August and October, respectively.

Considering point 1, observed = 1.4 mm, FFNN = 1.5 mm, ANFIS = 1.6 mm, SVR = 1.6 mm and MLR = 2.4 mm, this shows that FFNN is more close to the target than the rest models. At point 2, observed = 5.0 mm, FFNN = 5.3 mm, ANFIS = 5.0 mm, SVR = 5.1 mm and MLR = 5.6 mm, this indicates that the agreement between observed and predicted values is higher using ANFIS model, FFNN model which was the best in the month of February is at 3rd rank in June. At point 3, observed = 4.8 mm, FFNN = 5.5 mm, ANFIS = 5.5 mm, SVR = 5.4 mm and MLR = 4.4 mm, this shows that MLR is less deviated from the observed value than the other models and SVR is 2nd performing model at point 3. At point 4, almost all models performances converged together. Observed = 2.6 mm, FFNN = 2.6 mm, ANFIS = 2.7 mm, SVR = 2.6 mm and MLR = 2.6 mm. From the models' outputs at these four points, it can be deduced that different data aspects can be captured by different models in different ways at different time points. Hence, amalgamation of models via ensemble approaches could enhance the capability of the model in more precisely capturing the target. To this end, two linear (SA, WA) and one nonlinear (NE) ensemble techniques are applied in strategy 1 (for black box models) and strategy 2 (for empirical models) in the next section.

It should be noted that the ensemble modeling was performed in strategies 1 and 2 instead of combining all the models (FFNN, ANFIS, SVR, MLR, HS, MHS, MK and RT) for the following reasons; (i) we tried to assess the responses of both AI and empirical models to ensemble modeling, if we combine the models all together, we cannot know the influence of each technique towards ensemble performance, (ii) to see if it's possible to use empirical models for performance improvement in case of data lack for AI based modeling and (iii) to see the difference in performance improvement between ensemble models derived from low performance single models and the improvement achieved from higher performance single models.

4.1.4 Results of the ensemble techniques

4.1.4.1 Results of strategy 1

In strategy 1, the outputs of 3 AI based (FFNN, ANFIS, SVR) and MLR models were used as inputs to the ensemble models. To ensure that the higher performance is achieved, three methods were applied in obtaining the weights for WA ensembles; (i) using only DC of the training phase, (ii) using only DC of the validation phase, (iii) using both DCs of training

and validation phases of the single models. The weights generated by the 3rd method provided better simulation and hence, applied in both strategies 1 and 2. Figure 4.5 shows the overall methodology of the SA, WA and NE models.

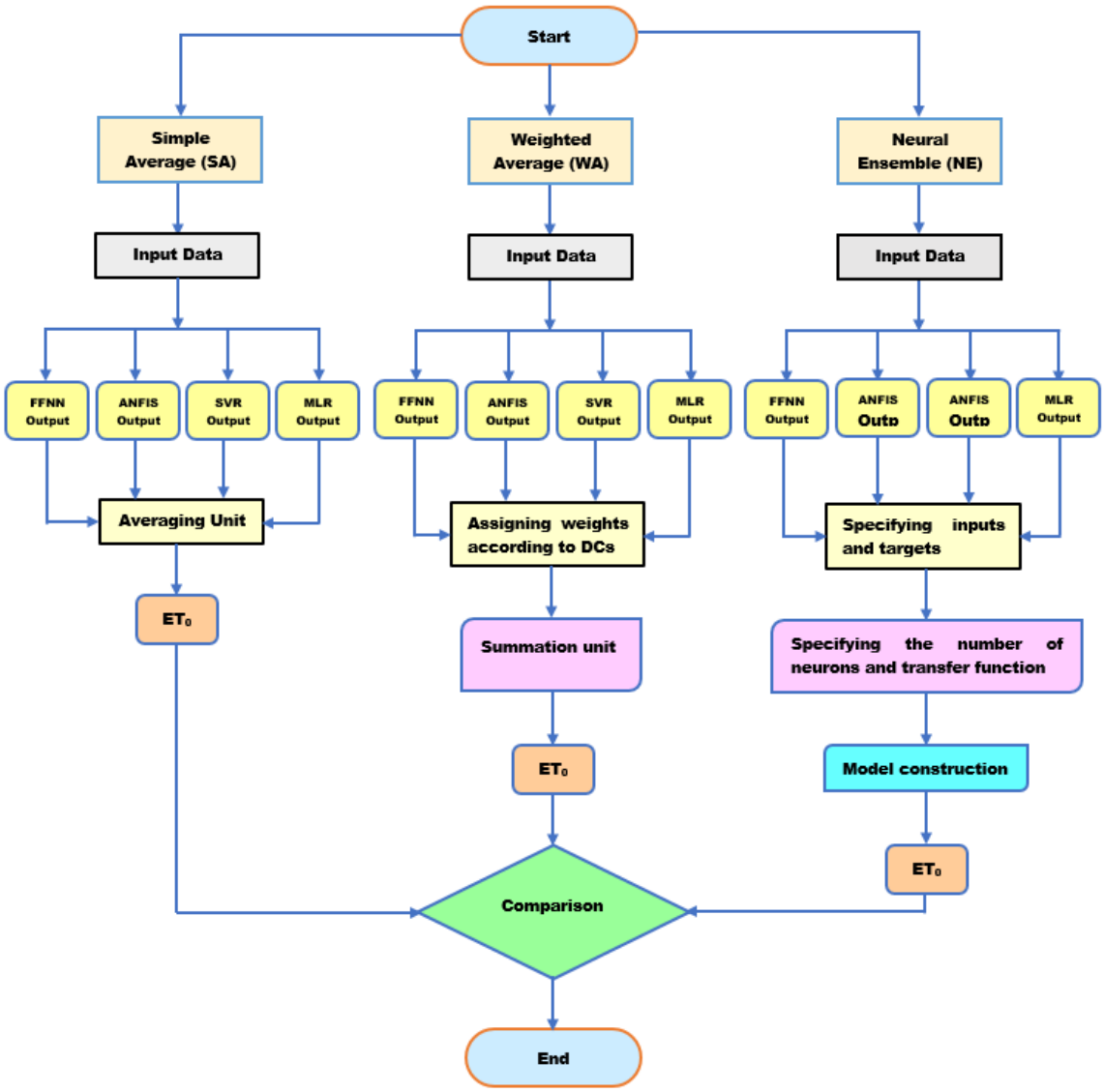

Figure 4.5: Flowchart showing the methodology of the proposed ensemble modeling

Similar to the single FFNN models, the NE models were developed using LM training algorithm with tangent sigmoid as activation functions for both hidden and output layers. The schematic diagram of the developed procedure for NE modeling is given in Figure 4.6.

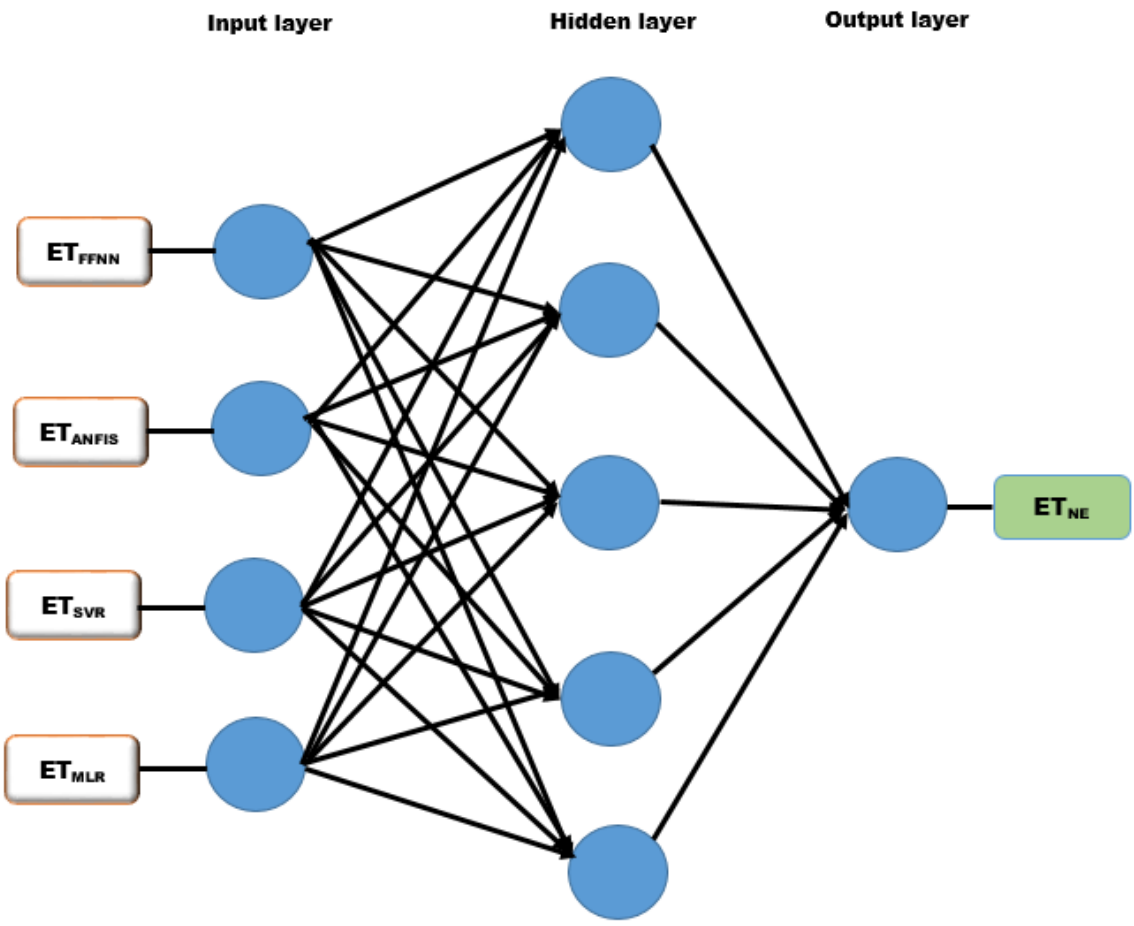

Figure 4.6: Schematic diagram of the NE method

Trial and error procedure was applied to determine the best epoch number and structure (number of hidden neurons) of the ensemble network. The choice of ANN in this study as the nonlinear ensemble technique over other AI models was made due to its popularity, compatibility, and above all high reported performance by many ensemble modeling studies, including Yu et al. (2005); Kiran and Ravi (2008); Sharghi et al. (2018), while other AI models may also be employed as the kernel of ensembling.

The obtained results for the ensemble models in strategy 1 are presented in Table 4.4. For model structure, a-b represent number of inputs and output for SA, w, x, y, z imply the generated weights by FFNN, ANFIS, SVR, and MLR that were applied for WA and finally, FFNN ensemble structure is same as explained previously for single FFNN models.

Table 4.4: The results of the ensemble models via strategy 1

				Training		Validation	
Country	**Station**	**Model**	**Model Structure**	**DC**	**RMSE[a]**	**DC**	**RMSE[a]**
Turkey	Adana	SA	4-1	0.9321	0.0632	0.9078	0.0793
		WA	0.2630, 0.2614, 0.2517, 0.2247	0.9332	0.0624	0.9085	0.0788
		NE	4-8-1	0.9567	0.0501	0.9331	0.0687
	Ankara	SA	4-1	0.8825	0.0879	0.8643	0.0821
		WA	0.2741, 0.2742, 0.2643, 0.1876	0.8876	0.0848	0.8657	0.0833
		NE	4-12-1	0.9264	0.0707	0.8996	0.0729
	Izmir	SA	4-1	0.9328	0.0769	0.9346	0.0757
		WA	0.2648, 0.2658, 0.2581, 0.2103	0.9287	0.0773	0.9287	0.0781
		NE	4-7-1	0.9565	0.0614	0.9586	0.0610
	Samsun	SA	4-1	0.8491	0.0973	0.8251	0.0891
		WA	0.2839, 0.2863, 0.2592, 0.1711	0.8598	0.0935	0.8376	0.0857
		NE	4-10-1	0.8943	0.0816	0.8587	0.0811
Cyprus	Famagusta	SA	4-1	0.9086	0.1263	0.8261	0.1172
		WA	0.2578, 0.2622, 0.2572,0.2234	0.9477	0.1164	0.9138	0.1243
		NE	4-10-1	0.9495	0.1129	0.9197	0.1189
	Kyrenia	SA	4-1	0.9643	0.0824	0.8121	0.1135
		WA	0.2620, 0.2616, 0.2544,0.2228	0.9678	0.0818	0.8158	0.1127
		NE	4-9-1	0.9692	0.0802	0.9015	0.0826
	Morphou	SA	4-1	0.9264	0.1451	0.8132	0.1313
		WA	0.2553, 0.2672, 0.2473,0.2281	0.9274	0.1442	0.8156	0.1306
		NE	4-8-1	0.9373	0.1354	0.8765	0.1086
	Nicosia	SA	4-1	0.9381	0.1266	0.8812	0.0876
		WA	0.2617, 0.2626, 0.2598,0.2154	0.9397	0.1246	0.8856	0.0863
		NE	4-12-1	0.9547	0.1118	0.8993	0.0805
Iraq	Erbil	SA	4-1	0.9325	0.0724	0.9139	0.0848
		WA	0.2616, 0.2582, 0.2549, 0.2243	0.9323	0.0726	0.9124	0.0857
		NE	4-11-1	0.9496	0.0623	0.9472	0.0681
	Salahaddin	SA	4-1	0.8524	0.0926	0.7868	0.1104
		WA	0.2693, 0.2741, 0.2668, 0.1913	0.8592	0.0902	0.7887	0.1090

		NE	4-10-1	0.8976	0.0779	0.8340	0.0971
Iran	Tabriz	SA	4-1	0.9278	0.0768	0.8835	0.1002
		WA	0.2529, 0.2546, 0.2473, 0.2448	0.9279	0.0767	0.8842	0.0999
		NE	4-12-1	0.9317	0.0747	0.9271	0.0793
	Urmia	SA	4-1	0.8936	0.0935	0.8492	0.1112
		WA	0.2505, 0.259, 0.2526, 0.2379	0.8942	0.0933	0.8498	0.1110
		NE	4-8-1	0.9265	0.0778	0.8957	0.0925
Libya	Sabha	SA	4-1	0.9116	0.0872	0.7384	0.1323
		WA	0.2509, 0.2853, 0.2496, 0.2142	0.9134	0.0864	0.7449	0.1306
		NE	4-14-1	0.9401	0.0718	0.9290	0.0689
	Tripoli	SA	4-1	0.7942	0.0990	0.7343	0.1079
		WA	0.2626, 0.2798, 0.2451, 0.2125	0.7980	0.0981	0.7379	0.1072
		NE	4-9-1	0.8576	0.0824	0.8446	0.0825

RMSE[a] : Since the data were normalized, RMSE has no unit

The results in Table 4.4 indicate that ensemble modeling certainly improved accuracy of performance over single models. The performances of the models improved up to 20%, 31%, 22%, 34%, 13%, 11%, 7%, 10%, 15%, 29%, 4%, 11%, 8% and 14% over MLR models in the training phases, and 4%, 13%, 12%, 8%, 13%, 7%, 14%, 2%, 9%, 6%, 10%, 7%, 22% and 15% over SVR models in the validation phases for Adana, Ankara, Izmir, Samsun, Famagusta, Kyrenia, Morphou Nicosia, Erbil, Salahaddin, Tabriz, Urmia, Sabha and Tripoli stations, respectively. It is observed that not much improvement in DCs was attained in the training phase over AI models, but remarkably higher performances were achieved over all models in the validation phase which was the primary focused area in this study. As explained earlier, at different points in time, different behaviors of the data could be captured with underestimation and overestimation of ET_0 by different models and with unique capability of each model, the underlying process could be simulated better than in case of single models. The deduced ensemble results (Table 4.4) in this study show that the performances of the SA and WA are almost equal in most cases across the study stations. This could be because of the linear (direct) relationship they shared with the single models. The performances of the nonlinear FFNN ensemble (NE) models are far better than SA and WA ensemble models, this could be because: (i) FFNN uses nonlinear kernel to simulate the behavior of a system, hence simulation by FFNN would yield better results than the other

linear (SA and WA) methods. (ii) The performances of single models may influence overall results of SA and WA models, implying that poor performing models may result in lesser ensemble performances because of the direct relationship that the methods (SA and WA) share with the single models. (iii) The errors generated by single models might be propagated and incorporated by SA and WA ensemble techniques due to the direct amalgamation of the single models.

It is observed from Table 4.4 that for Turkey stations, the results for Adana and Izmir stations are better than those for Ankara and Samsun stations. Also, ensemble results for Ankara are superior to the results obtained for Samsun station. Similarly, for Iraq stations, ensemble model result for Erbil station surpassed that obtained for Salahaddin station. This clarifies that the climate conditions at these stations not only affect the performance of the single models, but also accuracy and efficiency of the ensemble models that are generated from the single models. To compare the performances of the ensemble models for the 4 study stations in NC, the DC values of the best performance single models were subtracted from the DC values of the strategy 1 ensemble models (Tables 4.3 and 4.4). The differences are 0.0912, 0.0136, 0.0073 and 0.0026 for Famagusta, Kyrenia, Morphou and Nicosia, respectively. This shows that the differences (which indicate the best performing ensemble models) are higher in the first 2 stations than in the last 2 stations. This could be because the heat capacity of soil for inland stations is lower than that of water (ocean) for coastal stations, implying that the ocean cools down and heats up relatively slowly and in contrast, the land heats faster and cools faster. The sudden cooling and heating of inland areas make ET_0 phenomenon difficult to predict, thus ensemble modeling predicts ET_0 better in coastal stations (Famagusta and Kyrenia) than inland stations (Morphou and Nicosia). Considering the improvement in performance achieved by ensemble model in the validation phase of Tabriz and Urmia (10% and 7%) stations, by examining the difference in performance between the best performed single models (ANFIS) of two stations, it could be seen that ANFIS model for Tabriz station is a bit superior to ANFIS model for Urmia station. This signifies that ensemble models increase prediction of single models (according to single model performance) by same amount for station under same climatological condition (such as Tabriz and Urmia of Iran's semi-arid region). For Libya stations, the 22% increment in performance for arid (Sabha)

station compared to 15% increment for semi-arid Mediterranean (Tripoli) station means ensemble techniques are capable of delivering superb performance in an extreme climate.

4.1.4.2 Results of strategy 2

The strategy 2 of ensemble simulation was applied to the four empirical models (HS, MHS, MK, RT) in this study to see how ensemble approaches could cope with less performing models (when compared to AI models). The modeling was performed via three ensemble approaches (SA, WA and NE) same as those used in strategy 1. Table 4.5 shows the results of strategy 2 of ensemble models.

Table 4.5: The results of strategy 2 ensemble modeling

				Training		Validation	
Country	**Station**	**Model**	**Model Structure**	**DC**	**RMSE[a]**	**DC**	**RMSE[a]**
Turkey	Adana	SA2	4-1	0.8135	0.1123	0.7024	0.1276
		WA2	0.2873, 0.3064, 0.1910, 0.2151	0.8278	0.0934	0.7385	0.1205
		NE2	4-13-1	0.9184	0.0748	0.9469	0.0541
	Ankara	SA2	4-1	0.7967	0.1138	0.6810	0.1284
		WA2	0.2573, 0.2659, 0.2169, 0.2576	0.7992	0.1123	0.6854	0.1276
		NE2	4-11-1	0.8901	0.0843	0.8857	0.0789
	Izmir	SA2	4-1	0.8677	0.1053	0.8567	0.1110
		WA2	0.2392, 0.2574, 0.2527, 0.2507	0.8690	0.1041	0.8579	0.1107
		NE2	4-9-1	0.9505	0.0649	0.9490	0.0649
	Samsun	SA2	4-1	0.6843	0.1409	0.5078	0.1510
		WA2	0.2297, 0.2425, 0.2618, 0.2663	0.6857	0.1402	0.5132	0.1491
		NE2	4-9-1	0.8595	0.0940	0.8267	0.0895
Cyprus	Famagusta	SA2	4-1	0.7760	0.1314	0.7421	0.2128
		WA2	0.2591, 0.2673, 0.2312, 0.2403	0.7776	0.1312	0.7447	0.2112
		NE2	4-8-1	0.8908	0.1382	0.7985	0.1247
	Kyrenia	SA2	4-1	0.8456	0.1663	0.7879	0.1190
		WA2	0.2519, 0.2535, 0.2423, 0.2516	0.8462	0.1660	0.7876	0.1193
		NE2	4-7-1	0.9577	0.0883	0.8652	0.0949
	Morphou	SA2	4-1	0.8937	0.1765	0.7368	0.1550

		WA2	0.2489, 0.2442, 0.2524, 0.2534	0.8951	0.1752	0.7374	0.1547
		NE2	4-10-1	0.9293	0.1447	0.7648	0.1473
	Nicosia	SA2	4-1	0.9183	0.1449	0.8067	0.1119
		WA2	0.2496, 0.2543, 0.2462, 0.2491	0.9185	0.1448	0.8070	0.1118
		NE2	4-8-1	0.9359	0.1280	0.8731	0.0910
Iraq	Erbil	SA2	4-1	0.9272	0.0748	0.8950	0.0946
		WA2	0.2644, 0.2562, 0.2381, 0.2403	0.9285	0.0744	0.8970	0.0931
		NE2	4-7-1	0.9543	0.0598	0.9399	0.0756
	Salahaddin	SA2	4-1	0.6133	0.1500	0.4223	0.1816
		WA2	0.2072, 0.2685, 0.2396, 0.2852	0.6198	0.1488	0.4277	0.1802
		NE2	4-8-1	0.8858	0.0819	0.7699	0.1144
Iran	Tabriz	SA2	4-1	0.8715	0.1024	0.8248	0.1229
		WA2	0.2621, 0.277, 0.1899, 0.271	0.8823	0.0981	0.8304	0.1210
		NE2	4-12-1	0.9871	0.0325	0.9840	0.0372
	Urmia	SA2	4-1	0.8914	0.0945	0.8815	0.0986
		WA2	0.243, 0.2484, 0.2553, 0.2533	0.8904	0.0949	0.8817	0.0985
		NE2	4-15-1	0.9813	0.0393	0.9696	0.0499
Libya	Sabha	SA2	4-1	0.8451	0.1155	0.6495	0.1531
		WA2	0.2602, 0.2632, 0.2304, 0.2462	0.8446	0.1157	0.6511	0.1528
		NE2	4-9-1	0.9134	0.0864	0.7950	0.1171
	Tripoli	SA2	4-1	0.6119	0.1360	0.4239	0.1589
		WA2	0.2675, 0.2692, 0.2572, 0.2061	0.6189	0.1347	0.4275	0.1584
		NE2	4-8-1	0.9897	0.0222	0.9846	0.0260

RMSE[a] : Since the data were normalized, RMSE has no unit

Table 4.5 demonstrates the capability of ensemble approaches to improve the performances of all models irrespective of their applied simulation method. The performances of the models were improved up to 5%, 9%, 10%, 18%, 7%, 8%, 6%, 1%, 8%, 29%, 12%, 11%, 8% and 33% over MHS models in the training phases, and 8%, 15%, 11%, 37%, 1%, 12%, 7%, 7%, 14%, 31%,17%, 19%, 13% and 55% over same MHS models of validation phases for Adana, Ankara, Izmir, Samsun, Famagusta, Kyrenia, Morphou Nicosia, Erbil, Salahaddin, Tabriz, Urmia, Sabha and Tripoli stations, respectively. It is observed that

almost all the features of strategy 2 resemble those of strategy 1 ensemble techniques including the closeness of the results obtained by SA and WA models, higher performance of NE over SA and WA ensembles, etc. which their reasons are discussed in strategy 1. This shows that these features are peculiar to ensemble models irrespective of the single models used because of the processes and methodologies followed in carrying out the three ensemble simulations. It is observed that there is huge gap in performance between the two linear ensemble models (SA and WA) and NE model in the second ensemble strategy than in the first ensemble strategy. This is because empirical models provided lower estimates of ET_0 in the single modeling, NE model in the second ensemble modeling overcomes the obstacle posed by the lower estimations, whereas the other ensemble models due to their linear behavior could only adapt the nature of the single models. The result shows that the improvement in ET_0 modeling is higher in strategy 2 ensemble modeling (up to 55%) than in the strategy 1 (maximum 22%) in the verification phase. But owing to the capability of AI based models to handle uncertainty of system, strategy 1 ensemble remains superior to the strategy 2. This means that with low performance single models, more room for improvement will be left to be filled by ensemble models, but with high performance single models, higher predictions would be achieved by ensemble models.

It is worth mentioning that by comparing the two ensemble strategies (Tables 4.4 and 4.5), strategy 1 outperformed strategy 2 (in terms of higher DC and lower RMSE) in the similar manner AI models outperformed empirical models (see Tables 4.1 and 4.3). This implies that the ensemble model performance follows the trend and direction of the performance of single models, that is to say with high performance of single models, ensemble modeling yields better simulations, while in contrast, less accurate but improved performance ensemble modeling could be achieved from poor performance single models. Therefore, for more efficient and accurate estimation of ET_0, AI based models are preferable over empirical models. However, obviously the ensemble of empirical models may be used in the case of data lack for AI based modeling. Figure 4.7 compares the performances of strategies 1 and 2 ensemble techniques in form of computed versus observed ET_0 time series for stations in Turkey, NC, Iraq, Iran and Libya.

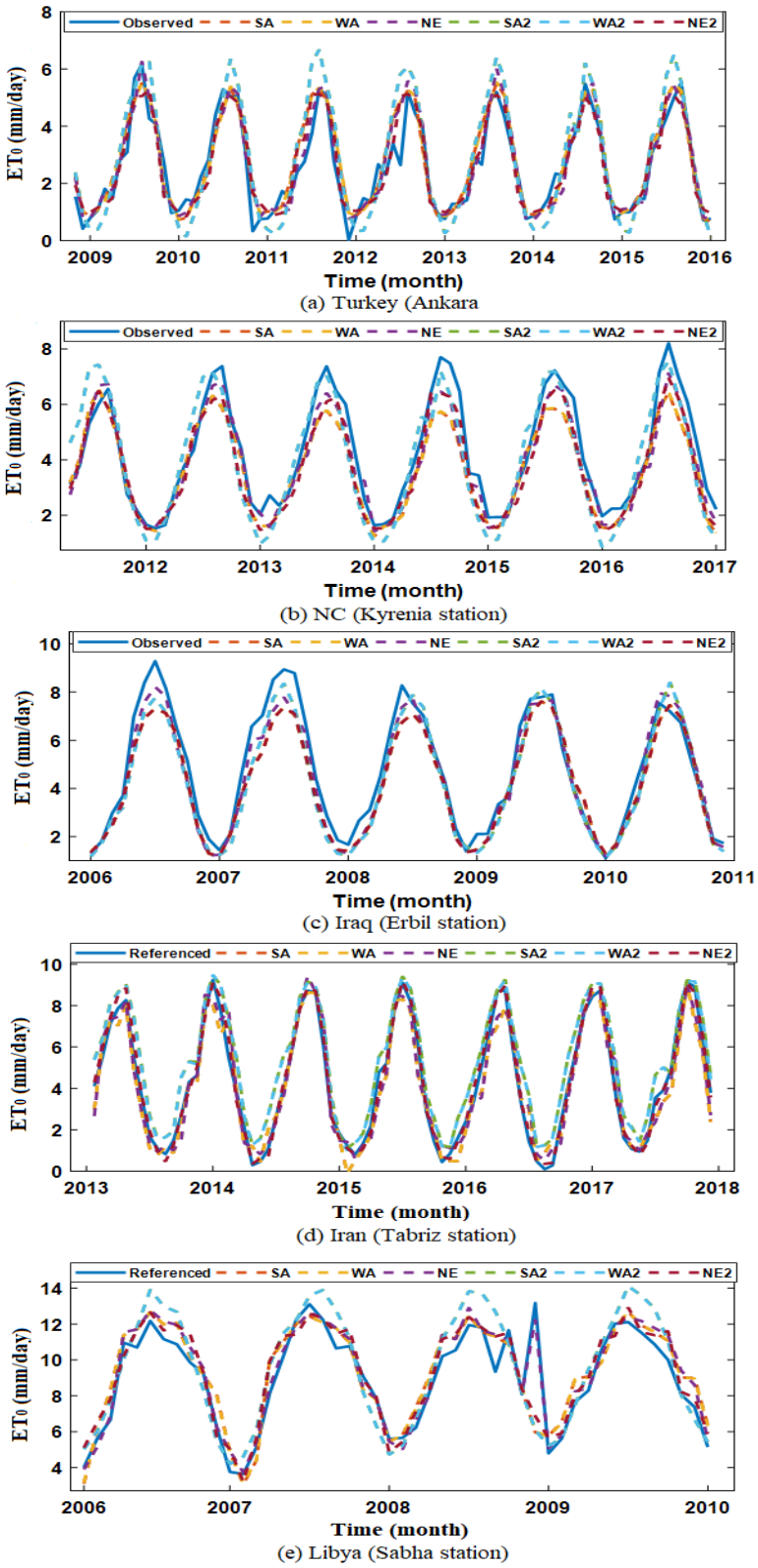

(a) Turkey (Ankara

(b) NC (Kyrenia station)

(c) Iraq (Erbil station)

(d) Iran (Tabriz station)

(e) Libya (Sabha station)

Figure 4.7: Observed vs computed time series for ensemble models at strategy 1 and strategy 2

According to Figure 4.7, it is apparent that AI based ensemble models are more accurate than empirical based ensemble models. The SA, WA and NE follow closely the fluctuations of the observed data, whereas SA2, WA2 and NE2 are unable to have close correlation with the observed data.

However, to further assess the performance of the individual models for both scenarios, Taylor diagrams were plotted. A Taylor diagram summarizes the overall performance of the models by taking in to account the variability, pattern correlations, as well as the RMSE between observed data and predictions by the models (Mehr et al., 2019). In the diagram, the similarity between observed records and predictive models is determined in terms of standard deviation (SD) and correlation coefficient (CC), while RMSE is centered as a measure of distance from observed point (reference point) (Yaseen et al., 2019). In general, if the SD of the observed values surpasses the SD of the predicted values, then underestimation occurs. On the other hand, if the SD of the observed values is lower than the SD of the predicted values, then overestimation occurs (Elkiran et al., 2019). Figures 4.8-4.12 compare the performances of all the applied single models with respect to NE model in terms of the Taylor diagrams for all the 14 stations. The Figures are presented in accordance with the station's country. It is worthy to mention that for each station, the best performance model for each category (e.g. conventional models or AI models) was selected for the comparison.

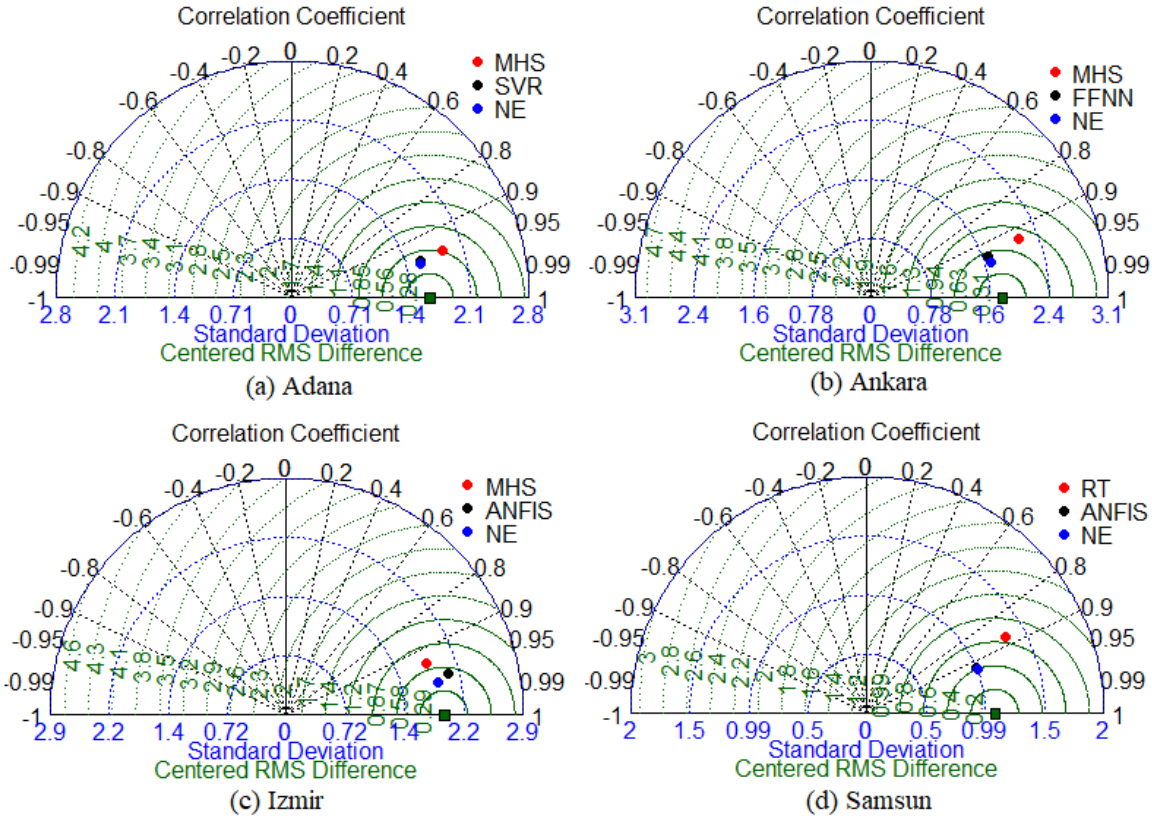

Figure 4.8: Performance comparison between NE and single models for Turkey stations

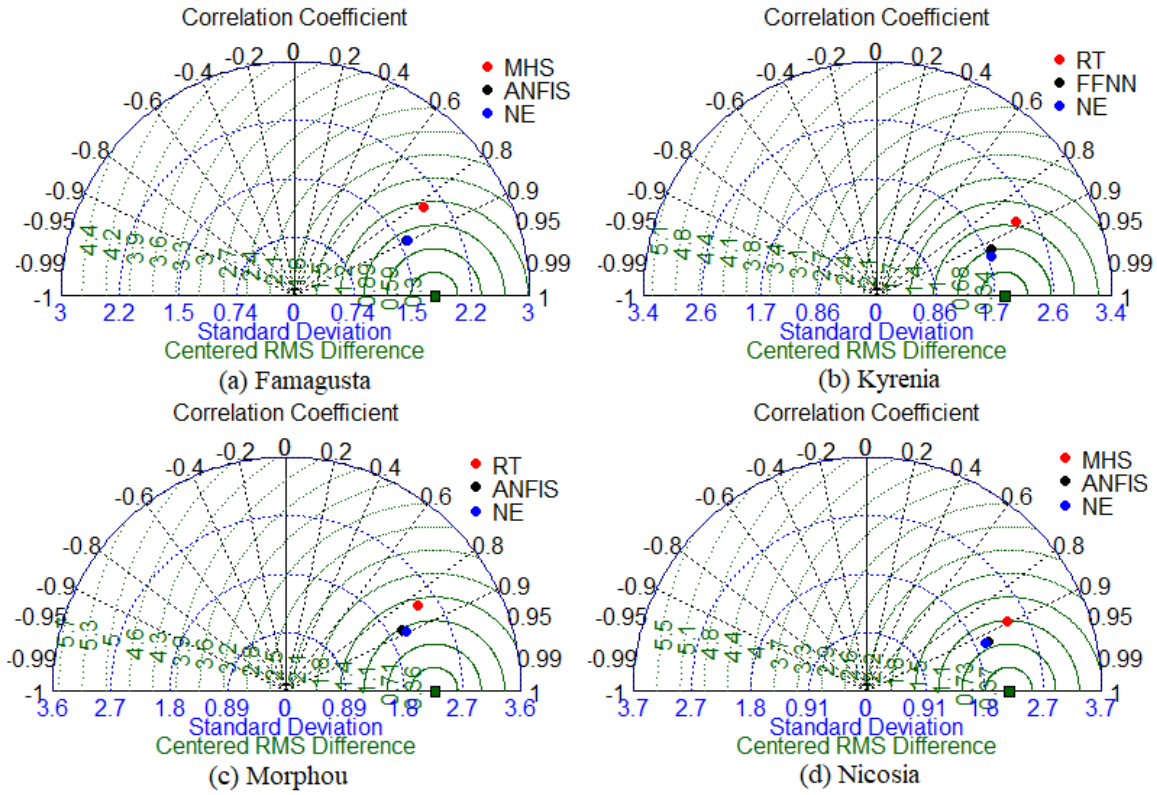

Figure 4.9: Performance comparison between NE and single models for Cyprus stations

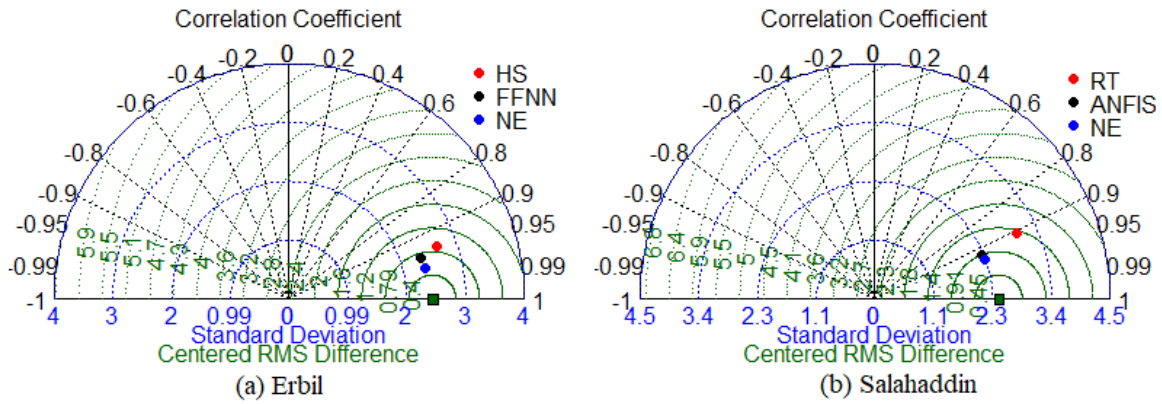

Figure 4.10: Performance comparison between NE and single models for Iraq stations

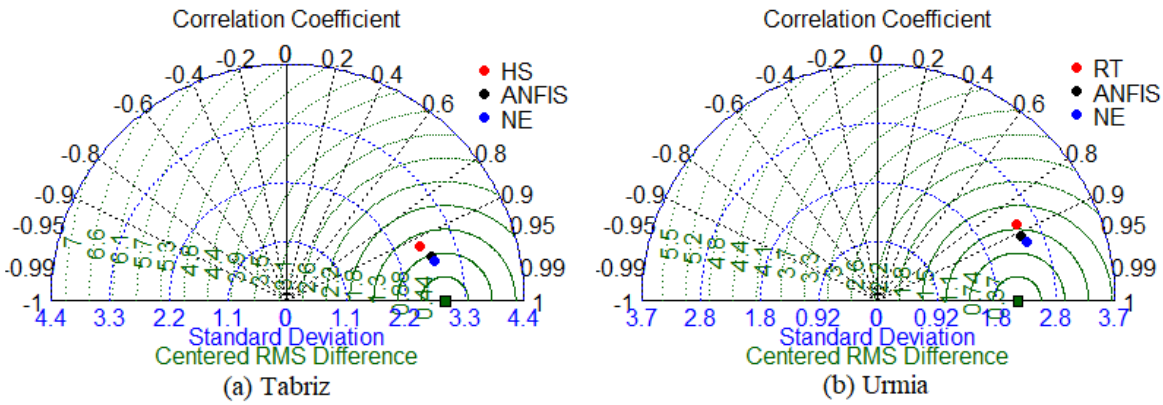

Figure 4.11: Performance comparison between NE and single models for Iran stations

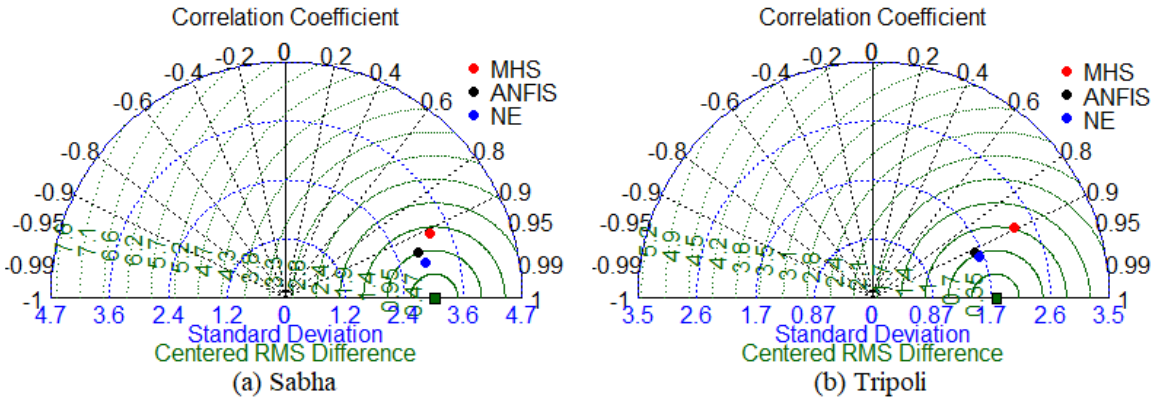

Figure 4.12: Performance comparison between NE and single models for Libya stations

As demonstrated by Figures 4.8-4.12, for all stations across all regions and countries, the NE model provided the best efficiency and reliability based on the three performance indicators (SD, CC and RMSE) despite selecting the best performing single models. In the above plotted Taylor diagrams, for Turkey stations, it can be seen that NE (blue round dot) has SD values more close to the observed value (green square dot), higher CC values and least RMSE values. The AI models demonstrated their capabilities of dealing with complicity of the process by following closely the performance of NE models and lastly the empirical models though with appreciable performance but performed the least in comparison to AI and NE models.

For Cyrus stations, the NE models and AI models are very close in performance but a wide difference can be seen with respect to the applied empirical models, this justifies and confirm

the suitability of AI models in dealing with complex ET_0 process. The NE and FFNN models for Kyrenia station have the highest CC of about 0.99 and 0.97 and the lowest RMSE of 0.57 and 0.68, respectively. The better performances of the models in Kyrenia station could be due to its uniqueness, the nature of the terrain, the coast surrounded by high rocks, the hills and valley area, the commercial activities in the area and the climatological characteristics of the area, which result in frequent and heavy rainfall in comparison to other Cyprus stations.

For Iraq stations, the results displayed by the Taylor diagrams show that, the NE, FFNN and HS models provided more reliable performances in Erbil station than Salahaddin station. This indicates that due to unstable nature of the climate for Salahaddin station (as described by Sarlak and Agha, 2018), despite promising performance of NE model, the ET_0 modeling in the station cannot be as efficient as in the case of Erbil station. These results are in conformity with the results shown in Table 4.1 and Tables 4.3-4.5 where the models performed better for Erbil than Salahaddin station for both single and ensemble models. This implies that different statistical or performance indicators may yield different results but the general revelation by the indicators will lead to same outcome.

For Iran stations, the NE, ANFIS and HS models were found to have better performances in Tabriz station with CCs of 0.99, 0.97 and 0.96 and RMSEs of 0.71, 0.88 and 1.21, respectively. Whereas for Urmia station, their CCs are 0.97, 0.96 and 0.94 and RMSEs are 0.88, 0.94 and 1.26, respectively.

For the performances of the applied models for Libya stations as shown by the plotted Taylor diagrams, the performances of the models are superior in Sabha station than Tripoli station. This could be because Tripoli is the capital city of Libya and has much higher number of inhabitants than Sabha. The human activities couple with environmental degradation due to industrialization and the release of toxic waste cause harm to climatological variables and thereby affects the precise estimation of ET_0 in the area.

4.2 Results for Phase 2 Study

This study was conducted in two steps. The first step involves the application of FFNN, ANFIS, SVR, and MLR models for one- three-step ahead predictions of ET_0. In the second step, linear and nonlinear ensemble modeling was carried out for the assessment of performance improvement of the single models. Hence, the results obtained are presented accordingly.

4.2.1 Results of one and multi-step ahead predictions via single models

For single and multi-step ahead predictions, the three AI based and MLR approaches were applied for the ET_0 prediction. For better forecasting precision, the 12 input parameters were subjected to several time lags (up to 12 months) to check for Markovian strength of the parameters and to ensure that the seasonality of the process is covered. The results showed that Ep and R_S have strong Markov chain while T_{mean}, T_{min}, T_{max}, T_D, R_H, P_R, U_{min}, U_{max}, U_{mean} and S_P are weak in Markovian process, implying that for Ep and R_S, the next step ahead ET_0 values are dependent on sequence of previous events whereas for T_{mean}, T_{min}, T_{max}, T_D, R_H, P_R, U_{min}, U_{max}, U_{mean} and S_P, ET_0 values for the next step are dependent only on its current values. This could be because of the strong correlation that exists between Ep and R_S for determination of ET_0, which keeps their bonding together despite lagging in time. Owing to this development, several input combinations were formed for the single and multi-step ahead predictions containing only the time lags for Ep and R_S as:

$$ET_{0\,(t+h)} = f\left(R_s, E_p, E_{p\,(t-1)}, \dots, E_{p\,(t-12)},\ R_{s\,(t-1)}, \dots, R_{s\,(t-12)}\right) \tag{4.15}$$

Where $ET_{0\,(t+h)}$, is the predicted values for single and multi-step ahead ET_0 (h = 1, 2, 3), *t-1,…, t-12* are monthly time lags, R_s, E_p have been previously defined.

The FFNN was trained using Levenberg Marquardt algorithm with sole hidden layer and varied hidden neurons number for the simulation of ET_0. To ascertain the suitable hidden layer nodes optimal number for each region, trial and error approach was adopted. For the ANFIS model in this study, Sugeno type fuzzy inference algorithm was used, which via hybrid optimization algorithm, a given input-output dataset calibrated the membership function parameters. For the development of ANFIS model structure and to determine the

best ANFIS construction, trial and error procedure was also applied. Gaussian-shaped, Triangular, and Trapezoidal membership functions (MFs) were used across all stations due to their suitability in the simulation of ET_0. For most optimum performance, the training epochs were modified. RBF was used as the kernel for the creation of SVR models for the entire study stations. The two sigmoid and polynomial kernels tuning parameters are more than that of the RBF kernel. The RBF kernel considering smoothness assumptions also shows better SVR modeling performance (Sharghi et al., 2018). For efficient, reliable and best ET_0 modeling performance in the study stations, the SVR parameters were tuned using RBF kernel. Finally, this study also employs the application of MLR model, which linearly expresses the relationship between independent and dependent variables.

Tables 4.6, 4.7 and 4.8 present the obtained results for the best performing FFNN, ANFIS, SVR, and MLR models across the study stations. It is worth mentioning that only the best output results of the applied models are given. x-y-z for FFNN model structure mean the number of inputs used for the model development, hidden neurons number and the ET_0 output. MF-x imply type and number of MFs used for ANFIS structure. For SVR model, RBF represents the kernel function applied for SVR construction. For MLR model, the structure x-y describe the input and output number of parameters used.

4.2.1.1 Results for Turkey stations

With different climate conditions, the results for Turkey stations differ with location and time step prediction. Table 4.6 shows the results of the single and multi-step ahead modeling of ET_0 for Turkey stations.

Table 4.6: Single and multi-step ahead modeling results for Turkey stations

					Training		Verification	
Step ahead	**Station**	**Model**	**Inputs**	**Structure**	**DC**	**RMSE[a]**	**DC**	**RMSE[a]**
One step ahead ($ET_{0\ t+1}$)	Adana	FFNN	E_P, R_S, $E_{P\ (t-1)}$	3-6-1	0.7099	0.1409	0.6729	0.1346
		ANFIS		Triangular-5	0.7334	0.1351	0.7186	0.1248
		SVR		RBF	0.7162	0.1394	0.7069	0.1274
		MLR		3-1	0.708	0.1412	0.6268	0.1438
	Ankara	FFNN	E_P, R_S, $E_{P\ (t-1)}$, $R_{S\ (t-1)}$	4-9-1	0.7826	0.1177	0.7136	0.1219
		ANFIS		Triangular-5	0.7792	0.1186	0.7272	0.119
		SVR		RBF	0.7258	0.1322	0.6504	0.1347
		MLR		4-1	0.559	0.1513	0.549	0.1696
	Izmir	FFNN	E_P, R_S, $E_{P\ (t-1)}$	3-7-1	0.7534	0.1449	0.6153	0.1785
		ANFIS		Gausian-5	0.7382	0.1496	0.6176	0.178
		SVR		RBF	0.7107	0.1572	0.5972	0.1827
		MLR		3-1	0.6829	0.1646	0.5742	0.1878
	Samsun	FFNN	E_P, R_S, $E_{P\ (t-1)}$, $R_{S\ (t-1)}$, $E_{P\ (t-2)}$	5-12-1	0.6651	0.1453	0.5179	0.1495
		ANFIS		Triangular-5	0.7123	0.1347	0.6535	0.1268
		SVR		RBF	0.5079	0.1761	0.4064	0.1659
		MLR		5-1	0.5127	0.1752	0.3355	0.1756
Two step ahead ($ET_{0\ t+2}$)	Adana	FFNN	E_P, R_S, $E_{P\ (t-6)}$	3-9-1	0.7484	0.1313	0.7094	0.1269
		ANFIS		Trapezoidal-5	0.7129	0.1402	0.6945	0.1301
		SVR		RBF	0.6756	0.149	0.5843	0.1517
		MLR		3-1	0.663	0.1519	0.6156	0.1459
	Ankara	FFNN	E_P, R_S, $E_{P\ (t-4)}$, $R_{S\ (t-3)}$	4-11-1	0.6825	0.1423	0.5018	0.1608
		ANFIS		Triangular-5	0.7361	0.1297	0.4861	0.1633
		SVR		RBF	0.7014	0.138	0.4702	0.1658
		MLR		4-1	0.573	0.1489	0.5577	0.168
	Izmir	FFNN	E_P, R_S, $E_{P\ (t-5)}$	3-5-1	0.6395	0.1728	0.4272	0.2212
		ANFIS		Trapezoidal-5	0.6252	0.1762	0.4422	0.2183
		SVR		RBF	0.5425	0.1947	0.3354	0.2383
		MLR		3-1	0.4444	0.2146	0.3673	0.2325
	Samsun	FFNN	E_P, R_S, $E_{P\ (t-2)}$, $R_{S\ (t-2)}$, $E_{P\ (t-6)}$	5-11-1	0.5773	0.14	0.4397	0.1879
		ANFIS		Guasian-5	0.6641	0.1248	0.4932	0.1787
		SVR		RBF	0.422	0.1637	0.3145	0.2079
		MLR		5-1	0.407	0.1658	0.2838	0.2125
Three step ahead ($ET_{0\ t+3}$)	Adana	FFNN	E_P, R_S, $E_{P\ (t-12)}$	3-6-1	0.6228	0.1445	0.5955	0.1664
		ANFIS		Gausian-5	0.6228	0.1607	0.6205	0.145
		SVR		RBF	0.7206	0.1383	0.5875	0.1512
		MLR		3-1	0.582	0.1692	0.5488	0.1581
	Ankara	FFNN		4-9-1	0.7312	0.1309	0.4736	0.1653

	ANFIS	E_P, R_S, $E_{P\,(t-6)}$, $R_{S\,(t-12)}$	Gausian-5	0.738	0.1293	0.482	0.164
	SVR		RBF	0.6914	0.1402	0.4314	0.1798
	MLR		4-1	0.2531	0.1969	0.1765	0.2291
Izmir	FFNN	E_P, R_S, $E_{P\,(t-12)}$	3-8-1	0.7575	0.1418	0.5666	0.1924
	ANFIS		Trapezoidal-5	0.7384	0.1472	0.6139	0.1816
	SVR		RBF	0.6696	0.1655	0.4239	0.2219
	MLR		3-1	0.572	0.1883	0.4341	0.2199
Samsun	FFNN	E_P, R_S, $E_{P\,(t-2)}$, $R_{S\,(t-2)}$, $E_{P\,(t-12)}$	5-13-1	0.5743	0.1405	0.4239	0.1905
	ANFIS		Triangular-5	0.6641	0.1248	0.4932	0.1787
	SVR		RBF	0.4219	0.1637	0.2932	0.2243
	MLR		5-1	0.401	0.1721	0.2618	0.2196

[a]RMSE : RMSE has no unit due to normalized data

The results in Table 4.6 show that the efficiency of the models to predict ET_0 decreases with increased step ahead, implying that the correlation between the inputs and output decreases as precedence horizon goes on, which weakens the Markovian characteristic of the inputs on output thereby lessening the models performances. The results also demonstrated the superiority in performance of AI models over MLR model whereby the AI models produced better performances across all of the modeling steps, which could be due to the inability of MLR model to deal with nonlinear behavior of the system. Drastic reduction in the performance and increase in error of MLR model could also be noticed which make it difficult to cope with future forecast of ET_0. For example, considering Ankara station, the DC and RMSE in the validation phase for single step ahead are 0.5490 and 0.1696 while the DC and RMSE in the validation phase for three step ahead are 0.1765 and 0.2291.

The results in Table 4.6 also show that the performances of the AI and MLR models in term of lower RMSE and higher DC in Adana station are better than in Samsun station across all steps of the modeling. This could be attributed to higher amount of precipitation receives by the MED climate, and based on water cycle concept, frequent evapotranspiration lead to condensation and eventual precipitation. This demonstrates that AI models estimate evapotranspiration easier when there is higher frequency of precipitation. The obtained results also show superior performance of Ankara station over Samsun station for the applied models. This is because Ankara station has semi-arid climate being located in CCAN environment, whereas Samsun station constitutes temperate climate of BLS region and AI models were developed to provide efficient predictions where empirical models fail to have

accurate predictions due to severe climate condition (more specifically arid and semi-arid climates), hence AI models may not produce peak performance in predicting ET_0 for stations with less extremity of climate.

In view of the results in Table 4.6 it can be seen that, both AI and MLR models provided lesser performances for Samsun station in comparison to other stations in all three steps of ET_0 predictions. The least performance among AI models is for SVR model, in Samsun station for three-step ahead ET_0 prediction, which has DC = 0.2932 and RMSE = 0.2243. This reveals that AI and MLR models performances are affected negatively by the BLS temperate climate of Samsun station, but the threat caused by the region climate can be resisted by AI based models, which across all modeling steps, provided efficient performance owing to their nonlinear nature and capability to overcome the uncertainty of the climate behavior. Moreover, despite the robustness of the AI based models and their ability to provide efficient and dependable results for BLS climate region, other stations have superior performances than Samsun station. This implies that even with the application of AI based models in such region, reliable results could be produced but not at the peak. The overall results of the stations located in Turkey show that ET_0 modeling is affected by the climate of the regions, with the least models performance from BLS region, followed by CCAN region, and best performance was achieved in MED region.

Figure 4.13 shows observed vs predicted scatter plots in the verification phase for the best performing ANFIS model for Turkey stations.

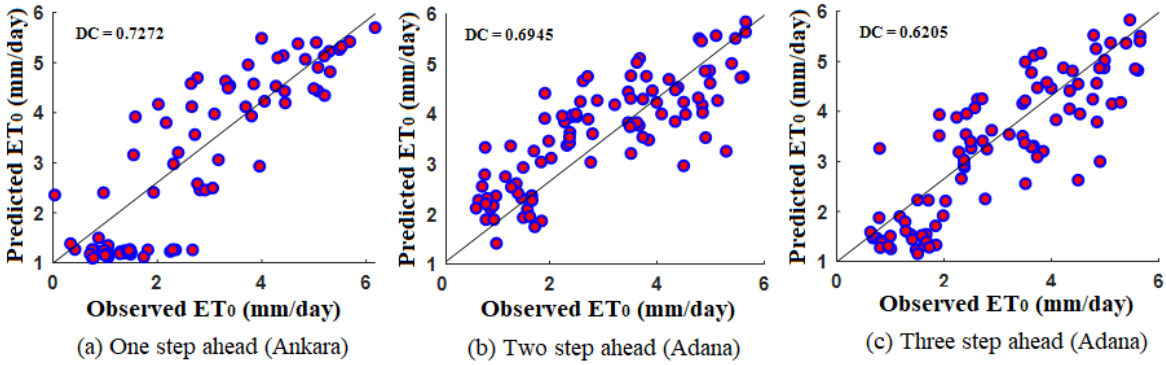

Figure 4.13: Observed vs computed scatter plots in the validation phase for the best-predicted ANFIS models, note that ET_0 values are daily values averaged over the month (i.e., $\frac{\sum ET_{0i}}{D}$ which D is number of days in that month)

4.2.1.2 Results for North Cyprus stations

Table 4.7 shows the models performances for single and multi-step ahead predictions of ET_0 for North Cyprus stations.

Table 4.7: Single and multi-step ahead modeling results for North Cyprus stations

					Training		Verification	
Step ahead	**Station**	**Model**	**Inputs**	**Structure**	**DC**	**RMSE[a]**	**DC**	**RMSE[a]**
One step ahead ($ET_{0\ t+1}$)	Famagusta	FFNN	E_P, R_S, $E_{P\ (t-1)}$, $R_{S\ (t-1)}$	4-10-1	0.7757	0.1227	0.7713	0.1304
		ANFIS		Triangular-4	0.7942	0.1225	0.772	0.1249
		SVR		RBF	0.773	0.1258	0.7599	0.1312
		MLR		4-1	0.6533	0.1622	0.5421	0.1737
	Kyrenia	FFNN	E_P, R_S, $E_{P\ (t-1)}$, $R_{S\ (t-1)}$	4-9-1	0.8114	0.102	0.7089	0.1409
		ANFIS		Triangular-4	0.8056	0.1035	0.7584	0.1283
		SVR		RBF	0.8278	0.0974	0.6341	0.1579
		MLR		4-1	0.4458	0.1845	0.3758	0.1989
	Morphou	FFNN	E_P, R_S, $E_{P\ (t-1)}$, $R_{S\ (t-1)}$	4-8-1	0.7692	0.1451	0.7133	0.151
		ANFIS		Gausian-4	0.7839	0.1404	0.7382	0.1442
		SVR		RBF	0.7577	0.1487	0.7169	0.1499
		MLR		4-1	0.6213	0.1859	0.4514	0.2088
	Nicosia	FFNN	E_P, R_S, $E_{P\ (t-1)}$, $R_{S\ (t-1)}$	4-12-1	0.6378	0.1518	0.6075	0.176
		ANFIS		Triangular-4	0.6992	0.1383	0.6197	0.1733
		SVR		RBF	0.7422	0.1281	0.6802	0.1589
		MLR		4-1	0.4397	0.1927	0.3545	0.2236
	Famagusta	FFNN		4-11-1	0.5791	0.166	0.5453	0.1868

		ANFIS	E_P, R_S, $E_{P\,(t-3)}$, $R_{S\,(t-6)}$	Trapezoidal-4	0.5808	0.1657	0.5778	0.18
		SVR		RBF	0.626	0.1565	0.5779	0.1799
		MLR		4-1	0.3918	0.216	0.2684	0.2189
	Kyrenia	FFNN	E_P, R_S, $E_{P\,(t-3)}$, $R_{S\,(t-6)}$	4-10-1	0.7906	0.114	0.764	0.12
		ANFIS		Triangular-4	0.8053	0.1035	0.7643	0.1273
		SVR		RBF	0.8275	0.0974	0.6433	0.1566
		MLR		4-1	0.4024	0.1851	0.3771	0.2028
Two step ahead ($ET_{0\,t+2}$)	Morphou	FFNN	E_P, R_S, $E_{P\,(t-3)}$, $R_{S\,(t-6)}$	4-11-1	0.5916	0.1935	0.5176	0.1951
		ANFIS		Trapezoidal-4	0.6345	0.183	0.504	0.1978
		SVR		RBF	0.6238	0.1857	0.5597	0.1864
		MLR		4-1	0.6208	0.1864	0.4526	0.2078
	Nicosia	FFNN	E_P, R_S, $E_{P\,(t-3)}$, $R_{S\,(t-6)}$	4-13-1	0.6535	0.1492	0.6099	0.1747
		ANFIS		Gaussian-4	0.6836	0.1426	0.6221	0.1719
		SVR		RBF	0.7322	0.1312	0.6809	0.158
		MLR		4-1	0.3431	0.2054	0.2454	0.243
	Famagusta	FFNN	E_P, R_S, $E_{P\,(t-6)}$, $R_{S\,(t-12)}$	4-9-1	0.5907	0.1665	0.5741	0.1791
		ANFIS		Gaussian-4	0.587	0.1656	0.579	0.1799
		SVR		RBF	0.6241	0.1564	0.5876	0.1797
		MLR		4-1	0.4123	0.2146	0.2661	0.2186
	Kyrenia	FFNN	E_P, R_S, $E_{P\,(t-6)}$, $R_{S\,(t-12)}$	4-10-1	0.7569	0.1152	0.7508	0.1334
		ANFIS		Gaussian-4	0.8013	0.1041	0.7774	0.1261
		SVR		RBF	0.8261	0.0974	0.6688	0.1538
		MLR		4-1	0.3793	0.1853	0.3769	0.2057
Three step ahead ($ET_{0\,t+3}$)	Morphou	FFNN	E_P, R_S, $E_{P\,(t-6)}$, $R_{S\,(t-12)}$	4-12-1	0.5646	0.1952	0.5112	0.203
		ANFIS		Trapezoidal-4	0.6465	0.1829	0.5005	0.1973
		SVR		RBF	0.6316	0.1862	0.5551	0.1867
		MLR		4-1	0.5552	0.2051	0.4112	0.2143
	Nicosia	FFNN	E_P, R_S, $E_{P\,(t-6)}$, $R_{S\,(t-12)}$	4-13-1	0.6744	0.1469	0.6544	0.1636
		ANFIS		Triangular-4	0.677	0.1463	0.6207	0.1714
		SVR		RBF	0.7359	0.1323	0.676	0.1584
		MLR		4-1	0.3846	0.1979	0.2368	0.2454

[a]RMSE : RMSE has no unit due to normalized data

More accurate and reliability estimates of ET_0 are provided by AI based models in comparison to linear models among the applied models. For one-step ahead modeling, the MLR models yielded acceptable results based on the performance evaluation criteria applied for the ET_0 prediction in both training and validation phases. Nevertheless, with further predictions ahead, MLR models failed to give reliable performance especially in the validation phase. This could be because MLR model generates more error with further predictions ahead due to the presence of nonlinear behavior of ET_0. It is apparent from the

results shown in Table 4.7 that both AI and MLR models produced better results for Famagusta station for single step ahead prediction (compared to their performances in other stations) but provided better predictions for two and three-step ahead predictions in Kyrenia station. The better performance of MLR model in Famagusta station could be due to the effect of the input combination applied, so that the data for the station behave more linear which led to less error and better efficiency than the other stations but magnified with further predictions ahead. Kyrenia on the other hand, has unique characteristics among the stations, the hills and valley nature of its terrain, the presence of rocks surrounding the region, higher precipitation frequency etc. These could strengthen the bond between previous and future ET_0.

Despite the reduction in performance due to increase in error and uncertainty for future ET_0 prediction, the performances of all the AI based models are found to be promising across the study stations, which could be attributed to their capability of containing the complex ET_0 process. Considering single step ahead predictions, ANFIS achieved better predictions in both training and validation phases for Famagusta and Morphou stations with DC = 0.7942, RMSE = 0.1225 and DC = 0.7720, RMSE = 0.1249 for Famagusta, DC = 0.7839, RMSE = 0.1404 and DC = 0.7382, RMSE = 0.1442 for Morphou in the training and validation phases, respectively. In the validation phase of Kyrenia station, SVR was found to have inferior performance compared to ANFIS by 2%, but produced better results in the training phase. In Nicosia station, also higher prediction accuracy was demonstrated by SVR model over ANFIS and FFNN models. The efficient performance of the ANFIS in Famagusta, Morphou and Kyrenia in the validation phase despite ANN's ability of handling various real world problems, may likely be associated with the ANN shortcomings in dealing with less accurate and uncertain data. Consequently, with incorporation of fuzzy logic ability and neural network concept for handing uncertainty of a process, the better option might be ANFIS (Moghaddamnia et al., 2009).

Table 4.7 also shows the multi-step ahead time series predictions for two and three-step ahead. With the implementation of machine learning models such as neural networks, more robust and more reliable performances were achieved despite increase in time lags and 3 AI models (FFNN, ANFIS, and SVR) were found to have promising performances by maintaining good generalization capability up to three step ahead. In contrast, MLR model

performance was relatively poor for further time step ahead. The underperformance of MLR could be because (a) most time series data contain nonlinear property and MLR being a linear model could not cope with a nonlinear process (b) it is difficult to achieve multi-step ahead prediction successfully with a linear model due to lack of real data to adjust the performance of the model for the future (c) Error from the first step ahead prediction could be accumulated at the beginning and propagates to the future, which could lead to poor prediction.

It is observed from the single and multi-step ahead prediction results in Table 4.7 that, the ability to achieve high correlation by almost all models decreases with further step ahead which could be obvious owing to decrease in generalization capabilities and error propagation of the models, but certain models for certain stations achieved higher predictions with further step ahead (for instance, ANFIS model in the validation phase of Kyrenia station which has DCs = 0.7584, 0.7643, 0.7774 and RMSEs = 0.1283, 0.1273, 0.1261 for one-step, two-step, and three-step ahead predictions, respectively). This could be because the models were developed with increasing time lags for further steps ahead, thus by the first few lags, perhaps an important period (value) that has great influence on the ET_0 is removed which may distort the entire data and subsequently affects the performance of the data driven models. On the other hand, as the lagging continuous, a point would be reached where the time lags covered the entire season which balanced the missing values and hence, results in better performance of the model.

Figure 4.14 shows observed vs predicted scatter plots in the verification phase for the best performing ANFIS model for North Cyprus stations, as example.

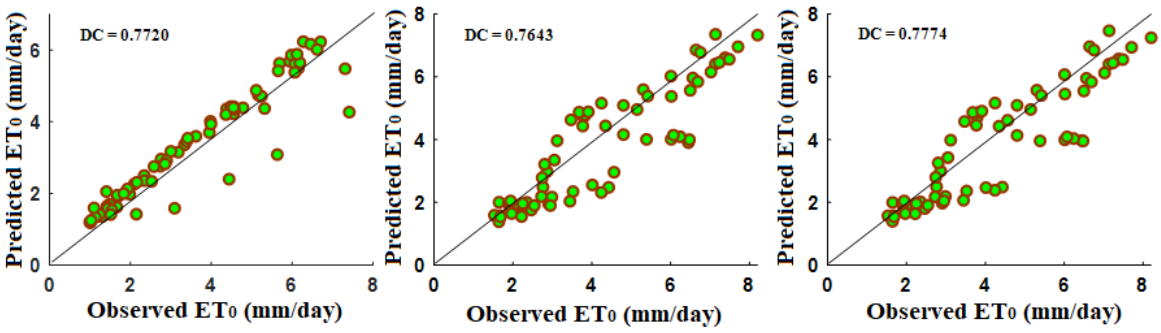

(a) One step ahead (Famagusta) (b) Two step ahead (Kyrenia) (c) Three step ahead (Kyrenia)

Figure 4.14: Observed vs computed scatter plots in the validation phase for the best-predicted ANFIS models

4.2.1.3 Results for Iraq stations

The single and multi-step ahead results for Erbil and Salahaddin stations are presented in Table 4.8.

Table 4.8: Single and multi-step ahead modeling results for Iraq stations

					Training		Verification	
Step ahead	**Station**	**Model**	**Inputs**	**Structure**	**DC**	**RMSE[a]**	**DC**	**RMSE[a]**
One step ahead ($ET_{0\ t+1}$)	Erbil	FFNN	E_P, R_S, E_P $_{(t-1)}$	3-7-1	0.8237	0.1166	0.725	0.1526
		ANFIS		Triangular-3	0.8245	0.1163	0.7632	0.1416
		SVR		RBF	0.8001	0.1242	0.6892	0.1622
		MLR		3-1	0.6776	0.1577	0.5939	0.1854
	Salahaddin	FFNN	E_P, R_S, E_P $_{(t-1)}$, R_S $_{(t-1)}$	4-10-1	0.6421	0.1446	0.539	0.1621
		ANFIS		Triangular-4	0.7331	0.1248	0.6167	0.1478
		SVR		RBF	0.6274	0.1475	0.5655	0.1573
		MLR		4-1	0.3549	0.1941	0.2436	0.2078
Two step ahead ($ET_{0\ t+2}$)	Erbil	FFNN	E_P, R_S, E_P $_{(t-6)}$	3-6-1	0.8355	0.1126	0.7125	0.156
		ANFIS		Trapezoidal-3	0.8011	0.1239	0.7255	0.1524
		SVR		RBF	0.7938	0.1261	0.7172	0.1547
		MLR		3-1	0.6306	0.1688	0.5622	0.1925
	Salahaddin	FFNN	E_P, R_S, E_P $_{(t-2)}$, R_S $_{(t-3)}$	4-9-1	0.6393	0.1451	0.5208	0.1652
		ANFIS		Triangular-4	0.6633	0.1402	0.5901	0.1528
		SVR		RBF	0.6028	0.1523	0.5597	0.1584
		MLR		4-1	0.3184	0.1995	0.2083	0.2124
Three step ahead ($ET_{0\ t+3}$)	Erbil	FFNN	E_P, R_S, E_P $_{(t-12)}$	3-7-1	0.7012	0.1518	0.6779	0.1651
		ANFIS		Gausian-3	0.7809	0.1299	0.6849	0.1633
		SVR		RBF	0.6919	0.1541	0.5591	0.1932

	MLR		3-1	0.4989	0.1966	0.4004	0.2253
Salahaddin	FFNN	E_P, R_S, $E_{P(t-2)}$, $R_{S(t-12)}$	4-10-1	0.4656	0.1767	0.381	0.1878
	ANFIS		Gausian-4	0.4655	0.1767	0.374	0.1889
	SVR		RBF	0.3657	0.1925	0.2761	0.2031
	MLR		4-1	0.3096	0.2008	0.2044	0.2129

[a]RMSE : RMSE has no unit due to normalized data

Based on the results given in Table 4.8, it can be seen that, the performances of the models for single and multi-step ahead ET_0 predictions are higher for Erbil station than Salahaddin station. This revealed that climate of the region not only affects the ET_0 prediction for current time but also affects ET_0 predictions for further time ahead. Although the climate of Salahaddin station has been categorized as semi-arid, Sarlak and Agha (2018) study reveals that the station's aridity changes depending on the applied aridity index and the time of investigation. For instance, between 1980 – 2011 the station was identified as sub-humid using UNEP (1992) aridity index, semi-arid between 1998 – 2011 and sub-humid between 1980 – 1997. The fluctuating nature of the climate makes ET_0 estimation difficult in the Salahaddin station. As elements of different climatic regions are contained in the long time data record, the AI and MLR models fail to provide much reliable estimations in comparison to Erbil station. This results in least performance of the applied models in Salahaddin compared to Erbil stations. The models applied for single and multi-step ahead ET_0 predictions in Erbil station led to higher values of ET_0 estimates but AI models provided superior performance than MLR model. Figure 4.15 shows observed vs predicted scatter plots in the verification phase for the best performing ANFIS model for Iraq stations.

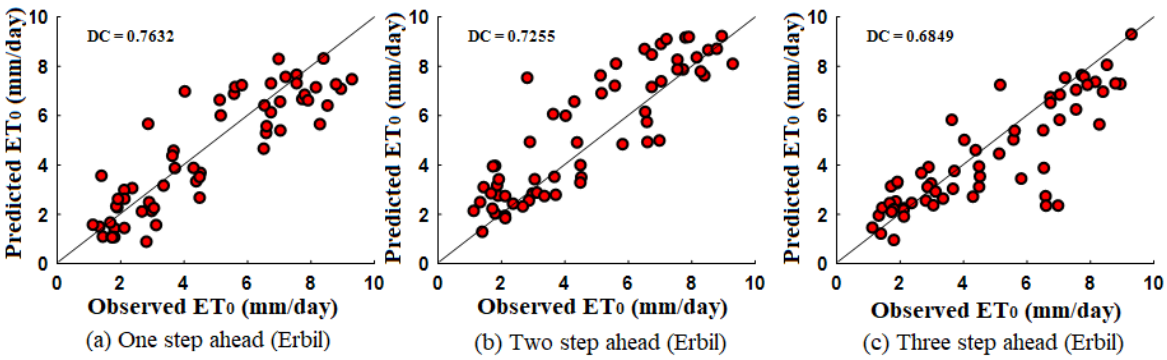

Figure 4.15: Observed vs computed scatter plots in the validation phase for the best-predicted ANFIS models

Comparing the results in Tables 4.6-4.8, it could be seen that for Turkey, Cyprus and Iraq stations, the black box models performances are inferior to that of Nourni et al. (2019a) study across all the 3 steps of the modeling. This is because current data have a strong bond with the correlation of inputs and output which in turns bonded to Markov chain of ET_0 process. As data lag occurs, the correlation bond between inputs and output weakens, thereby resulting in weak Markov chain and thus, reduces the performance of the black box models. Whereas in the case of first phase of this study, with no data lag, correlation (between inputs and output) and the Markovian process are of strong agreement and consequently, resulting in higher performance of the black box models.

For instance, Figure 4.16 shows a section of three step ahead time series modeling of Kyrenia station by FFNN, ANFIS, SVR and MLR. For better visibility of each model estimated values of ET_0, only 12 months' period of the time series is shown (January, 2011 – December, 2011).

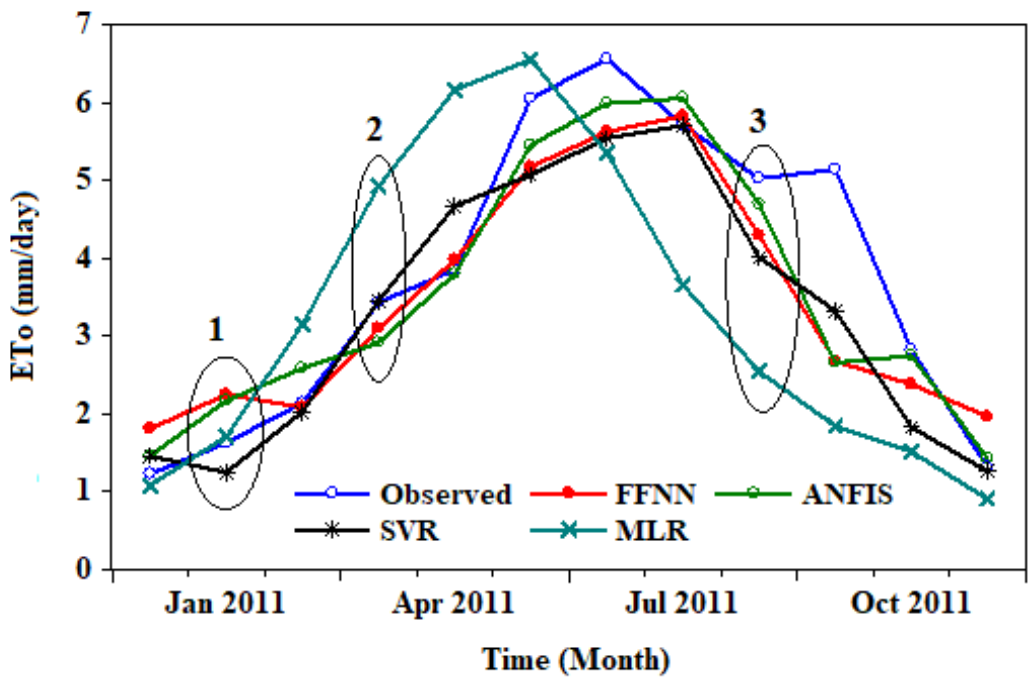

Figure 4.16: Observed versus predicted ET_0 values for three-step ahead predictions for Kyrenia station

As revealed in Figure 4.16, the months of February, April and September are selected randomly as points 1, 2, and 3, respectively. With regards to the first point (point 1), MLR = 1.7 mm/day, SVR = 1.2 mm/day, ANFIS = 2.2 mm/day, FFNN = 2.2 mm/day and observed = 1.6 mm/day. This implies that MLR value is more fitted to the observed than the other models which in turn revealed that even the poorest performing model, at certain point of the time series could be the best. At point 2, MLR = 4.9 mm/day, SVR = 3.4 mm/day, ANFIS = 2.9 mm/day, FFNN = 3.1 mm/day and observed = 3.4 mm/day. This shows that the SVR model performed better in terms of predicted vs observed agreement, MLR model has the least accuracy at 4th rank in April compared to being the best in the month of February. At the final point (point 3), MLR = 2.5 mm/day, SVR = 4.0 mm/day, ANFIS = 4.7 mm/day, FFNN = 4.3 mm/day and observed = 5.0 mm/day. This shows less deviation of the ANFIS model from the observed value in contrast to the others, and SVR model performed better at point 2 and 3rd at point 3. From the results of these three selected points, it is apparent that at different time points, different models could exhibit varied performance from different data aspects. Therefore, the precise target can be captured better via ensemble approaches, which amalgamate the outputs of the single models. In this respect, SA, WA and NE ensemble models were developed for single and multi-step ahead modeling.

4.2.2 Results of the ensemble techniques

The individual models outputs were used as the ensemble models inputs. For higher achievement of performance, the weights for WA ensembles were generated via three methods; (i) using only training data set, (ii) using only validation data set, (iii) using both data sets of validation and training. The third weights generation method led to superior result and hence, applied for the weight generation in all Turkey, North Cyprus and Iraq stations.

Similar to FFNN single models, the LM algorithm was used to train the NE models and for both hidden and output layers, tangent sigmoid was utilized as the activation function. To determine the number of hidden neurons and best epoch number, trial and error approach was employed. ANN was chosen for the NE modeling in this study over ANFIS and SVR models due to its compatibility, popularity as well as its accuracy in ensemble modeling as demonstrated in many studies, such as Kiran and Ravi (2008); Sharghi et al. (2018); Nourani

et al. (2019 a,b). Nevertheless, other AI models (ANFIS and SVR) could also be used as the kernel.

Tables 4.9-4.11 depict the obtained ensemble models results for all modeling steps across all stations. The SA structure a-b serve as number of inputs and ET_0 as output, w, x, y, z for WA express the weights generated by the applied models and lastly, the ensemble structure of FFNN is as previously explained for single FFNN model.

Table 4.9 gives the single and multi-step ahead results of the ensemble predictions for Samsun Izmir, Ankara, and Adana stations of Turkey.

Table 4.9: The results of the ensemble models for Turkey stations

				Training		Validation	
Step ahead	**Station**	**Model**	**Model structure**	**DC**	**RMSE[a]**	**DC**	**RMSE[a]**
One step ahead	Adana	SA	4-1	0.7982	0.1175	0.7887	0.1082
		WA	0.2473, 0.2596, 0.2545, 0.2387	0.7962	0.1181	0.7866	0.1087
		NE	4-8-1	0.8952	0.0847	0.8775	0.0824
	Ankara	SA	4-1	0.7730	0.1203	0.7495	0.1140
		WA	0.2727, 0.2745, 0.2508, 0.2019	0.7767	0.1193	0.7472	0.1172
		NE	4-6-1	0.8291	0.1044	0.8083	0.0998
	Izmir	SA	4-1	0.7322	0.1513	0.6153	0.1785
		WA	0.2589, 0.2562, 0.2472, 0.2376	0.7330	0.1510	0.6159	0.1784
		NE	4-10-1	0.7594	0.1434	0.6352	0.1739
	Samsun	SA	4-1	0.6451	0.1496	0.5457	0.1452
		WA	0.2744, 0.3168, 0.2120, 0.1967	0.6652	0.1459	0.5701	0.1412
		NE	4-7-1	0.7181	0.1143	0.6905	0.1397
Two step ahead	Adana	SA	4-1	0.7209	0.1382	0.6791	0.1333
		WA	0.2486, .2537, 0.2669, 0.2308	0.7233	0.1376	0.6826	0.1326
		NE	4-9-1	0.8024	0.1163	0.7648	0.1141
	Ankara	SA	4-1	0.7505	0.1261	0.6275	0.1391
		WA	0.2515, 0.2596, 0.2488, 0.2401	0.7504	0.1261	0.6239	0.1397
		NE	4-11-1	0.8294	0.1043	0.7498	0.1139
	Izmir	SA	4-1	0.5933	0.1836	0.4236	0.2219
		WA	0.2790, 0.2792, 0.2296, 0.2123	0.6006	0.1819	0.4285	0.2209
		NE	4-13-1	0.6564	0.1687	0.5230	0.2019
	Samsun	SA	4-1	0.5731	0.1407	0.4275	0.1899
		WA	0.2823, 0.3213, 0.2003, 0.1960	0.5975	0.1366	0.4463	0.1868

		NE	4-6-1	0.7212	0.1137	0.5433	0.1697
Three step ahead	Adana	SA	4-1	0.6568	0.1533	0.6343	0.1423
		WA	0.2698, 0.2605, 0.2366, 0.2332	0.6597	0.1526	0.6359	0.1420
		NE	4-11-1	0.7852	0.1213	0.7379	0.1205
	Ankara	SA	4-1	0.7284	0.1316	0.6057	0.1431
		WA	0.2993, 0.3030, 0.2910, 0.1067	0.7435	0.1279	0.5534	0.1523
		NE	4-10-1	0.8536	0.0966	0.7800	0.1069
	Izmir	SA	4-1	0.7243	0.1512	0.5477	0.1966
		WA	0.2772, 0.2831, 0.2290, 0.2107	0.7322	0.1489	0.5572	0.1945
		NE	4-12-1	0.7977	0.1295	0.7529	0.1453
	Samsun	SA	4-1	0.5759	0.1403	0.4284	0.1898
		WA	0.2786, 0.3230, 0.197, 0.1954	0.6004	0.1361	0.4467	0.1867
		NE	4-8-1	0.7154	0.1149	0.5794	0.1628

[a]RMSE : RMSE has no unit due to normalized data

The results in Table 4.9 show the ability of ensemble models for improving the prediction accuracy of single and multi-step ahead models. The results indicate that SA, WA and NE models could be employed successfully for performance improvement of single and multi-step ahead models. Nevertheless, NE model performed better than the other methods due to nonlinear kernel applied for its development. NE improved accuracy of the highest performing model (ANFIS) for single and multi-step ahead predicts for Turkey stations in the validation phase by 16%, 8%, 2% and 4% for one-step ahead modeling, 7%, 26%, 8%, and 5% for two-step ahead modeling and 12%, 30%, 14%, and 8% for three-step ahead modeling for Adana, Ankara, Izmir and Samsun, respectively. The NE approach improved the efficiency of the lowest performing model (MLR) for single and multi-step ahead predicts of ET_0 for Turkey stations in the validation phase by 25%, 26%, 4% and 35% for one-step ahead modeling, 15%, 19%, 15%, and 26% for two-step ahead modeling and 19%, 60%, 32%, and 32% for three-step ahead modeling for Adana, Ankara, Izmir and Samsun, respectively.

Comparing the results from Tables 4.6 and 4.9, it can be deduced that, unlike in the case of single models where the modeling accuracy decreases with further time step ahead, the capability of ensemble approaches to improve prediction accuracy increases with further step ahead. For instance, for performance improvement over ANFIS, the models for Ankara, Izmir and Samsun stations were improved by 8%, 2% and 4% for one-step ahead but

improved by 30%, 14%, and 8% for three-step ahead modeling. Similarly, for Ankara and Izmir, the MLR models were initially improved by 26% and 4% for one-step ahead modeling but improved to 60% and 32% for three-step ahead.

The ensemble results for single and multi-step ahead predictions of ET_0 for Nicosia, Morphou, Kyrenia and Famagusta (North Cyprus) stations are presented in Table 4.10.

Table 4.10: The results of the ensemble models for North Cyprus stations

				Training		Validation	
Step ahead	**Station**	**Model**	**Model structure**	**DC**	**RMSE[a]**	**DC**	**RMSE[a]**
One step ahead	Famagusta	SA	4-1	0.7973	0.1240	0.7621	0.1252
		WA	0.2648, 0.2681, 0.2624, 0.2046	0.7974	0.1239	0.7665	0.1240
		NE	4-10-1	0.8111	0.1177	0.7896	0.1197
	Kyrenia	SA	4-1	0.7558	0.1160	0.6730	0.1493
		WA	0.2867, 0.2950, 0.2757, 0.1426	0.7916	0.1072	0.6989	0.1433
		NE	4-8-1	0.9483	0.0534	0.9188	0.0744
	Morphou	SA	4-1	0.7779	0.1424	0.7062	0.1528
		WA	0.2670, 0.2742, 0.2656, 0.1932	0.7800	0.1417	0.7147	0.1506
		NE	4-9-1	0.7498	0.1410	0.7446	0.1527
	Nicosia	SA	4-1	0.6699	0.1449	0.5808	0.1819
		WA	0.2702, 0.2862, 0.3087, 0.1349	0.6976	0.1387	0.6167	0.1739
		NE	4-10-1	0.8366	0.1019	0.7842	0.1305
Two step ahead	Famagusta	SA	4-1	0.5744	0.1686	0.5659	0.1807
		WA	0.2711, 0.2794, 0.2903, 0.1592	0.5907	0.1637	0.5884	0.1777
		NE	4-12-1	0.7492	0.1282	0.7351	0.1425
	Kyrenia	SA	4-1	0.7450	0.1184	0.7184	0.1392
		WA	0.2893, 0.2920, 0.2737, 0.1450	0.7789	0.1103	0.7445	0.1326
		NE	4-8-1	0.9514	0.0517	0.9339	0.0675
	Morphou	SA	4-1	0.6502	0.1791	0.5245	0.1937
		WA	0.2462, 0.2527, 0.2710, 0.2383	0.6530	0.1783	0.5233	0.1940
		NE	4-9-1	0.6729	0.1732	0.6341	0.1699
	Nicosia	SA	4-1	0.6582	0.1482	0.5859	0.1800
		WA	0.2764, 0.2857, 0.3092, 0.1287	0.6912	0.1408	0.6225	0.1719
		NE	4-10-1	0.8077	0.1115	0.8063	0.1227
Three step ahead	Famagusta	SA	4-1	0.5918	0.1696	0.5583	0.1788
		WA	0.2760, 0.2762, 0.2871, 0.1607	0.6050	0.1649	0.5822	0.1760
		NE	4-8-1	0.7140	0.1406	0.6963	0.1497

Kyrenia	SA	4-1	0.7404	0.1189	0.7172	0.1421
	WA	0.2887, 0.3023, 0.2862, 0.1573	0.7636	0.1146	0.7592	0.1299
	NE	4-11-1	0.9487	0.0529	0.8745	0.0947
Morphou	SA	4-1	0.6256	0.1882	0.5139	0.1947
	WA	0.2458, 0.2621, 0.2712, 0.2208	0.7764	0.1412	0.7442	0.1455
	NE	4-9-1	0.8717	0.1102	0.8265	0.1163
Nicosia	SA	4-1	0.6760	0.1466	0.6135	0.1730
	WA	0.2750, 0.2685, 0.2922, 0.1643	0.6939	0.1424	0.6340	0.1684
	NE	4-8-1	0.8065	0.1194	0.7849	0.1224

[a]RMSE : RMSE has no unit due to normalized data

The results in Table 4.10 affirm the ability of ensemble modeling in improving the performance of the single and multi-step ahead models. For instance, NE models improved performance of ANFIS model in the validation phase up to 2%, 16%, 1% and 16% for one-step ahead modeling, 15%, 17%, 13%, and 19% for two-step ahead modeling and 12%, 9%, 33%, and 16% for three-step ahead modeling for Famagusta, Kyrenia, Morphou and Nicosia, respectively. It is discovered that not significant improvement in DCs and RMSEs were attained by SA and WA ensembles over single and multi-step ahead AI models in both phases of training and validation, but remarkably higher performance was achieved by NE models. As earlier clarified, different data behavior at different points in time could be grabbed with overestimation and underestimation of ET_0 by distinct models. Yet, with each model particular capability, in comparison to the case of single models, better simulation of the underlying process could be achieved. In this study, the referred ensemble results (Table 4.10) show that the difference in performance between SA and WA ensemble models are not wide in most cases but WA models are superior in performance. This is due to linear or direct relationship that SA and WA ensemble models shared with the single and multi-step ahead models. However, WA model produced better prediction performance due to weights applied for its development, which were generated according to the relative importance of the models. The performances of SA and WA ensemble models are by far inferior to NE models, owing to the following reasons: (i) nonlinear kernel was used in FFNN to simulate the system behavior, thus simulation by FFNN led to higher accuracy than the linear system of SA and WA methods. (ii) The SA and WA models overall results may be influenced by the performances of single models, signifying that lesser ensemble performances may be

achieved from poor performing single models due to the linear correlation that exists between the single models and SA and WA ensemble methods.

It is worth mentioning in view of the results that, the performance of ensemble models is not based on one, two or three-step ahead predictions, rather based on the ability of the single models to produce desired output. For instance, considering Table 4.10, Kyrenia has the highest performance among all stations, which is derived from the single and multi-step ahead models performance in Table 4.7. This shows that ensemble modeling follows the trend of models development. Signifying that input combination influences the performances of single and multi-step ahead models, and improvement in prediction by ensemble models increases with increased performances of the single and multi-step ahead models and vice versa.

Finally, the obtained results for single and multi-step ensemble models across two Iraq stations are presented in Table 4.11.

Table 4.11: The results of the ensemble models for Iraq stations

				Training		Validation	
Step ahead	**Station**	**Model**	**Model structure**	**DC**	**RMSE[a]**	**DC**	**RMSE[a]**
One step ahead	Erbil	SA	4-1	0.8597	0.1040	0.7895	0.1335
		WA	0.2626, 0.2692, 0.2525, 0.2156	0.8632	0.1027	0.7954	0.1316
		NE	4-8-1	0.9262	0.0754	0.9032	0.0905
	Salahaddin	SA	4-1	0.7436	0.1224	0.6465	0.1419
		WA	0.2779, 0.3003, 0.2784, 0.1434	0.7688	0.1162	0.6786	0.1353
		NE	4-8-1	0.8457	0.0949	0.8118	0.1035
Two step ahead	Erbil	SA	4-1	0.8275	0.1153	0.7229	0.1531
		WA	0.2679, 0.2642, 0.2615, 0.2064	0.8289	0.1149	0.7251	0.1525
		NE	4-9-1	0.8963	0.0894	0.8602	0.1088
	Salahaddin	SA	4-1	0.6567	0.1416	0.5632	0.1577
		WA	0.2779, 0.3176, 0.2806, 0.1239	0.6826	0.1362	0.5875	0.1533
		NE	4-13-1	0.7621	0.1179	0.6720	0.1367
Three step ahead	Erbil	SA	4-1	0.7343	0.1432	0.6395	0.1747
		WA	0.2760, 0.2934, 0.2504, 0.1800	0.7454	0.1401	0.6528	0.1714
		NE	4-9-1	0.8118	0.1205	0.7204	0.1538
	Salahaddin	SA	4-1	0.4426	0.1804	0.3506	0.1924
		WA	0.2979, 0.2954, 0.2258, 0.1809	0.4535	0.1786	0.3629	0.1905
		NE	4-8-1	0.5122	0.1688	0.4625	0.1750

[a]RMSE : RMSE has no unit due to normalized data

The results in Table 4.11 indicate that SA, WA and NE models could be employed successfully for performance improvement of the single and multi-step ahead models. However, NE model performed better than the other methods. It improved the accuracy of SVR model for Iraq stations in the validation phase by 21% and 24% for one-step ahead modeling, 14%, and 11% for two-step ahead modeling and 16% and 18% for three-step ahead modeling for Erbil and Salahaddin, respectively.

For example, Figure 4.17 shows observed vs predicted time series for the best ensemble models for one station from each country.

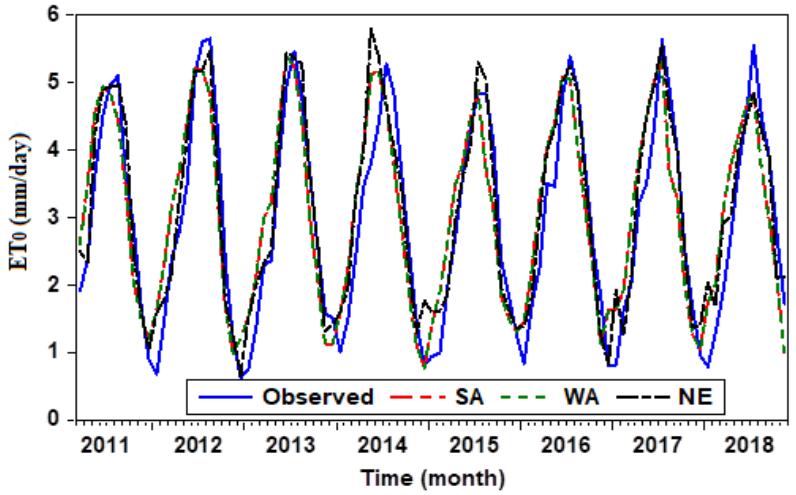

(a) Adana station (Turkey)

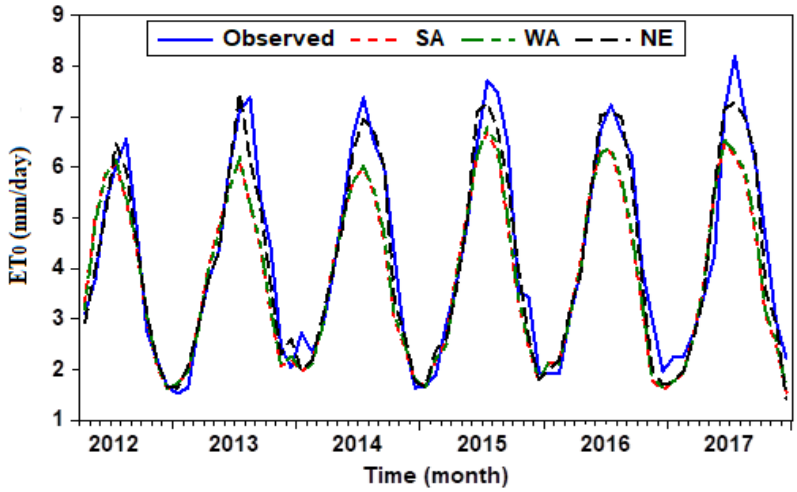

(b) Kyrenia station (North Cyprus)

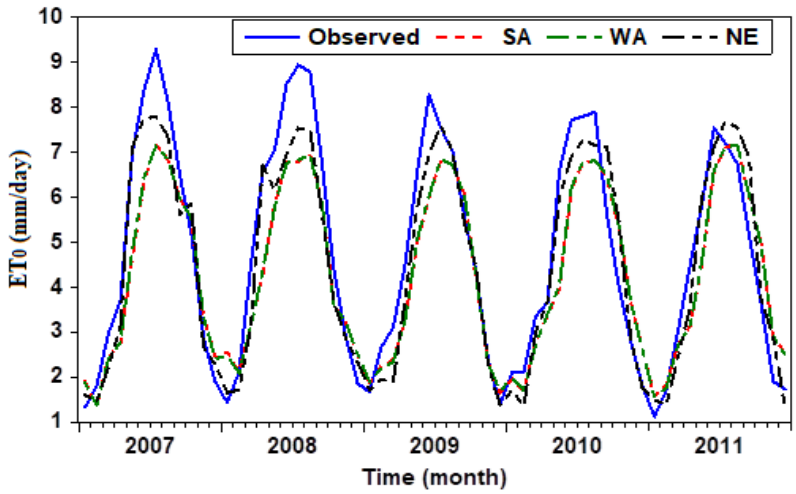

(c) Erbil station (Iraq)

Figure 4.17: Time series for the best performance ensemble models vs observed values

From the given Figure 4.17, it is apparent that SA and WA models are less accurate than NE models. The observed data are more fitted with values of the NE models, whereas fluctuations between observed and predicted values are wider in the case of SA and WA ensembles.

To ascertain the performance of all models across the study stations for single and ensemble modeling, DCs, and RMSEs average values of the models (MLR, SVR, ANFIS, FFNN and SA, WA, NE) were taken and presented in Table 4.12.

Table 4.12: Average performances of single and ensemble models across the study stations

		Single modeling				Ensemble modeling			
		Training		Validation		Training		Validation	
Step ahead	**Station**	**DC**	**RMSE[a]**	**DC**	**RMSE[a]**	**DC**	**RMSE[a]**	**DC**	**RMSE[a]**
One step ahead	Adana	0.7169	0.1392	0.6813	0.1327	0.8299	0.1068	0.8176	0.0998
	Ankara	0.7117	0.1300	0.6601	0.1363	0.7929	0.1147	0.7683	0.1103
	Izmir	0.7213	0.1541	0.6011	0.1818	0.7415	0.1486	0.6221	0.1769
	Samsun	0.5995	0.1578	0.4783	0.1545	0.6761	0.1366	0.6021	0.1420
	Famagusta	0.7491	0.1333	0.7113	0.1401	0.8019	0.1219	0.7727	0.1230
	Kyrenia	0.7227	0.1219	0.6193	0.1565	0.8319	0.0922	0.7636	0.1223
	Morphou	0.7330	0.1550	0.6550	0.1635	0.7692	0.1417	0.7218	0.1520
	Nicosia	0.6297	0.1527	0.5655	0.1830	0.7347	0.1285	0.6606	0.1621
	Erbil	0.7815	0.1287	0.6928	0.1605	0.8830	0.0940	0.8294	0.1185
	Salahaddin	0.5894	0.1528	0.4912	0.1688	0.7860	0.1112	0.7123	0.1269
Two step ahead	Adana	0.7000	0.1431	0.6510	0.1387	0.7489	0.1307	0.7088	0.1267
	Ankara	0.6733	0.1397	0.5040	0.1645	0.7768	0.1188	0.6671	0.1309
	Izmir	0.5629	0.1896	0.3930	0.2276	0.6168	0.1781	0.4584	0.2149
	Samsun	0.5176	0.1486	0.3828	0.1968	0.6306	0.1303	0.4724	0.1821
	Famagusta	0.5444	0.1761	0.4924	0.1914	0.6381	0.1535	0.6298	0.1670
	Kyrenia	0.7065	0.1250	0.6372	0.1517	0.8251	0.0935	0.7989	0.1131
	Morphou	0.6177	0.1872	0.5085	0.1968	0.6587	0.1769	0.5606	0.1859
	Nicosia	0.6031	0.1571	0.5396	0.1869	0.7190	0.1335	0.6716	0.1582
	Erbil	0.7653	0.1329	0.6794	0.1639	0.8509	0.1065	0.7694	0.1381
	Salahaddin	0.5560	0.1593	0.4697	0.1722	0.7005	0.1319	0.6076	0.1492
Three step ahead	Adana	0.6371	0.1532	0.5881	0.1552	0.7006	0.1424	0.6694	0.1349
	Ankara	0.6034	0.1493	0.3909	0.1846	0.7752	0.1187	0.6464	0.1341
	Izmir	0.6844	0.1607	0.5096	0.2040	0.7514	0.1432	0.6193	0.1788
	Samsun	0.5153	0.1503	0.3680	0.2033	0.6306	0.1304	0.4848	0.1798
	Famagusta	0.5535	0.1758	0.5017	0.1893	0.6369	0.1584	0.6123	0.1682

Kyrenia	0.6909	0.1255	0.6435	0.1548	0.8176	0.0955	0.7836	0.1222
Morphou	0.5995	0.1924	0.4945	0.2003	0.7579	0.1465	0.6949	0.1522
Nicosia	0.6180	0.1559	0.5470	0.1847	0.7255	0.1361	0.6775	0.1546
Erbil	0.6682	0.1581	0.5806	0.1867	0.7638	0.1346	0.6709	0.1666
Salahaddin	0.4016	0.1867	0.3089	0.1982	0.4694	0.1759	0.3920	0.1860

[a]RMSE : RMSE has no unit due to normalized data

As seen in Table 4.12 in single modeling for one time step ahead predictions in the validation phase, the models show identical performances with a narrow difference for Erbil, Morphou, Kyrenia, Famagusta, Izmir, Ankara, and Adana stations, which were because, all the climates of the stations are semiarid. This shows that despite the distance and locations of the stations from different countries, similarity of the climates led to similarity in models performances. Although Nicosia station is a Mediterranean semiarid climate as Famagusta, Kyrenia and Morphou, being an inland city reduces the Mediterranean (sea) effect of the station, thereby resulting in inferior modeling performance compared to the other stations. The average performance of the models in Samsun station is lower than other Turkey stations, which was because, Samsun station is BLS climate. The BLS climate has a uniform rainfall through the year, but selection of dominant input parameters showed that P_R is weak in Markovian process which made it to be poor input for single and multi-step ahead predictions of ET_0. This could be why the models performed better in other stations than Samsun station.

For two-step ahead predictions shown in Table 4.12, the average of models, performances are superior in Erbil station than all other stations in the verification phase. This could be because apart from being semiarid climate, the station is characterized by Sahara Desert, which could lead to increases in U_2 which in turn increases the rate of evapotranspiration. According to Nourani et al. (2019), U_2 could produce poor performance for single-input single-output prediction, but inclusion of U_2 in combination with other parameters could increase the prediction efficiency.

For three-step ahead predictions, the results in Table 4.12 for validation phase show that, Kyrenia station has the highest models performances. This is because R_S was found to have stronger bond with ET_0 among the input parameters, and due to the presence of higher mountains surrounding Kyrenia station, the radiant energy could reach the earth surface faster and with more effects than for flat surrounding stations.

As ensemble modeling improved performance of the single models, the average models results in Table 4.12 show that higher ensemble results were achieved by higher single models, but with the ability of nonlinear ensemble to deal with complex and uncertain problems, lower performance average models could produce highest performance ensemble models.

It can be seen that contrary to single modeling where less accurate results were obtained by this study compared to phase 1 study, more improvements were achieved by multi-step ahead ensemble modeling of ET_0 than the first phase of this study. For instance, in the validation phase of this study, the prediction improvements over SVR models were achieved up to 17%, 18% and 15% for Adana station, 10%, 13% and 11% for Nicosia station, and 25%, 11% and 19% for Salahaddin station for one, two and three step ahead ET_0 modeling against 4%, 2% and 6% improvements for Adana, Nicosia and Salahaddin stations by Nourani et al. (2019a) study. The results of this study affirmed the earlier assertion that lower performance models could lead to higher performance ensemble results (due to wider space for improvement) but more accurate and most efficient ET_0 modeling would be achieved from single models with higher performance. For examples, phase 1 ensemble study (because of the effect of more efficient single modeling) produced higher DCs, 0.9331, 0.8993, 0.8340 and RMSEs, 0.0687, 0.0805, 0.0971 for Adana, Nicosia, and Salahaddin stations, respectively. In comparison, in this study, lower DCs were obtained 0.8775, 0.7842, 0.8118 for one step ahead modeling, 0.7648, 0.8063, 0.6720 for two step ahead modeling, 0.7379, 0.7849, 0.4625 for three step ahead modeling and higher RMSEs, 0.0824, 0.1305, 0.1305 for one step ahead modeling, 0.1141, 0.1227, 0.1367 for two step ahead modeling and 0.1205, 0.1224, 0.1750 for three step ahead modeling.

ET process, just like any other natural process, may show both linear and nonlinear behaviors at different time spans. For example, in frozen days of winter, the ET time series gets small values having less complexity without significant fluctuations. In this case, a linear model may sufficiently lead to reliable results. When time series of the process includes both linear and nonlinear patterns, it is expected that the combination of linear and nonlinear models could lead to better final outcome. Such superior efficiency is reached via training of a black box ensemble method which learns using historical observations to apply appropriate weight to the components of the model at different patterns.

CHAPTER 5

CONCLUSION AND RECOMMENDATION

5.1 Conclusions

In this study, SA, WA and NE models were applied in phase 1 for ET_0 modeling and phase 2 for single and multi-step ET_0 modeling to improve performance of FFNN, ANFIS, SVR, MLR, HS, MHS, RT and MK models. Initially, sensitivity analysis was performed to determine the dominant inputs among the 12 variables obtained from Turkey (Adana, Ankara, Izmir and Samsun stations), Cyprus (Famagusta, Kyrenia, Morphou and Nicosia stations), Iraq (Erbil and Salahaddin stations), Iran (Tabriz and Urmia stations) and Libya (Sabha and Tripoli stations). In the absence of Lysimeter, a widely accepted method of ET_0 for practical problems is pan evaporation method. Therefore, pan evaporation method of ET_0 was used as the benchmark ET_0 for determining the performance of the developed models.

The results for phase 1 study showed that with location of most of the study stations to harsh climate conditions (arid and semi-arid), T_{mean}, T_{min}, T_{max} and R_S were generally the most effective variables for ET_0 modeling according to the sensitivity analysis results. Both the results of MLR and empirical models could be acceptable for ET_0 predictions. Due to the combine benefits of both fuzzy logic and neural network learning, the AI based models results demonstrated more efficiency of ANFIS over FFNN and SVR models. The results also exhibited that promising improvement could be achieved by ensemble models over single models. The application of ensemble learning led to increase in performance up to 22% over AI based models and up to 55% over empirical models.

The results for phase 2 study showed that AI models could be used to carry out multi-step ahead ET_0 predictions up to three step ahead successfully. With further step ahead predictions, mostly the AI based models performance decreased and MLR could not provide sufficient reliability in ET_0 modeling beyond one step ahead forecast. The results also emphasized that a successful application of ensemble modeling could lead to successful forecast of ET_0 up to three step ahead. The applied ensemble learning improved predictions

of single models averagely up to 23%, 19% and 35% for one step ahead, two step ahead and three step ahead ET_0 modeling, respectively.

The general results of this study demonstrated promising impact of combining models for ET_0 estimation. The obtained results from the ensemble methods more especially, neural ensemble method implied that better accuracy in ET_0 simulation can be achieved by combined outputs than individual models.

5.2 Recommendation

In view of the methodology applied and the results obtained, the following recommendations can be made:

- It is suggested to apply other emerging AI based techniques such as M5 model tree, random forest, genetic algorithm, multivariate adaptive regression splines, etc. as single models for ensemble modeling studies.
- The ensemble method should be applied for other hydro-climatic parameters such as precipitation, temperature, etc. to ascertain the difference in performance of ensemble learning for different processes. However, this study only used ANN as a kernel for nonlinear ensemble models, other models including ANFIS, SVR, etc. should be tested as nonlinear ensemble kernels to see their response to ensemble application.
- As the second phase of this study is limited to three step ahead predictions, further steps ahead should be investigated in future studies to see how efficient or otherwise could ensemble model performs with further forecast.
- In both phases of this studies, local calibration was done by training and validating models using data of own stations. Further studies should also perform external calibration which uses data from one station to train and validate models in another station. This might give idea on the applicability of ensemble learning for both local and external calibrations.

REFERENCES

Abdullah, S. S., Malek, M. A., Abdullah, N. S., and Mustapha, A. (2015a). Feedforward backpropagation, genetic algorithm approaches for predicting reference evapotranspiration. *Sains Malaysiana*, *44*(7), 1053-1059.

Abdullah, S. S., Malek, M. A., Abdullah, N. S., Kisi, O., and Yap, K. S. (2015b). Extreme learning machines: a new approach for prediction of reference evapotranspiration. *Journal of Hydrology*, *527*, 184-195.

Abdullah, S. S., Malek, M. A., Mustapha, A., and Aryanfar, A. (2014). Hybrid of Artificial Neural Network-Genetic Algorithm for Prediction of Reference Evapotranspiration (ET^ sub 0^) in Arid and Semiarid Regions. *Journal of Agricultural Science*, *6*(3), 191.

Abdullahi, J., and Elkiran, G. (2017). Prediction of the future impact of climate change on reference evapotranspiration in Cyprus using artificial neural network. *Procedia computer science*, *120*, 276-283.

Abdullahi, J., Elkiran, G., and Nourani, V. (2017). Application of Artificial Neural Network to predict reference evapotranspiration in Famagusta, North Cyprus. In *11th International Scientific Conference on Production Engineering Development And Modernization of Production* (pp. 549-554).

Adamala, S., Raghuwanshi, N. S., Mishra, A., and Singh, R. (2019). Generalized wavelet neural networks for evapotranspiration modeling in India. *ISH Journal of Hydraulic Engineering*, *25*(2), 119-131.

Ageena, I. (2013). *Trends and patterns in the climate of Libya (1945-2010)* (Doctoral dissertation), University of Liverpool, United Kingdom.

Akrami, S. A., Nourani, V., and Hakim, S. J. S. (2014). Development of nonlinear model based on wavelet-ANFIS for rainfall forecasting at Klang Gates Dam. *Water Resources Management*, *28*(10), 2999-3018.

Ali, A. A. (1997). Estimation of evapotranspiration in Libya under the impact of plausible global climate change. *Polish National Committee International Geosphere-Biosphere Programme*, *25*.

Aljumaili, K. K., Al-Khafaji, M. S., and Al-Awadi, A. T. (2014). Assessment of Evapotranspiration Estimation Models for Irrigation Projects in Karbala, Iraq. *Engineering and Technology Journal*, *32*(5), 1149-1157.

Allen, R. G., Pereira, L. S., Raes, D., and Smith, M. (1998). Crop evapotranspiration-Guidelines for computing crop water requirements-FAO Irrigation and drainage paper 56. *FAO, Rome*, *300*(9), D05109.

Aqil, M., Kita, I., Yano, A., and Nishiyama, S. (2007). Analysis and prediction of flow from local source in a river basin using a Neuro-fuzzy modeling tool. *Journal of Environmental Management*, *85*(1), 215-223.

Aschonitis, V. G., Lekakis, E., Tziachris, P., Doulgeris, C., Papadopoulos, F., Papadopoulos, A., and Papamichail, D. (2019). A ranking system for comparing models' performance combining multiple statistical criteria and scenarios: The case of reference evapotranspiration models. *Environmental modelling and software*, *114*, 98-111.

Awchi, T. A. (2008). Application of radial basis function neural networks for reference evapotranspiration prediction. *AL Rafdain Engineering Journal*, *16*(1), 117-130.

Bao, Y., Xiong, T., and Hu, Z. (2014). Multi-step-ahead time series prediction using multiple-output support vector regression. *Neurocomputing*, *129*, 482-493.

Bates, J. M., and Granger, C. W. J. (1969). The combination of forecasts. *Operations Research Quarterly 20*, 451–468.

Benediktsson, J. A., Sveinsson, J. R., Ersoy, O. K., and Swain, P. H. (1997). Parallel consensual neural networks. *IEEE Transactions on Neural Networks*, *8*(1), 54-64.

Benzaghta, M. A., and Lawgali, Y. F. (2014) Estimation of evapotranspiration using different climate models: A case study in semi-arid region-Libya. *Sirte University Scientific Journal*, *4*(1), 27-34.

Beven, K. (1979). A sensitivity analysis of the Penman-Monteith actual evapotranspiration estimates. *Journal of Hydrology*, *44*(3-4), 169-190.

Blaney, H. F. (1952). Determining water requirements in irrigated areas from climatological and irrigation data. *Food and Agricultural Organization of the United Nations (FAO).*

Breiman, L. (1996). Bagging predictors. *Machine Learning*, *24*(2), 123-140.

Brutsaert, W. (1982). The surface roughness parameterization. In *Evaporation into the Atmosphere*, 113-127.

Čadro, S., Cherni-Čadro, S., Marković, M., and Žurovec, J. (2019). A reference evapotranspiration map for Bosnia and Herzegovina. *International Soil and Water Conservation Research*, *7*(1), 89-101.

Carter, C., and Liang, S. (2019). Evaluation of ten machine learning methods for estimating terrestrial evapotranspiration from remote sensing. *International Journal of Applied Earth Observation and Geoinformation*, *78*, 86-92.

Chen, D., Gao, G., Xu, C. Y., Guo, J., and Ren, G. (2005). Comparison of the Thornthwaite method and pan data with the standard Penman-Monteith estimates of reference evapotranspiration in China. *Climate Research*, *28*(2), 123-132.

Citakoglu, H., Cobaner, M., Haktanir, T., and Kisi, O. (2014). Estimation of monthly mean reference evapotranspiration in Turkey. *Water Resources Management*, *28*(1), 99-113.

Cobaner, M., Citakoğlu, H., Haktanir, T., and Kisi, O. (2016). Modifying Hargreaves–Samani equation with meteorological variables for estimation of reference evapotranspiration in Turkey. *Hydrology Research*, *48*(2), 480-497.

Cuenca, R. H. (1989). *Irrigation system design: an engineering approach.* 1st ed. Englewood Cliffs (NJ): Prentice-Hall; p. 552.

Dinpashoh, Y. (2006). Study of reference crop evapotranspiration in IR of Iran. *Agricultural Water Management*, *84*(1-2), 123-129.

Dinpashoh, Y., Jhajharia, D., Fakheri-Fard, A., Singh, V. P., and Kahya, E. (2011). Trends in reference crop evapotranspiration over Iran. *Journal of Hydrology*, *399*(3-4), 422-433.

Dinpashoh, Y., Jahanbakhsh-Asl, S., Rasouli, A. A., Foroughi, M., and Singh, V. P. (2019). Impact of climate change on potential evapotranspiration (case study: west and NW of Iran). *Theoretical and applied climatology*, *136*(1-2), 185-201.

Djaman, K., Irmak, S., Kabenge, I., and Futakuchi, K. (2016). Evaluation of FAO-56 penman-monteith model with limited data and the valiantzas models for estimating grass-reference evapotranspiration in Sahelian conditions. *Journal of Irrigation and Drainage Engineering*, *142*(11), 04016044.

Djaman, K., O'Neill, M., Diop, L., Bodian, A., Allen, S., Koudahe, K., and Lombard, K. (2019). Evaluation of the Penman-Monteith and other 34 reference evapotranspiration equations under limited data in a semiarid dry climate. *Theoretical and Applied Climatology*, *137*(1-2), 729-743.

Doğan, E. (2009). Reference evapotranspiration estimation using adaptive neuro-fuzzy inference systems. *Irrigation and Drainage*, *58*(5), 617-628.

Dou, X., and Yang, Y. (2018). Evapotranspiration estimation using four different machine learning approaches in different terrestrial ecosystems. *Computers and electronics in agriculture*, *148*, 95-106.

Ekhmaj, A. I. (2012). Prediction of Evapotranspiration using Artificial Neural Networks Model. *Buhri Arifin, SitiNurAfifah Jaafar and Sayed Mohamed. Universiti Malaysia Terengganu. Terengganu, Malaysia*, 937-943.

Elkiran, G., and Ergil, M. (2006). The assessment of a water budget of North Cyprus. *Building and Environment*, *41*(12), 1671-1677.

Elkiran, G., and Ongul, Z. (2009). Implications of excessive water withdrawals to the environment of Northern Cyprus. *Water and Environment Journal*, *23*(2), 145-154.

Elkiran, G., Nourani, V., Abba, S. I., and Abdullahi, J. (2018). Artificial intelligence-based approaches for multi-station modelling of dissolve oxygen in river. *Global Journal of Environmental Science and Management*, *4*(4), 439-450.

Elkiran, G., Nourani, V., and Abba, S. I. (2019). Multi-step ahead modelling of river water quality parameters using ensemble artificial intelligence-based approach. *Journal of Hydrology*, *577*, 123962.

El-Wahed, M. H. A., and El-Mageed, T. A. A. (2014). Estimating reference evapotranspiration using modified Blaney-Criddle equation in arid region.

Eslamian, S. S., Gohari, S. A., Zareian, M. J., and Firoozfar, A. (2012). Estimating Penman–Monteith reference evapotranspiration using artificial neural networks and genetic algorithm: a case study. *Arabian Journal for Science and Engineering*, *37*(4), 935-944.

Estévez, J., Gavilán, P., and Berengena, J. (2009). Sensitivity analysis of a Penman–Monteith type equation to estimate reference evapotranspiration in southern Spain. *Hydrological Processes*, *23*(23), 3342-3353.

Estévez, J., Gavilán, P., and Giráldez, J. V. (2011). Guidelines on validation procedures for meteorological data from automatic weather stations. *Journal of Hydrology*, *402*(1-2), 144-154.

Estévez, J., García-Marín, A. P., Morábito, J. A., and Cavagnaro, M. (2016). Quality assurance procedures for validating meteorological input variables of reference evapotranspiration in mendoza province (Argentina). *Agricultural Water Management*, *172*, 96-109.

Farzanpour, H., Shiri, J., Sadraddini, A. A., and Trajkovic, S. (2018). Global comparison of 20 reference evapotranspiration equations in a semi-arid region of Iran. *Hydrology Research*, *50*(1), 282-300.

Feng, S., Hu, Q., and Qian, W. (2004). Quality control of daily meteorological data in China, 1951–2000: a new dataset. *International Journal of Climatology: A Journal of the Royal Meteorological Society*, *24*(7), 853-870.

Feng, Y., Cui, N., Zhao, L., Hu, X., and Gong, D. (2016). Comparison of ELM, GANN, WNN and empirical models for estimating reference evapotranspiration in humid region of Southwest China. *Journal of Hydrology*, *536*, 376-383.

Feng, Y., Cui, N., Zhao, L., Hu, X., and Gong, D. (2016). Comparison of ELM, GANN, WNN and empirical models for estimating reference evapotranspiration in humid region of Southwest China. *Journal of Hydrology*, *536*, 376-383.

Ferreira, L. B., da Cunha, F. F., de Oliveira, R. A., and Fernandes Filho, E. I. (2019a). Estimation of reference evapotranspiration in Brazil with limited meteorological data using ANN and SVM–A new approach. *Journal of Hydrology*, *572*, 556-570.

Ferreira, L. B., Duarte, A. B., Cunha, F. F. D., and Fernandes Filho, E. I. (2019b). Multivariate adaptive regression splines (MARS) applied to daily reference evapotranspiration modeling with limited weather data. *Acta Scientiarum. Agronomy*, *41*.

Fotovatikhah, F., Herrera, M., Shamshirband, S., Chau, K. W., Faizollahzadeh Ardabili, S., and Piran, M. J. (2018). Survey of computational intelligence as basis to big flood management: Challenges, research directions and future work. *Engineering Applications of Computational Fluid Mechanics*, *12*(1), 411-437.

Gao, F., Feng, G., Ouyang, Y., Wang, H., Fisher, D., Adeli, A., and Jenkins, J. (2017). Evaluation of reference evapotranspiration methods in arid, semiarid, and humid regions. *JAWRA Journal of the American Water Resources Association*, *53*(4), 791-808.

Ghorbani, M. A., Kazempour, R., Chau, K. W., Shamshirband, S., and Taherei Ghazvinei, P. (2018). Forecasting pan evaporation with an integrated artificial neural network quantum-behaved particle swarm optimization model: A case study in Talesh, Northern Iran. *Engineering Applications of Computational Fluid Mechanics*, *12*(1), 724-737.

Granata, F. (2019). Evapotranspiration evaluation models based on machine learning algorithms—A comparative study. *Agricultural Water Management*, *217*, 303-315.

Granata, F. (2019). Evapotranspiration evaluation models based on machine learning algorithms—A comparative study. *Agricultural Water Management*, *217*, 303-315.

Guitjens, J. C. (1982). Models of alfalfa yield and evapotranspiration. *Journal of the Irrigation and Drainage Division*, *108*(3), 212-222.

Haghiabi A. H., Azamathulla H.M. and Parsaie A. (2016) Prediction of head loss on cascade weir using ANN and SVM. *ISH Journal of Hydraulic Engineering*, 23, 102-110.

Harbeck, G. E. (1962). A practical field technique for measuring reservoir evaporation utilizing mass-transfer theory. Geological Survey Professional Paper 272-E. Government Printing Office, Washington, DC, p 101–105

Hargreaves, G. H., and Samani, Z. A. (1985). Reference crop evapotranspiration from temperature. *Applied Engineering in Agriculture*, *1*(2), 96-99.

Heydari, M. M., and Heydari, M. (2014). Evaluation of pan coefficient equations for estimating reference crop evapotranspiration in the arid region. *Archives of Agronomy and Soil Science*, *60*(5), 715-731.

Hornik, K., Stinchcombe, M., and White, H. (1989). Multilayer feedforward networks are universal approximators. *Neural Networks*, *2*(5), 359-366.

Hu, Q. F., Yang, D. W., Wang, Y. T., and Yang, H. B. (2011). Global calibration of Hargreaves equation and its applicability in China. *Advances in Water Sciences*, 22 (2), 160–167.

Huang, G., Wu, L., Ma, X., Zhang, W., Fan, J., Yu, X., ... and Zhou, H. (2019). Evaluation of CatBoost method for prediction of reference evapotranspiration in humid regions. *Journal of Hydrology*, *574*, 1029-1041.

Irmak, S., Haman, D. Z., and Jones, J. W. (2002). Evaluation of class A pan coefficients for estimating reference evapotranspiration in humid location. *Journal of Irrigation and Drainage Engineering*, *128*(3), 153-159.

Jaber, H. S., Mansor, S., Pradhan, B., and Ahmad, N. (2016). Evaluation of SEBAL model for Evapotranspiration mapping in Iraq using remote sensing and GIS. *Int. J. Appl. Eng. Res*, *11*, 3950-3955.

Jain, S. K., Nayak, P. C., and Sudheer, K. P. (2008). Models for estimating evapotranspiration using artificial neural networks, and their physical interpretation. *Hydrological Processes*, *22*(13), 2225-2234.

Jang, J. S. (1993). ANFIS: adaptive-network-based fuzzy inference system. *IEEE Transactions on Systems, Man, and Cybernetics*, *23*(3), 665-685.

Jang, J. S. R., Sun, C. T., and Mizutani, E. (1997). *Neuro-fuzzy and soft computing—A Computational Approach to Learning and Machine Intelligence*. New Jersey: Prentice Hall.

Jang, J. S., and Sun, C. T. (1995). Neuro-fuzzy modeling and control. *Proceedings of the IEEE*, *83*(3), 378-406.

Jassas, H., Kanoua, W., and Merkel, B. (2015). Actual evapotranspiration in the Al-Khazir Gomal Basin (Northern Iraq) using the surface energy balance algorithm for land (SEBAL) and water balance. *Geosciences*, *5*(2), 141-159.

Jones, J. W., and Ritchie, J. T. (1990). Crop growth models. In: Hoffman, G.J., Howel, T.A., Solomon, K. H. (Eds.), *Management of Farm Irrigation System.* ASAE Monograph No. 9. ASAE, St. Joseph, Mich, pp. 63–89

Karbasi, M. (2018). Forecasting of multi-step ahead reference evapotranspiration using Wavelet-Gaussian Process Regression model. *Water resources management*, *32*(3), 1035-1052.

Karimaldini, F., Teang Shui, L., Ahmed Mohamed, T., Abdollahi, M., and Khalili, N. (2011). Daily evapotranspiration modeling from limited weather data by using neuro-fuzzy computing technique. *Journal of Irrigation and Drainage Engineering*, *138*(1), 21-34.

Keshtegar, B., Kisi, O., and Zounemat-Kermani, M. (2019). Polynomial chaos expansion and response surface method for nonlinear modelling of reference evapotranspiration. *Hydrological Sciences Journal*, *64*(6), 720-730.

Khoob, A. R. (2008). Artificial neural network estimation of reference evapotranspiration from pan evaporation in a semi-arid environment. *Irrigation Science*, 27(1), 35-39.

Kiran, N. R., and Ravi, V. (2008). Software reliability prediction by soft computing techniques. *Journal of Systems and Software*, *81*(4), 576-583.

Kisi, O. (2006). Evapotranspiration estimation using feed-forward neural networks. *Hydrology Research*, *37*(3), 247-260.

Kişi, Ö. (2011). Evapotranspiration modeling using a wavelet regression model. *Irrigation science*, *29*(3), 241-252.

Kisi, O. (2013a). Applicability of Mamdani and Sugeno fuzzy genetic approaches for modeling reference evapotranspiration. *Journal of hydrology*, *504*, 160-170.

Kisi, O. (2013b). Comparison of different empirical methods for estimating daily reference evapotranspiration in Mediterranean climate. *Journal of Irrigation and Drainage Engineering*, *140*(1), 04013002.

Kisi, O. (2016). Modeling reference evapotranspiration using three different heuristic regression approaches. *Agricultural Water Management*, *169*, 162-172.

Kisi, O., and Oztürk, O. (2007). Adaptive neurofuzzy computing technique for evapotranspiration estimation. *Journal of Irrigation and Drainage Engineering*, *133*(4), 368-379.

Kisi, O., and Cengiz, T. M. (2013). Fuzzy genetic approach for estimating reference evapotranspiration of Turkey: Mediterranean region. *Water resources management*, *27*(10), 3541-3553.

Kisi, O., and Zounemat-Kermani, M. (2014). Comparison of two different adaptive neuro-fuzzy inference systems in modelling daily reference evapotranspiration. *Water resources management*, *28*(9), 2655-2675.

Kisi, O., and Kilic, Y. (2016). An investigation on generalization ability of artificial neural networks and M5 model tree in modeling reference evapotranspiration. *Theoretical and Applied Climatology*, *126*(3-4), 413-425.

Kumar, M., Raghuwanshi, N. S., Singh, R., Wallender, W. W., and Pruitt, W. O. (2002). Estimating evapotranspiration using artificial neural network. *Journal of Irrigation and Drainage Engineering*, *128*(4), 224-233.

Legates, D. R., and McCabe Jr, G. J. (1999). Evaluating the use of "goodness-of-fit" measures in hydrologic and hydroclimatic model validation. *Water Resources Research*, *35*(1), 233-241.

Makkink, G. F. (1957). Testing the Penman formula by means of lysimeters. *Journal of the Institution of Water Engineers*, *11*, 277-288.

Makridakis, S., Andersen, A., Carbone, R., Fildes, R., Hibon, M., Lewandowski, R., and Winkler, R. (1982). The accuracy of extrapolation (time series) methods: Results of a forecasting competition. *Journal of Forecasting*, *1*(2), 111-153.

Manikumari, N., Murugappan, A., and Vinodhini, G. (2017). Time Series Forecasting of Daily Reference Evapotranspiration by Neural Network Ensemble Learning for Irrigation

System. In *IOP Conference Series: Earth and Environmental Science* (Vol. 80, No. 1, p. 012069). IOP Publishing.

Mehdizadeh, S. (2018). Estimation of daily reference evapotranspiration (ET_0) using artificial intelligence methods: Offering a new approach for lagged ETo data-based modeling. *Journal of Hydrology*, *559*, 794-812.

Mehdizadeh, S., Behmanesh, J., and Khalili, K. (2017). Using MARS, SVM, GEP and empirical equations for estimation of monthly mean reference evapotranspiration. *Computers and Electronics in Agriculture*, *139*, 103-114.

Mehr, A. D., Nourani, V., Khosrowshahi, V. K., and Ghorbani, M. A. (2019). A hybrid support vector regression–firefly model for monthly rainfall forecasting. *International Journal of Environmental Science and Technology*, *16*(1), 335-346.

Moazenzadeh, R., Mohammadi, B., Shamshirband, S., and Chau, K. W. (2018). Coupling a firefly algorithm with support vector regression to predict evaporation in northern Iran. *Engineering Applications of Computational Fluid Mechanics*, *12*(1), 584-597.

Moghaddamnia, A., Gousheh, M. G., Piri, J., Amin, S., and Han, D. (2009). Evaporation estimation using artificial neural networks and adaptive neuro-fuzzy inference system techniques. *Advances in Water Resources*, *32*(1), 88-97.

Mohammadrezapour, O., Piri, J., and Kisi, O. (2018). Comparison of SVM, ANFIS and GEP in modeling monthly potential evapotranspiration in an arid region (Case study: Sistan and Baluchestan Province, Iran). *Water Supply*, *19*(2), 392-403.

Monteith, J.L. (1965). *Evaporation and environment.* Proc Symp Soc Exp Biol 19:205–234

Najmaddin, P. M., Whelan, M. J., and Balzter, H. (2017). Estimating daily reference evapotranspiration in a semi-arid region using remote sensing data. *Remote Sensing*, *9*(8), 779.

Nourani, V., and Fard, M. S. (2016). Sensitivity analysis of the artificial neural network outputs in simulation of the evaporation process at different climatologic regimes. *Advances in Engineering Software*, *47*(1), 127-146.

Nourani, V., and Komasi, M. (2013). A geomorphology-based ANFIS model for multi-station modeling of rainfall–runoff process. *Journal of Hydrology*, *490*, 41-55.

Nourani, V., Kalantari, O., and Baghanam, A. H. (2012). Two semidistributed ANN-based models for estimation of suspended sediment load. *Journal of Hydrologic Engineering*, *17*(12), 1368-1380.

Nourani, V., Khanghah, T. R., and Baghanam, A. H. (2015). Application of Entropy Concept for Input Selection of Wavelet-ANN Based Rainfall-Runoff Modeling. *Journal of Environmental Informatics*, *26*(1).

Nourani, V., Mousavi, S., Dabrowska, D., and Sadikoglu, F. (2017). Conjunction of radial basis function interpolator and artificial intelligence models for time-space modeling of contaminant transport in porous media. *Journal of Hydrology*, *548*, 569-587.

Nourani, V., Elkiran, G., Abdullahi, J., and Tahsin, A. (2019). Multi-region modeling of daily global solar radiation with artificial intelligence ensemble. *Natural Resources Research*, *28*(4), 1217-1238.

Odhiambo, L. O., Yoder, R. E., and Yoder, D. C. (2001). Estimation of reference crop evapotranspiration using fuzzy state models. *Transactions of the ASAE*, *44*(3), 543.

Oladipo, E. O. (1993). Is the climate of northern Nigeria becoming more arid. In *36th Annual Conference of the Nigerian Geographical Association* (pp. 18-22).

Papadavid, G., and Diofantos, H. (2010). Integrated approach of remote sensing and micro-sensor technology for estimating evapotranspiration in Cyprus. *Agricultural Engineering International: CIGR Journal*, *12*(3-4), 1-11.

Papadavid, G., Hadjimitsis, D., Michaelides, S., and Nisantzi, A. (2011). Crop evapotranspiration estimation using remote sensing and the existing network of meteorological stations in Cyprus. *Advances in Geosciences*, *30*, 39-44.

Papadavid, G., Hadjimitsis, D. G., Toulios, L., and Michaelides, S. (2013). A modified SEBAL modeling approach for estimating crop evapotranspiration in semi-arid conditions. *Water resources management*, *27*(9), 3493-3506.

Penman, H. L. (1948). Natural evaporation from open water, bare soil and grass. Proc R Soc Lond 193:120–145

Perrone, M.P., and Cooper, L.N. (1993). When networks disagree: ensemble methods for hybrid neural netwoks. In: Mammone, R.J. (Ed.), Neural Networks for speech and Image processing. Chapman Hall, pp. 126– 142.

Petković, D., Gocic, M., Trajkovic, S., Shamshirband, S., Motamedi, S., Hashim, R., and Bonakdari, H. (2015). Determination of the most influential weather parameters on reference evapotranspiration by adaptive neuro-fuzzy methodology. *Computers and Electronics in Agriculture*, *114*, 277-284.

Pour-Ali Baba, A., Shiri, J., Kisi, O., Fard, A. F., Kim, S., and Amini, R. (2012). Estimating daily reference evapotranspiration using available and estimated climatic data by adaptive neuro-fuzzy inference system (ANFIS) and artificial neural network (ANN). *Hydrology Research*, *44*(1), 131-146.

Rahimikhoob, A. (2010). Estimation of evapotranspiration based on only air temperature data using artificial neural networks for a subtropical climate in Iran. *Theoretical and Applied Climatology*, *101*(1-2), 83-91.

Rahimikhoob, A. (2014). Comparison between M5 model tree and neural networks for estimating reference evapotranspiration in an arid environment. *Water resources management*, *28*(3), 657-669.

Rahimikhoob, A., Asadi, M., and Mashal, M. (2013). A comparison between conventional and M5 model tree methods for converting pan evaporation to reference evapotranspiration for semi-arid region. *Water resources management*, *27*(14), 4815-4826.

Ranjbar, S., Hooshyar, M., Singh, A., and Wang, D. (2018). Quantifying climatic controls on river network branching structure across scales. *Water Resources Research*, *54*(10), 7347-7360.

Raoof, M., and Mobaser, J. A. (2019). Reference Evapotranspiration Estimation Using Locally Adjusted Coefficient of Angstrom's Radiation Model in an Arid-Cold Region. *Journal of Agricultural Science and Technology*, *21*(2), 487-499.

Rasul, A., Balzter, H., and Smith, C. (2015). Spatial variation of the daytime surface urban cool island during the dry season in Erbil, Iraqi Kurdistan, from Landsat 8. *Urban Climate*, *14*, 176-186.

Saggi, M. K., and Jain, S. (2019). Reference evapotranspiration estimation and modeling of the Punjab Northern India using deep learning. *Computers and electronics in agriculture*, *156*, 387-398.

Sahoo, G. B., Ray, C., and Wade, H. F. (2005). Pesticide prediction in ground water in North Carolina domestic wells using artificial neural networks. *Ecological Modelling*, *183*(1), 29-46.

Sanikhani, H., Kisi, O., Maroufpoor, E., and Yaseen, Z. M. (2019). Temperature-based modeling of reference evapotranspiration using several artificial intelligence models: application of different modeling scenarios. *Theoretical and applied climatology*, *135*(1-2), 449-462.

Sarlak, N., and Agha, O. M. M. (2018). Spatial and temporal variations of aridity indices in Iraq. *Theoretical and Applied Climatology*, *133*(1-2), 89-99.

Shafer, M. A., Fiebrich, C. A., Arndt, D. S., Fredrickson, S. E., and Hughes, T. W. (2000). Quality assurance procedures in the Oklahoma Mesonetwork. *Journal of Atmospheric and Oceanic Technology*, *17*(4), 474-494.

Sharghi, E., Nourani, V., and Behfar, N. (2018). Earthfill dam seepage analysis using ensemble artificial intelligence based modeling. *Journal of Hydroinformatics*, jh2018151.

Sharma, A., Vijay, R., Bodhe, G. L., and Malik, L. G. (2018). An adaptive neuro-fuzzy interface system model for traffic classification and noise prediction. *Soft Computing*, *22*(6), 1891-1902.

Shiri, J. (2017). Evaluation of FAO56-PM, empirical, semi-empirical and gene expression programming approaches for estimating daily reference evapotranspiration in hyper-arid regions of Iran. *Agricultural water management*, *188*, 101-114.

Shiri, J., Kişi, Ö., Landeras, G., López, J. J., Nazemi, A. H., and Stuyt, L. C. (2012). Daily reference evapotranspiration modeling by using genetic programming approach in the Basque Country (Northern Spain). *Journal of Hydrology*, *414*, 302-316.

Shiri, J., Sadraddini, A. A., Nazemi, A. H., Kisi, O., Marti, P., Fard, A. F., and Landeras, G. (2013). Evaluation of different data management scenarios for estimating daily reference evapotranspiration. *Hydrology Research*, *44*(6), 1058-1070.

Shiri, J., Nazemi, A. H., Sadraddini, A. A., Landeras, G., Kisi, O., Fard, A. F., and Marti, P. (2014a). Comparison of heuristic and empirical approaches for estimating reference evapotranspiration from limited inputs in Iran. *Computers and Electronics in Agriculture*, *108*, 230-241.

Shiri, J., Sadraddini, A. A., Nazemi, A. H., Kisi, O., Landeras, G., Fard, A. F., and Marti, P. (2014b). Generalizability of gene expression programming-based approaches for estimating daily reference evapotranspiration in coastal stations of Iran. *Journal of hydrology*, *508*, 1-11.

Shiri, J., Nazemi, A. H., Sadraddini, A. A., Marti, P., Fard, A. F., Kisi, O., and Landeras, G. (2019). Alternative heuristics equations to the Priestley–Taylor approach: assessing reference evapotranspiration estimation. *Theoretical and Applied Climatology*, 1-18.

Snyder RL, Orang M, Matyac S, and Grismer ME. (2005). Simplified estimation of reference evapotranspiration from pan evaporation data in California. *Journal of Irrigation and Drainage Engineering*, 131, 249–253.

Sudheer K. P., Gosain A. K., and Ramasastri K. S. (2003). Estimating actual evapotranspiration from limited climatic data using neural computing technique. *Journal of Irrigation and Drainage Engineering 129*(3), 214–218.

Tabari, H., and Talaee, P. H. (2011). Local calibration of the Hargreaves and Priestley-Taylor equations for estimating reference evapotranspiration in arid and cold climates of Iran based on the Penman-Monteith model. *Journal of Hydrologic Engineering*, *16*(10), 837-845.

Tabari, H., Kisi, O., Ezani, A., and Talaee, P. H. (2012). SVM, ANFIS, regression and climate based models for reference evapotranspiration modeling using limited climatic data in a semi-arid highland environment. *Journal of Hydrology*, *444*, 78-89.

Todorovic, M., Karic, B., and Pereira, L. S. (2013). Reference evapotranspiration estimate with limited weather data across a range of Mediterranean climates. *Journal of Hydrology*, *481*, 166-176.

Turkes, M. (1996). Spatial and temporal analysis of annual rainfall variations in Turkey. *International Journal of Climatology*, *16*(9), 1057-1076.

UNEP (1992). *World atlas of desertification.* Edward Arnold, London.

Valipour, M. (2012). Ability of Box-Jenkins models to estimate of reference potential evapotranspiration (A case study: Mehrabad Synoptic Station, Tehran, Iran). *IOSR Journal of Agriculture and Veterinary Science*, *1*(5), 1-11.

Valipour, M. (2015a). Temperature analysis of reference evapotranspiration models. *Meteorological Applications*, *22*(3), 385-394.

Valipour, M. (2015b). Investigation of Valiantzas' evapotranspiration equation in Iran. *Theoretical and applied climatology*, *121*(1-2), 267-278.

Vapnik, V. (1998). *Statistical learning theory.* (Vol. 3). Wiley, New York.

Wang, W. C., Xu, D. M., Chau, K. W., and Chen, S. (2013). Improved annual rainfall-runoff forecasting using PSO–SVM model based on EEMD. *Journal of Hydroinformatics*, *15*(4), 1377-1390.

Wang, S., Lian, J., Peng, Y., Hu, B., and Chen, H. (2019). Generalized reference evapotranspiration models with limited climatic data based on random forest and gene expression programming in Guangxi, China. *Agricultural Water Management*, *221*, 220-230.

Wang, Y. M., Traore, S., Kerh, T., and Leu, J. M. (2011). Modelling reference evapotranspiration using feed forward backpropagation algorithm in arid regions of Africa. *Irrigation and Drainage*, *60*(3), 404-417.

Wen, X., Si, J., He, Z., Wu, J., Shao, H., and Yu, H. (2015). Support-vector-machine-based models for modeling daily reference evapotranspiration with limited climatic data in extreme arid regions. *Water Resources Management*, *29*(9), 3195-3209.

Wu, L., Zhou, H., Ma, X., Fan, J., and Zhang, F. (2019). Daily reference evapotranspiration prediction based on hybridized extreme learning machine model with bio-inspired optimization algorithms: Application in contrasting climates of China. *Journal of Hydrology*, *577*, 123960.

Yang, Y., Cui, Y., Bai, K., Luo, T., Dai, J., Wang, W., and Luo, Y. (2019). Short-term forecasting of daily reference evapotranspiration using the reduced-set Penman-Monteith model and public weather forecasts. *Agricultural water management*, *211*, 70-80.

Yaseen, Z. M., Sulaiman, S. O., Deo, R. C., and Chau, K. W. (2018). An enhanced extreme learning machine model for river flow forecasting: State-of-the-art, practical applications in water resource engineering area and future research direction. *Journal of Hydrology*, 569, 387-408.

Yaseen, Z. M. Ebtehaj, S. Kim, H. Sanikhani, H. Asadi, M. I. Ghareb and S. Shahid, Novel hybrid data-intelligence model for forecasting monthly rainfall with uncertainty analysis, *Water*, *11* (2019) 502.

Yin, Z., Wen, X., Feng, Q., He, Z., Zou, S., and Yang, L. (2017). Integrating genetic algorithm and support vector machine for modeling daily reference evapotranspiration in a semi-arid mountain area. *Hydrology Research*, *48*(5), 1177-1191.

Yu, L., Wang, S., and Lai, K. K. (2005). A novel nonlinear ensemble forecasting model incorporating GLAR and ANN for foreign exchange rates. *Computers and Operations Research*, *32*, 2523-2541.

Zanetti, S. S., Sousa, E. F., Oliveira, V. P., Almeida, F. T., and Bernardo, S. (2007). Estimating evapotranspiration using artificial neural network and minimum climatological data. *Journal of Irrigation and Drainage Engineering*, *133*(2), 83-89.

Zhang, G. P. (2003). Time series forecasting using a hybrid ARIMA and neural network model. *Neurocomputing*, 50, 159–175.

Zhang, L., Traore, S., Cui, Y., Luo, Y., Zhu, G., Liu, B., and Singh, V. (2019). Assessment of spatiotemporal variability of reference evapotranspiration and controlling climate factors over decades in China using geospatial techniques. *Agricultural water management*, *213*, 499-511.

Zhu, X., Luo, T., Luo, Y., Yang, Y., Guo, L., Luo, H., and Cui, Y. (2019). Calibration and Validation of the Hargreaves-Samani Model for Reference Evapotranspiration Estimation in China. *Irrigation and Drainage*.

APPENDICES

APPENDIX 1

DESCRIPTIVE STATISTICS OF THE USED DATA

Appendix 1a: Data Descriptive Statistics for Turkey Stations

Station	Location	Coordinates	Parameters	Unit	Min	Max.	Average	St. Deviation
Adana	Latitude	$36^0$99'N	Relative Humidity (R_H)	%	42.54	78.50	62.02	7.22
			Surface Pressure (S_P)	Kpa	99.21	101.15	100.14	0.47
			Precipitation (P_R)	mm/day	0.00	9.13	1.61	1.52
	Longitude	$35^0$33'E	Dew-point Temperature (T_D)	^{0}C	0.70	21.56	11.69	5.35
			Maximum Temperature (T_{max})	^{0}C	10.19	35.51	23.56	7.26
			Minimum Temperature (T_{min})	^{0}C	4.08	27.64	16.69	6.59
			Mean Temperature (T_{mean})	^{0}C	6.89	31.17	19.90	6.92
			Minimum Wind Speed (U_{min})	m/s	0.46	2.42	1.05	0.41
			Maximum Wind Speed (U_{max})	m/s	2.23	4.64	3.37	0.53
	Altitude	27 m	Mean Wind Speed (U_{mean})	m/s	1.79	3.83	2.68	0.40
			Solar Radiation (R_S)	MJ/m^2/day	1.30	30.54	18.19	7.35
			Pan Evaporation (E_P)	mm/day	0.81	9.64	4.30	2.30
Ankara	Latitude	$39^0$93'N	Relative Humidity (R_H)	%	30.10	89.93	61.83	15.40
			Surface Pressure (S_P)	Kpa	89.04	90.51	89.65	0.24
			Precipitation (P_R)	mm/day	0.00	4.99	1.08	0.82
	Longitude	$32^0$86'E	Dew-point Temperature (T_D)	^{0}C	-8.04	12.60	2.68	4.84
			Maximum Temperature (T_{max})	^{0}C	-1.35	34.70	17.21	9.63
			Minimum Temperature (T_{min})	^{0}C	-9.01	17.79	4.75	7.09
			Mean Temperature (T_{mean})	^{0}C	-4.48	26.25	10.70	8.56
			Minimum Wind Speed (U_{min})	m/s	0.56	1.86	0.92	0.19
			Maximum Wind Speed (U_{max})	m/s	1.74	3.85	2.76	0.38
	Altitude	938 m	Mean Wind Speed (U_{mean})	m/s	1.30	3.24	2.17	0.32
			Solar Radiation (R_S)	MJ/m^2/day	4.45	28.93	16.13	6.99
			Pan Evaporation (E_P)	mm/day	0.04	10.74	3.80	2.62
Izmir	Latitude	$38^0$42'N	Relative Humidity (R_H)	%	33.23	87.56	63.63	14.80
			Surface Pressure (S_P)	Kpa	98.50	100.26	99.18	0.36
			Precipitation (P_R)	mm/day	0.00	9.70	1.66	1.79
	Longitude	$27^0$14'E	Dew-point Temperature (T_D)	^{0}C	-0.73	16.05	8.96	3.79
			Maximum Temperature (T_{max})	^{0}C	7.79	37.68	22.49	8.51
			Minimum Temperature (T_{min})	^{0}C	0.30	23.34	11.71	6.38
			Mean Temperature (T_{mean})	^{0}C	3.74	30.23	16.80	7.53
			Minimum Wind Speed (U_{min})	m/s	0.80	2.64	1.58	0.37
			Maximum Wind Speed (U_{max})	m/s	3.03	5.75	4.34	0.52
	Altitude	30 m	Mean Wind Speed (U_{mean})	m/s	1.96	4.11	2.90	0.44
			Solar Radiation (R_S)	MJ/m^2/day	2.61	29.89	16.94	7.54
			Pan Evaporation (E_P)	mm/day	0.00	10.27	4.36	2.90
Samsun	Latitude	$41^0$28'N	Relative Humidity (R_H)	%	62.33	86.66	74.25	5.06
			Surface Pressure (S_P)	Kpa	96.15	97.72	96.71	0.30
			Precipitation (P_R)	mm/day	0.00	5.50	1.55	0.93
	Longitude	$36^0$34'E	Dew-point Temperature (T_D)	^{0}C	-3.16	17.77	7.53	5.98
			Maximum Temperature (T_{max})	^{0}C	2.42	30.85	16.69	7.34
			Minimum Temperature (T_{min})	^{0}C	-3.51	20.59	8.86	6.49
			Mean Temperature (T_{mean})	^{0}C	-0.49	25.20	12.30	6.91
			Minimum Wind Speed (U_{min})	m/s	0.42	2.39	1.09	0.34
			Maximum Wind Speed (U_{max})	m/s	2.60	5.93	3.99	0.60
	Altitude	4 m	Mean Wind Speed (U_{mean})	m/s	1.45	3.94	2.50	0.49
			Solar Radiation (R_S)	MJ/m^2/day	2.76	28.07	13.94	6.62
			Pan Evaporation (E_P)	mm/day	0.00	6.29	2.73	1.42

Appendix 1b: Data Descriptive Statistics for North Cyprus Stations

Station	Location	Coordinates	Parameters	Unit	Min	Max.	Average	St. Deviation
Famagusta	Latitude	$35^0$11'N	Relative Humidity (R_H)	%	53.18	75.50	64.22	4.96
			Surface Pressure (S_P)	Kpa	99.87	101.70	100.74	0.44
			Precipitation (P_R)	mm/day	0.00	5.33	0.77	0.93
	Longitude	$33^0$95'E	Dew-point Temperature (T_D)	^{0}C	5.17	22.24	14.17	4.61
			Maximum Temperature (T_{max})	^{0}C	14.02	34.11	23.79	6.31
			Minimum Temperature (T_{min})	^{0}C	10.72	28.58	19.32	5.46
			Mean Temperature (T_{mean})	^{0}C	12.37	31.23	21.47	5.88
	Altitude	20 m	Minimum Wind Speed (U_{min})	m/s	0.72	3.07	1.59	0.49
			Maximum Wind Speed (U_{max})	m/s	3.11	6.75	4.45	0.69
			Mean Wind Speed (U_{mean})	m/s	1.92	4.95	3.01	0.58
			Solar Radiation (R_S)	MJ/m^2/day	5.55	31.22	18.50	7.39
			Pan Evaporation (E_P)	mm/day	1.10	10.30	4.36	2.45
Kyrenia	Latitude	$35^0$33'N	Relative Humidity (R_H)	%	52.38	77.85	64.85	6.03
			Surface Pressure (S_P)	Kpa	98.77	100.50	99.58	0.41
			Precipitation (P_R)	mm/day	0.00	189.69	27.69	33.13
	Longitude	$33^0$31'E	Dew-point Temperature (T_D)	^{0}C	4.65	21.06	13.36	4.47
			Maximum Temperature (T_{max})	^{0}C	13.20	34.76	23.60	6.67
			Minimum Temperature (T_{min})	^{0}C	9.13	27.65	17.99	5.59
			Mean Temperature (T_{mean})	^{0}C	11.16	30.96	20.61	6.11
	Altitude	20 m	Minimum Wind Speed (U_{min})	m/s	1.03	2.97	1.71	0.38
			Maximum Wind Speed (U_{max})	m/s	2.98	6.85	4.77	0.58
			Mean Wind Speed (U_{mean})	m/s	2.03	5.03	3.27	0.46
			Solar Radiation (R_S)	MJ/m^2/day	5.55	31.22	18.50	7.39
			Pan Evaporation (E_P)	mm/day	0.90	11.55	4.84	2.61
Morphou	Latitude	$35^0$18'N	Relative Humidity (R_H)	%	53.27	80.25	67.83	6.33
			Surface Pressure (S_P)	Kpa	97.87	101.65	98.42	0.39
			Precipitation (P_R)	mm/day	0.00	6.12	0.91	1.08
	Longitude	$33^0$0'E	Dew-point Temperature (T_D)	^{0}C	2.86	19.26	12.98	4.97
			Maximum Temperature (T_{max})	^{0}C	14.20	37.34	25.62	6.32
			Minimum Temperature (T_{min})	^{0}C	10.76	29.14	18.53	6.27
			Mean Temperature (T_{mean})	^{0}C	12.19	32.71	22.53	6.09
	Altitude	45 m	Minimum Wind Speed (U_{min})	m/s	0.93	2.78	1.24	0.41
			Maximum Wind Speed (U_{max})	m/s	2.77	5.96	4.09	0.62
			Mean Wind Speed (U_{mean})	m/s	2.63	4.73	3.01	0.49
			Solar Radiation (R_S)	MJ/m^2/day	3.97	32.45	19.65	6.89
			Pan Evaporation (E_P)	mm/day	1.11	12.10	5.83	3.28
Nicosia	Latitude	$35^0$19'N	Relative Humidity (R_H)	%	51.28	75.76	62.83	5.39
			Surface Pressure (S_P)	Kpa	96.23	99.37	99.23	0.54
			Precipitation (P_R)	mm/day	0.00	5.83	0.94	1.11
	Longitude	$33^0$38'E	Dew-point Temperature (T_D)	^{0}C	3.76	22.48	14.93	6.32
			Maximum Temperature (T_{max})	^{0}C	10.19	39.26	25.18	5.82
			Minimum Temperature (T_{min})	^{0}C	4.36	22.63	14.36	6.30
			Mean Temperature (T_{mean})	^{0}C	10.76	33.26	24.17	6.85
	Altitude	220 m	Minimum Wind Speed (U_{min})	m/s	1.47	3.11	1.76	0.47
			Maximum Wind Speed (U_{max})	m/s	3.31	5.37	4.06	0.53
			Mean Wind Speed (U_{mean})	m/s	2.56	4.74	2.88	0.44
			Solar Radiation (R_S)	MJ/m^2/day	6.36	34.81	20.09	6.58
			Pan Evaporation (E_P)	mm/day	1.10	12.60	5.35	3.17

Appendix 1c: Data Descriptive Statistics for Iraq Stations

Station	Location	Coordinates	Parameters	Unit	Min	Max.	Average	St. Deviation
Erbil	Latitude	$35^0$55'N	Relative Humidity (R_H)	%	13.05	74.12	39.94	18.71
			Surface Pressure (S_P)	Kpa	92.13	93.96	93.18	0.48
			Precipitation (P_R)	mm/day	0.00	3.15	0.72	0.70
	Longitude	$43^0$57'E	Dew-point Temperature (T_D)	^{0}C	-6.78	9.70	1.84	3.11
			Maximum Temperature (T_{max})	^{0}C	6.19	44.03	25.65	11.08
			Minimum Temperature (T_{min})	^{0}C	-2.55	26.83	12.15	8.85
			Mean Temperature (T_{mean})	^{0}C	1.31	35.25	18.36	10.17
	Altitude	390 m	Minimum Wind Speed (U_{min})	m/s	0.34	0.92	0.55	0.09
			Maximum Wind Speed (U_{max})	m/s	1.48	3.38	2.27	0.43
			Mean Wind Speed (U_{mean})	m/s	1.16	2.49	1.54	0.22
			Solar Radiation (R_S)	MJ/m^2/day	5.14	30.47	17.86	7.08
			Pan Evaporation (E_P)	mm/day	1.00	16.00	6.80	4.41
Salahaddin	Latitude	$36^0$15'N	Relative Humidity (R_H)	%	24.00	92.00	52.27	16.01
			Surface Pressure (S_P)	Kpa	91.26	94.23	92.67	0.45
			Precipitation (P_R)	mm/day	0.00	2.18	0.67	0.73
	Longitude	$44^0$07'E	Dew-point Temperature (T_D)	^{0}C	-8.36	8.26	1.20	3.75
			Maximum Temperature (T_{max})	^{0}C	0.00	39.90	22.26	10.29
			Minimum Temperature (T_{min})	^{0}C	-1.60	29.20	13.35	8.57
			Mean Temperature (T_{mean})	^{0}C	0.00	34.60	18.02	9.27
	Altitude	1084 m	Minimum Wind Speed (U_{min})	m/s	0.28	0.95	0.61	0.08
			Maximum Wind Speed (U_{max})	m/s	1.35	4.13	2.13	0.49
			Mean Wind Speed (U_{mean})	m/s	1.00	4.00	2.36	0.64
			Solar Radiation (R_S)	MJ/m^2/day	3.89	28.78	16.25	8.12
			Pan Evaporation (E_P)	mm/day	0.00	15.50	5.55	3.86

Appendix 1d: Data Descriptive Statistics for Iran Stations

Station	Location	Coordinates	Parameters	Unit	Min	Max.	Average	St. Deviation
Tabriz	Latitude	$38^0$8'N	Relative Humidity (R_H)	%	29.43	82.05	53.28	13.29
			Surface Pressure (S_P)	Kpa	81.67	82.77	82.21	0.21
			Precipitation (P_R)	mm/day	0.00	2.91	0.59	0.55
	Longitude	$46^0$15'E	Dew-point Temperature (T_D)	^{0}C	-11.93	8.18	-0.19	5.25
			Maximum Temperature (T_{max})	^{0}C	-1.43	35.15	17.11	10.69
			Minimum Temperature (T_{min})	^{0}C	-11.46	16.82	3.78	7.59
			Mean Temperature (T_{mean})	^{0}C	-7.13	25.75	9.88	9.26
			Minimum Wind Speed (U_{min})	m/s	0.56	2.63	1.37	0.33
			Maximum Wind Speed (U_{max})	m/s	3.03	6.43	4.57	0.59
	Altitude	1350 m	Mean Wind Speed (U_{mean})	m/s	1.89	4.27	2.88	0.41
			Solar Radiation (R_S)	MJ/m^2/day	5.86	28.75	17.02	6.59
			Pan Evaporation (E_P)	mm/day	0.13	15.33	6.20	4.54
Urmia	Latitude	$37^0$34'N	Relative Humidity (R_H)	%	28.62	77.01	51.05	13.28
			Surface Pressure (S_P)	Kpa	83.99	85.05	84.47	0.23
			Precipitation (P_R)	mm/day	0.00	3.74	0.67	0.67
	Longitude	$44^0$58'E	Dew-point Temperature (T_D)	^{0}C	-11.15	10.28	1.29	5.12
			Maximum Temperature (T_{max})	^{0}C	-0.50	33.90	18.05	10.26
			Minimum Temperature (T_{min})	^{0}C	-9.07	20.17	7.17	8.14
			Mean Temperature (T_{mean})	^{0}C	-3.63	26.73	12.25	9.40
			Minimum Wind Speed (U_{min})	m/s	0.41	1.86	1.02	0.28
			Maximum Wind Speed (U_{max})	m/s	1.91	5.63	3.62	0.66
	Altitude	1332 m	Mean Wind Speed (U_{mean})	m/s	1.18	3.60	2.23	0.39
			Solar Radiation (R_S)	MJ/m^2/day	6.04	31.48	17.96	6.97
			Pan Evaporation (E_P)	mm/day	0.04	10.96	4.15	3.10

Appendix 1e: Data Descriptive Statistics for Libya Stations

Station	Location	Coordinates	Parameters	Unit	Min	Max.	Average	St. Deviation
Sabha	Latitude	$27^0$04'N	Relative Humidity (R_H)	%	15.52	61.70	28.73	10.40
			Surface Pressure (S_P)	Kpa	96.14	97.52	96.61	0.30
			Precipitation (P_R)	mm/day	0.00	1.42	0.05	0.16
	Longitude	$14^0$43'E	Dew-point Temperature (T_D)	^{0}C	-5.59	7.82	1.82	3.29
			Maximum Temperature (T_{max})	^{0}C	15.79	41.95	30.28	7.88
			Minimum Temperature (T_{min})	^{0}C	1.97	25.54	15.29	7.22
			Mean Temperature (T_{mean})	^{0}C	8.27	34.00	22.55	7.84
			Minimum Wind Speed (U_{min})	m/s	1.13	2.34	1.70	0.26
			Maximum Wind Speed (U_{max})	m/s	3.38	5.85	4.71	0.57
	Altitude	420 m	Mean Wind Speed (U_{mean})	m/s	2.28	3.98	3.14	0.39
			Solar Radiation (R_S)	MJ/m^2/day	9.41	29.35	20.99	5.64
			Pan Evaporation (E_P)	mm/day	4.90	24.70	15.09	5.65
Tripoli	Latitude	$32^0$89'N	Relative Humidity (R_H)	%	44.95	74.83	59.06	6.20
			Surface Pressure (S_P)	Kpa	99.96	101.45	100.41	0.29
			Precipitation (P_R)	mm/day	0.00	4.79	0.67	0.86
	Longitude	$13^0$19'E	Dew-point Temperature (T_D)	^{0}C	3.82	18.80	11.66	4.07
			Maximum Temperature (T_{max})	^{0}C	14.90	36.21	25.27	6.19
			Minimum Temperature (T_{min})	^{0}C	8.47	25.90	17.02	5.24
			Mean Temperature (T_{mean})	^{0}C	11.61	30.63	20.73	5.71
			Minimum Wind Speed (U_{min})	m/s	0.93	3.31	1.83	0.51
			Maximum Wind Speed (U_{max})	m/s	3.97	6.90	5.17	0.57
	Altitude	81 m	Mean Wind Speed (U_{mean})	m/s	2.56	5.03	3.59	0.53
			Solar Radiation (R_S)	MJ/m^2/day	7.20	29.71	18.71	7.01
			Pan Evaporation (E_P)	mm/day	2.20	14.10	7.52	2.65

APPENDIX 2

PEARSON CORRELATION MATRIX

Appendix 2a: Pearson Correlation Matrix between ET_0 and Input Parameters for Turkey Stations

Parameter	Adana	Ankara	Izmir	Samsun
P_R	0.8783	0.8759	0.9086	0.8264
R_H	0.9005	0.8786	0.9227	0.8199
S_P	-0.5869	-0.8080	-0.8833	-0.5713
T_D	-0.8847	-0.3907	-0.7753	-0.5644
T_{max}	-0.6643	-0.2469	-0.6512	-0.4355
T_{min}	0.8631	0.8311	0.8428	0.8319
T_{mean}	0.8956	0.8889	0.9262	0.8325
U_{min}	-0.5680	-0.1483	0.0497	-0.3162
U_{max}	0.7542	-0.0437	0.2092	-0.3130
U_{mean}	-0.1882	0.0670	0.1153	-0.3543
R_S	0.9143	0.8897	0.9388	0.8171
E_P	0.9987	0.9967	0.9970	0.9995

Appendix 2b: Pearson Correlation Matrix between ET_0 and Input Parameters for North Cyprus Stations

Parameter	Famagusta	Kyrenia	Morphou	Nicosia
P_R	0.7821	0.8140	0.8140	0.8140
R_H	0.8446	0.8697	0.8697	0.8697
S_P	-0.7521	-0.8477	-0.8477	-0.8477
T_D	-0.8784	-0.8787	-0.8787	-0.8787
T_{max}	-0.6789	-0.6919	-0.6959	-0.6959
T_{min}	0.7825	0.7922	0.7922	0.7922
T_{mean}	0.8218	0.8511	0.8511	0.8511
U_{min}	-0.6501	-0.4015	-0.4015	-0.4015
U_{max}	-0.4594	-0.0805	-0.0805	-0.0805
U_{mean}	-0.5584	-0.1855	-0.1855	-0.1855
R_S	0.9607	0.9634	0.9625	0.9634
E_P	0.9209	0.8818	0.9666	0.9684

Appendix 2c: Pearson Correlation Matrix between ET_0 and Input Parameters for Iraq Stations

Parameter	Erbil	Salahaddin
P_R	0.9367	0.8961
R_H	0.9463	0.8845
S_P	-0.8813	-0.8562
T_D	-0.9074	-0.8566
T_{max}	-0.5050	-0.5276
T_{min}	0.6023	0.5197
T_{mean}	0.9479	0.8794
U_{min}	0.7982	0.2055
U_{max}	0.1198	0.7656
U_{mean}	0.6640	0.1550
R_S	0.9270	0.8734
E_P	0.9952	0.9977

Appendix 2d: Pearson Correlation Matrix between ET_0 and Input Parameters for Iran Stations

Parameter	Tabriz	Urmia
P_R	0.9670	0.9000
R_H	0.9767	0.9134
S_P	-0.8884	-0.8441
T_D	-0.1060	-0.5202
T_{max}	-0.2850	-0.2482
T_{min}	0.9257	0.8864
T_{mean}	0.9765	0.9148
U_{min}	-0.1145	-0.2758
U_{max}	0.0479	0.3300
U_{mean}	0.1493	0.1783
R_S	0.9277	0.9345
E_P	0.9983	0.9979

Appendix 2e: Pearson Correlation Matrix between ET_0 and Input Parameters for Libya Stations

Parameter	Sabha	Tripoli
P_R	0.8891	-0.5551
R_H	0.9170	-0.8243
S_P	-0.8859	-0.6853
T_D	-0.8296	0.5962
T_{max}	-0.2400	0.7704
T_{min}	0.5292	0.6868
T_{mean}	0.9074	0.7377
U_{min}	0.4962	-0.4599
U_{max}	0.7674	-0.1743
U_{mean}	0.7814	-0.3563
R_S	0.8707	0.8172
E_P	0.9969	0.9986

APPENDIX 3

CURRICULUM VITAE

PERSONAL INFORMATION

Place of Birth: Wudil, Kano State, Nigeria

Citizenship: Nigerian

Gender: Male

Marital Status: Single

EDUCATION

Degree	Institution	Year of Graduation
M.Sc.	NEU Department of Civil Engineering	2016
B.Sc.	KUST Department of Civil Engineering	2012

WORK EXPERIENCE

Year	Place	Enrollment
2016 – 2020	Faculty of Civil and Environmental Engineering	Research Assistant
2013 – 2014	Kano Ministry of Works, Housing and Transport	Civil Engineer II
2012 – 2013	Abubakar Tatari Ali Polytechnic	Lecturer

LANGUAGES

Hausa and English

PUBLICATIONS IN INTERNATIONAL REFEREED JOURNALS (IN COVERAGE OF SCI/SCI-EXPANDED):

1. **Abdullahi, J.,** Iravanian, A., Nourani, V., & Elkiran, G. (2020). Application of artificial intelligence based and multiple regression techniques for monthly

precipitation modeling in coastal and inland stations. *Desalination and Water Treatment Journal* (accepted, awaiting publication) **(Q3)**.

2. Nourani, V., Elkiran, G., & **Abdullahi, J.** (2020). Multi-step ahead modeling of reference evapotranspiration using a multi-model approach. *Journal of Hydrology, 581*, 124434 **(Q1)**.
3. Nourani, V., Elkiran, G., & **Abdullahi, J.** (2019). Multi-station artificial intelligence based ensemble modeling of reference evapotranspiration using pan evaporation measurements. *Journal of Hydrology, 577*, 123958 **(Q1).**
4. Nourani, V., Elkiran, G., **Abdullahi, J.,** & Tahsin, A. (2019). Multi-region modeling of daily global solar radiation with artificial intelligence ensemble. *Natural Resources Research*, 1-22 **(Q3).**

PUBLICATIONS IN INTERNATIONAL REFEREED JOURNALS (IN COVERAGE OF British Education Index, ERIC, Science Direct, Scopus, IEEE):

- Elkiran, G., & **Abdullahi, J.** (2019). Assessment of water balance in food trade in the water-scarce regions of Nigeria. *International Transaction Journal of Engineering, Management, & Applied Sciences & Technologies*, 299-308**.**
- Elkiran, G., Nourani, V., Abba, S. I., & **Abdullahi, J.** (2018). Artificial intelligence-based approaches for multi-station modelling of dissolve oxygen in river. *Global Journal of Environmental Science and Management*, *4*(4), 439-450**.**
- Abba, S. I., Hadi, S. J., & **Abdullahi, J.** (2017). River water modelling prediction using multi-linear regression, artificial neural network, and adaptive neuro-fuzzy inference system techniques. *Procedia computer science*, *120*, 75-82**.**
- **Abdullahi, J.,** & Elkiran, G. (2017). Prediction of the future impact of climate change on reference evapotranspiration in Cyprus using artificial neural network. *Procedia computer science*, *120*, 276-283**.**

PAPERS PUBLISHED IN OTHER INTERNATIONAL INDEXED JOURNALS

1. **Abdullahi, J.,** Elkiran, G., & Nourani, V. (2017). Application of Artificial Neural Network to predict reference evapotranspiration in Famagusta, North Cyprus. In *11th International Scientific Conference on Production Engineering Development and Modernization of Production* (pp. 549-554).

2. **Abdullahi, J.,** and Elkiran, G. (2016). Determination of Crop Water Requirements of Maize in Nigeria by Using FAO CROPWAT 8.0. *International Multilingual Academic Journal, volume 3, No 2, May 2016,* 2330-6440.

PAPERS UNDER REVIEW FOR POSSIBLE PUBLICATIONS

1. **Abdullahi, J.,** Elkiran, G., Nourani, V., & Tahsin A. A novel approach for precipitation modeling using artificial intelligence based ensemble modeling.
2. Elkiran, G., **Abdullahi, J.,** Nourani, V., & Aslanova F. Linear and nonlinear ensemble concepts for pan evaporation modeling
3. Elkiran, G., & **Abdullahi, J.** Virtual water trade in the semi-arid regions of Nigeria.
4. Abba S.I., Hadi S.J., Abdulkadir R.A., Pham Q.B., **Abdullahi J.,** Gaya M.S, Albrka S.I., Esmaili P. Evolutionary computational intelligence techniques coupled with a non-tuned data intelligence model for modeling water quality index.
5. Abba S.I., Thuy L.N.T., **Abdullahi J.**, Albrka S.I., Pham Q.B., Abdulkadir R.A., Costache R. Hybrid Machine Learning Ensemble Techniques for Modeling Dissolved Oxygen Concentration

Book and Book Chapter published

1. **Abdullahi, J.,** Nourani, V., & Elkiran, J. (2020) Artificial Intelligence Based and Linear Conventional Techniques for Reference Evapotranspiration Modeling. In: Aliev R., Kacprzyk J., Pedrycz W., Jamshidi M., Babanli M., Sadikoglu F. (eds).
2. **Abdullahi, J.,** & Elkiran, G. (2017). Water footprint assessment in Nigeria: Evaluation of cropping pattern. LAMBERT Academic Publishing.

International Conferences Attended

1. 2nd International conference on the environment survival and sustainability, 7 – 11 October, 2019. Near East University, Nicosia, Cyprus.
2. 2nd International conference on Water problems in the Mediterranean Countries (WPMC 2019), 06 – 10 May, 2019. Near East University, Nicosia, Cyprus.
3. 3rd International Conference on Computational Mathematics and Engineering Sciences – CMES – 2018, 4 – 6 May, 2018, Girne, Cyprus.

4. The 11th International Conference on Research and Modernization of Production“ RIM” at Hotel Hills, Sarajevo, Bosnia & Herzegovina, October 4 -7, 2017.
5. AASRC SPEHES-IZMIR2016, Studies in Politics, Education, Health, Engineering and Sociology. April 22, 2016. http://aasrc.org. Conference Sponsor Ege University, Turkey.

Conferences Organized

- Member, Organization Committee, 2nd International conference on the environment survival and sustainability, 7 – 11 October 2019. Near East University, Nicosia, Cyprus.
- Member, Organization Committee, 2nd International conference on Water problems in the Mediterranean Countries (WPMC 2019), 06 – 10 May, 2019. Near East University, Nicosia, Cyprus.
- Member, Organization Committee, 2nd International conference on the Cyprus Issue: Past, Present and the Vision for the Future, 1 – 3 April, 2019. Near East University, Nicosia, Cyprus

THESISES

Master

Abdullahi, J. (2012). *Virtual Water Trade in the Semi-Arid Regions of Nigeria*. Unpublished Master thesis, Near East University, Department of Civil Engineering, Faculty of Civil and Environmental Engineering, Nicosia, Cyprus.

Project

Abdullahi, J. (2012). *Temperature Effect on the compressive strength of Concrete*. Unpublished Undergraduate project (B.SC.), Kano University of Science and Technology, Department of Civil Engineering, Faculty of Engineering, Wudil, Kano, Nigeria.

COURSES GIVEN

- (2012 – 2013) Building Construction and Introduction to Highway Engineering

- (2019 – 2020) CIV374 Engineering Hydrology
- (2020) CIV372 Hydromechanics

SPORTS

Football

HOBBIES

Reading, movies

APPENDIX 4

ETHICAL APPROVAL LETTER

TO GRADUATE SCHOOL OF APPLIED SCIENCES

REFERENCE: ENG. JAZULI ABDULLAHI (20167457)

I would like to inform you that the above candidate is one of our postgraduate students in Civil Engineering Department. He is taking thesis under my supervision and the thesis title is: **Multi-station artificial intelligence based ensemble modeling of reference evapotranspiration using pan evaporation measurements.** The data used in the study were obtained from the respective meteorological organizations of the study countries including Turkey, North Cyprus, Iraq, Iran and Libya.

Please do not hesitate to contact me if you have any further queries or questions.

Thank you very much indeed.

Best Regards.

Prof. Dr. Gozen Elkiran
Civil Engineering Department,
Faculty of Civil and Environmental Engineering,
Near East Boulevard, ZIP: 99138
Nicosia/TRNC, North Cyprus,
Mersin 10 – Turkey.
Email: gozen.elkiran@neu.edu.tr

APPENDIX 5

SIMILARITY REPORT

Jazuli Abdullahi

INBOX | NOW VIEWING: NEW PAPERS ▾

Submit File

Online Grading Report | Edit assignment settings | Email non-submitters

AUTHOR	TITLE	SIMILARITY	GRADE	RESPONSE	FILE	PAPER ID	DATE
Jazuli Abdullahi	Abstract	0%	--	--		1314396241	03-May-2020
Jazuli Abdullahi	Chapter 5	0%	--	--		1314399887	03-May-2020
Jazuli Abdullahi	Chapter 4	8%	--	--		1314495847	03-May-2020
Jazuli Abdullahi	All Thesis	9%	--	--		1314490324	03-May-2020
Jazuli Abdullahi	Chapter 3	10%	--	--		1314489250	03-May-2020
Jazuli Abdullahi	Chapter 2	11%	--	--		1314397135	03-May-2020
Jazuli Abdullahi	Chapter 1	13%	--	--		1314488941	03-May-2020

07/07/2020